



**NAVAL
POSTGRADUATE
SCHOOL**

MONTEREY, CALIFORNIA

THESIS

**HARDWARE INTERFACE TO CONNECT AN AN/SPS-65
RADAR TO AN SRC-6E RECONFIGURABLE COMPUTER**

by

Timothy L. King

March 2005

Thesis Advisor:

Douglas J. Fouts

Second Reader:

Phillip E. Pace

Approved for public release; distribution is unlimited

THIS PAGE INTENTIONALLY LEFT BLANK

REPORT DOCUMENTATION PAGE		Form Approved OMB No. 0704-0188	
<p>Public reporting burden for this collection of information is estimated to average 1 hour per response, including the time for reviewing instruction, searching existing data sources, gathering and maintaining the data needed, and completing and reviewing the collection of information. Send comments regarding this burden estimate or any other aspect of this collection of information, including suggestions for reducing this burden, to Washington headquarters Services, Directorate for Information Operations and Reports, 1215 Jefferson Davis Highway, Suite 1204, Arlington, VA 22202-4302, and to the Office of Management and Budget, Paperwork Reduction Project (0704-0188) Washington DC 20503.</p>			
1. AGENCY USE ONLY (Leave blank)	2. REPORT DATE	3. REPORT TYPE AND DATES COVERED	
	March 2005	Master's Thesis	
4. TITLE AND SUBTITLE: Hardware Interface to Connect an AN/SPS-65 Radar to an SRC-6E Reconfigurable Computer		5. FUNDING NUMBERS	
6. AUTHOR(S) LT Timothy L. King		7. PERFORMING ORGANIZATION NAME(S) AND ADDRESS(ES) Naval Postgraduate School Monterey, CA 93943-5000	
9. SPONSORING /MONITORING AGENCY NAME(S) AND ADDRESS(ES) NSA 9800 Savage Road Ft. George C. Meade, MD 20755		10. SPONSORING/MONITORING AGENCY REPORT NUMBER	
11. SUPPLEMENTARY NOTES The views expressed in this thesis are those of the author and do not reflect the official policy or position of the Department of Defense or the U.S. Government.			
12a. DISTRIBUTION / AVAILABILITY STATEMENT Approved for public release; distribution is unlimited		12b. DISTRIBUTION CODE	
13. ABSTRACT (maximum 200 words) A hardware interface is designed, developed, constructed, and tested to interface a naval radar to the SRC-6E reconfigurable computer. The U.S. Navy AN/SPS-65 radar provides in-phase (I) and quadrature (Q) channels along with the AGC voltage to the hardware interface in analog form. The hardware interface receives a sampling clock from the SRC-6E and in turn performs the requisite attenuation and digital conversion before presenting the signals to the SRC-6E through its CHAIN port. The results show that the SRC-6E can effectively generate a sampling clock to drive the analog-to-digital converters and that real-time radar data can be brought into the SRC-6E via its high speed CHAIN port for performing high speed digital signal processing			
14. SUBJECT TERMS Radar Signal Processing, Reconfigurable Computer, SRC-6E, SRC			15. NUMBER OF PAGES 127
			16. PRICE CODE
17. SECURITY CLASSIFICATION OF REPORT Unclassified	18. SECURITY CLASSIFICATION OF THIS PAGE Unclassified	19. SECURITY CLASSIFICATION OF ABSTRACT Unclassified	20. LIMITATION OF ABSTRACT UL

THIS PAGE INTENTIONALLY LEFT BLANK

Approved for public release; distribution is unlimited

**HARDWARE INTERFACE TO CONNECT AN AN/SPS-65 RADAR TO AN
SRC-6E RECONFIGURABLE COMPUTER**

Timothy L. King
Lieutenant, United States Naval Reserve
B.S., Virginia Polytechnic & State University, 2000

Submitted in partial fulfillment of the
requirements for the degree of

MASTER OF SCIENCE IN ELECTRICAL ENGINEERING

from the

**NAVAL POSTGRADUATE SCHOOL
March 2005**

Author: Timothy L. King

Approved by: Douglas J. Fouts
Thesis Advisor

Phillip E. Pace
Second Reader

John P. Powers
Chairman, Department of Electrical and Computer Engineering

THIS PAGE INTENTIONALLY LEFT BLANK

ABSTRACT

A hardware interface is designed, developed, constructed, and tested to interface a naval radar to the SRC-6E reconfigurable computer. The U.S. Navy AN/SPS-65 radar provides in-phase (I) and quadrature (Q) channels along with the AGC voltage to the hardware interface in analog form. The hardware interface receives a sampling clock from the SRC-6E and in turn performs the requisite attenuation and digital conversion before presenting the signals to the SRC-6E through its CHAIN port. The results show that the SRC-6E can effectively generate a sampling clock to drive the analog-to-digital converters and that real-time radar data can be brought into the SRC-6E via its high speed CHAIN port for performing high speed digital signal processing.

THIS PAGE INTENTIONALLY LEFT BLANK

TABLE OF CONTENTS

I.	INTRODUCTION	1
A.	PURPOSE.....	1
B.	DESIGN OVERVIEW	1
C.	THESIS OUTLINE.....	3
II.	SRC-6E ARCHITECTURE	5
A.	INTRODUCTION	5
B.	SRC-6E SYSTEM ARCHITECTURE OVERVIEW	5
C.	CHAIN PORT OVERVIEW	7
1.	CHAIN Port Physical Configuration	7
2.	Implementation as a General Purpose Port	8
D.	DESIGN IMPLEMENTATION.....	9
E.	CHAPTER SUMMARY	9
III.	AN/SPS-65.....	11
A.	INTRODUCTION	11
B.	RADAR SELECTION.....	11
C.	AN/SPS-65(V)1 OPERATIONAL OVERVIEW.....	11
D.	DESIGN IMPLEMENTATION.....	13
E.	CHAPTER SUMMARY	15
IV.	MAXIM MAX108EVKIT 8-BIT ADC BOARD.....	17
A.	INTRODUCTION	17
B.	OVERALL CAPABILITIES OF THE MAX108	17
C.	POWER REQUIREMENTS	19
D.	ANALOG AND CLOCK INPUTS	21
1.	Sample Clock Inputs.....	21
2.	Analog Inputs	21
E.	DIGITAL OUTPUTS	21
1.	Demultiplexer Operation	23
a.	<i>Non-Demultiplexed Mode</i>	24
b.	<i>Demultiplexed Mode</i>	24
c.	<i>Decimation Mode</i>	25
2.	Data Ready	26
F.	DESIGN IMPLEMENTATION.....	27
1.	Input Configuration.....	27
2.	Sample Clock and Demux Operation	27
3.	Data Ready	28
4.	Termination and Power Supplies.....	28
G.	INITIAL TESTING AND FAMILIARIZATION	29
H.	ADDITIONAL HARDWARE REQUIRED.....	30
I.	CHAPTER SUMMARY	31

V.	ANALOG PCB DESIGN	33
A.	INTRODUCTION	33
B.	ATTENUATION DESIGN OPTIONS	33
1.	Inline RF Attenuator and Buffer.....	33
2.	Op-Amp Attenuation Circuit	34
3.	Voltage Divider to High-Speed Buffer.....	35
C.	PRF TIMING REFERENCE AMPLIFICATION DESIGN	37
D.	PCB DESIGN AND LAYOUT	40
1.	PCB Software Selection.....	40
2.	Analog Board Schematic Layout.....	40
3.	Analog Board PCB Design.....	43
E.	TESTING.....	45
1.	I and Q Channel Testing	46
2.	AGC Voltage Testing	48
3.	PRF Timing Reference Testing	49
F.	CHAPTER SUMMARY	50
VI.	TRANSLATION BOARD DESIGN	51
A.	INTRODUCTION	51
B.	SIGNAL TRANSLATION	51
1.	LVPECL-to-LVTTL Translation.....	51
2.	LVTTL-to-ECL Translation.....	52
C.	MICTOR CONNECTOR ALTERNATIVES	52
1.	Custom Micro-Coaxial Cable	53
2.	MICTOR Connector Breakout Adapter.....	53
3.	Printed Circuit Board Implementation.....	53
D.	MAX108EVKIT-TO-TRANSLATION BOARD CABLING.....	54
E.	PCB DESIGN AND LAYOUT	55
1.	Initial Design Considerations	55
2.	Device Termination	56
3.	Power Distribution.....	58
4.	Translation Board Schematic Layout	59
5.	Translation Board PCB Layout	61
F.	TRANSLATION BOARD TESTING	62
1.	Sample Clock Translation Testing	64
2.	LVPECL-to-LVTTL Translation Testing	65
3.	LVPECL Termination Resistor Analysis	67
G.	CHAPTER SUMMARY	68
VII.	COMPLETE INTERFACE TESTING	71
A.	INTRODUCTION	71
B.	DESIGN MODIFICATION	71
C.	INTERFACE TEST.....	71
D.	CHAPTER SUMMARY	73
VIII.	CONCLUSIONS	75
A.	DESIGN SUMMARY.....	75

B.	DESIGN ACCOMPLISHMENT	76
C.	RECOMMENDATIONS FOR FUTURE WORK	77
APPENDIX A	CHAIN PORT PIN LISTING (AFTER REFS. 6 & 7.).....	79
APPENDIX B	SRC-6E PART NUMBERS.....	83
A.	USER LOGIC FPGAS [6].....	83
B.	MICRO-COAXIAL CABLE [6].....	83
C.	114-PIN AMP MICTOR CONNECTOR [6]	83
APPENDIX C	LOGIC ANALYZER DATA	85
APPENDIX D	MATLAB LOGIC ANALYZER PLOTTING SCRIPT	93
APPENDIX E	SPICE MODEL OF ATTENUATION CIRCUIT	95
APPENDIX F	SPICE MODEL OF PRF TIMING REFERENCE AMPLIFIER	97
APPENDIX G	EXPRESSPCB MANUFACTURING SPECIFICATIONS.....	99
APPENDIX H	MICTOR CONNECTOR SCHEMATIC	101
LIST OF REFERENCES		103
INITIAL DISTRIBUTION LIST.....		107

THIS PAGE INTENTIONALLY LEFT BLANK

LIST OF FIGURES

Figure 1.	AN/SPS-65 to SRC-6E Hardware Interface Block Diagram.....	2
Figure 2.	SRC-6E System Architecture Block Diagram (From Ref. 5.).....	6
Figure 3.	MAP Chassis Configuration (After Ref. 5.)	7
Figure 4.	AN/SPS-65 Receiver Block Diagram (After Ref. 8.)	13
Figure 5.	AN/SPS-65 Block Diagram Illustrating Test Point Taps (After Ref. 8.).....	14
Figure 6.	MAXIM MAX108EVKIT	18
Figure 7.	MAX108EVKIT Power Supply Connections	20
Figure 8.	MAX108EVKIT Digital Output Termination (From Ref. 10.).....	23
Figure 9.	Non-Demuxed, DIV1 Timing Diagram (From Ref. 9.).....	24
Figure 10.	Demuxed, DIV2 Timing Diagram (From Ref. 9.)	25
Figure 11.	Decimation, DIV4 Mode Timing Diagram (From Ref. 9.)	26
Figure 12.	CLK and DREADY Timing in DIV2 mode Showing the Two Possible Phases of DREADY (From Ref. 9.)	27
Figure 13.	Reconstructed Output from MAX108EVKIT Testing	30
Figure 14.	Two-Resistor Voltage Divider and Buffer Circuit.....	35
Figure 15.	AC Sweep Analysis of the LMH6559	37
Figure 16.	PRF Timing Reference LVTTL Amplification Circuit	38
Figure 17.	Simulation of PRF Timing Reference Amplifier Circuit	39
Figure 18.	Complete Analog Board Schematic	42
Figure 19.	PCB CAD Drawing for Analog Board	45
Figure 20.	Assembled Analog Board	46
Figure 21.	Test of I Channel Attenuation Circuit	47
Figure 22.	Test of Q Channel Attenuation Circuit	48
Figure 23.	Test of AGC Voltage Attenuation Circuit	49
Figure 24.	Test of PRF Timing Reference Amplification Circuit	50
Figure 25.	Shielded Controlled Impedance Cable	55
Figure 26.	Block Diagram of Translation Board and MAX108EVKIT Arrangement	56
Figure 27.	Translation Board Schematic.....	60
Figure 28.	PCB CAD Drawing of Translation Board	62
Figure 29.	Translation Board Trace Errors	63
Figure 30.	Assembled Translation Board.....	63
Figure 31.	10-MHz LVTTL Clock Translated to ECL	64
Figure 32.	200-MHz LVTTL Clock Translated to ECL	65
Figure 33.	Translation Board Output with a 200-MHz Sample Clock.....	66
Figure 34.	DREADY Immediately Following Translation (Terminator Located on MAX108EVKIT).....	68
Figure 35.	DREADY Immediately Following Translation (Terminator Located on Translation Board)	68
Figure 36.	Complete Hardware Interface Configuration	72
Figure 37.	Reconstructed Radar Data Collected by the SRC-6E (From Ref. 23.)	73

THIS PAGE INTENTIONALLY LEFT BLANK

LIST OF TABLES

Table 1.	SRC-6E CHAIN Port Signal Groupings (From Ref. 6.)	8
Table 2.	AN/SPS-65 Channel Parameters.....	14
Table 3.	Power Supply Requirements [9]	20
Table 4.	Ideal Input Voltage and Output Code Results for Single-ended Operation (From Ref. 10.)	22
Table 5.	Ideal Input Voltage and Output Code Results for Single-ended Operation (From Ref. 10.)	22
Table 6.	MAX108EVKIT Demultiplexer Jumper Settings [10].....	24
Table 7.	Resistor Values for Voltage Divider.....	35
Table 8.	Trace Impedance Calculation Results	43
Table 9.	Resistor Size and Power Handling Comparison.....	44
Table 10.	Shielded Controlled Impedance Cable Electrical Properties (From Ref. 20.)	55
Table 11.	Termination Resistor Power Calculations	58
Table 12.	Translation Board Voltage and Current Requirements	58
Table 13.	Trace Width Current Capacity (From Ref. 22.).....	62

THIS PAGE INTENTIONALLY LEFT BLANK

ACKNOWLEDGMENTS

I would like to thank my thesis advisor Douglas J. Fouts for his time, support and technical guidance. His involvement was essential in ensuring that this project stayed on track and succeeded not only in function, but also in providing a great learning experience that covered multiple electrical engineering disciplines.

A special thanks to David Rigmaiden for his printed circuit board expertise and soldering skills. His assistance was instrumental in the successful mounting of the MICTOR connector on the translation board and the implementation of corrective measures to work around design errors in both the analog and translation printed circuit boards.

SRC Computers, Inc. needs to be recognized for their design guidance and provisioning of specialized hardware. Without the micro-coaxial cables and breakout board they provided, the implementation and testing of the hardware interface would not have been possible in the time allotted for the project.

I would also like to Alan Hunsberger and the National Security Agency for providing me the opportunity to conduct this research.

Most importantly, I thank my wife Alice for being my strongest supporter. Over the past 27 months here at the Naval Postgraduate School she filled the role as sounding board, proofreader, and at times educator while simultaneously acting as wife, mother, and friend.

THIS PAGE INTENTIONALLY LEFT BLANK

EXECUTIVE SUMMARY

Reconfigurable computers provide the military a highly customizable and powerful way to process real-time data. The purpose of this research was to test the capability, exploit the functionality, and prove the feasibility of the SRC-6E reconfigurable computer to send and receive data via its high speed CHAIN port. The use of FPGAs on the reconfigurable MAP® boards of the SRC-6E provides the SRC-6E the ability to generate algorithm specific logic, with the potential for orders of magnitude speedup for computationally intensive algorithms [1]. Studies have been conducted proving that speedup can be obtained by reconfigurable computers but they have only addressed non-real-time computational intensive problems in which the data being analyzed is already stored on the machine. By bringing data straight to the reconfigurable computer, its parallel processing capabilities can be used to perform real-time data processing.

Reconfigurable computers offer high performance because they can be customized to the problem and they are relatively fast due to highly parallel and spatial execution [2]. Adding the ability to process large amounts of data in real-time gives reconfigurable computing the potential to evolve into efficient signal processors. Instead of having specialized gear for cryptographic analysis, radar processing, or electronic signal collection, a single SRC-6E, through its CHAIN port, can capture the requisite data and process it through hardware. This capability is very attractive in light of the ever increasing cost and complexity of signal processing equipment. Therefore, it was essential that this research use a valid real-world example to test the CHAIN port of the SRC-6E and determine its capabilities and limitations.

To prove the real-world applicability of such an interface, the AN/SPS-65 radar was selected as the data source. The goal of the hardware interface design was then to develop, implement, and test the requisite hardware needed to permit the SRC-6E to process the data received by the AN/SPS-65 to calculate the range of a target.

The data received by the AN/SPS-65 is carried on the ± 5.8 V in-phase (I) and quadrature (Q) channels while the internal amplification value of these two channels is

carried on the separate 0–12 V automatic gain control (AGC) voltage signal. The AN/SPS–65 pulse repetition frequency (PRF) is synchronized to 0 to 1.0–V pulse that generates a timing reference for the received radio frequency (RF) signals. The signals were connected to a custom-built analog board which buffered each signal and either amplified or attenuated the signal for proper compatibility with other parts of the design. The I, Q, and AGC voltage signals were attenuated to ± 225 mV to be compatible with the MAX108 ADC analog inputs and the PRF timing reference signal was amplified to low-voltage transistor-transistor-logic (LVTTL) to be compatible with the SRC–6E.

The I, Q, and AGC voltage signals were connected to individual MAX108 evaluation kits (MAX108EVKIT) where they were sampled at 100 MHz by the MAX108 ADCs. The low-voltage positive emitter coupled logic (LVPECL) outputs of each MAX108EVKIT were routed via shielded controlled impedance cables to a custom-built translation board. On the translation board, the LVPECL signals were translated to LVTTL and routed, along with the PRF timing reference signal from the analog board, to a 114-pin MICTOR™ connector. Micro-coaxial cable was then used to connect the MICTOR connector of the translation board to the MICTOR connector of the CHAIN port on the SRC–6E, completing the interface between the radar and the SRC–6E. The translation board also took the 100-MHz sample clock generated by the SRC–6E from the MICTOR connector and translated it into a differential emitter coupled logic (ECL) clock. This differential ECL clock was then routed through a clock driver for distribution to the three MAX108EVKITS.

The design met the established goal of interfacing the AN/SPS–65 radar to the SRC–6E reconfigurable computer. The design tested focused only on the single data rate (SDR) mode of the SRC–6E, but engineered all aspects of the design to be capable of exploiting the double data rate (DDR) capability of the SRC–6E allowing room for future speed-ups. To provide flexibility of implementation, the bandwidth of the analog board and the MAX108EVKITS allow the design to be capable of interfacing with other radars with similar output signals as the AN/SPS–65. Ultimately, the designed proved that the CHAIN port of the SRC–6E is a very capable high-speed port that can be effectively interfaced with external devices through user-defined hardware.

I. INTRODUCTION

A. PURPOSE

Reconfigurable computers provide the military a highly customizable and powerful way to process real-time data. The purpose of this research was to test the capability, exploit the functionality, and prove the feasibility of the ability of the SRC-6E reconfigurable computer to send and receive data via its high speed CHAIN port. The use of FPGAs on the reconfigurable MAP[®] boards of the SRC-6E provides the SRC-6E the ability to generate algorithm specific logic, with the potential for orders of magnitude speedup for computationally intensive algorithms [1]. Studies have been conducted proving that speedup can be obtained by reconfigurable computers, but they have only addressed non-real-time computational intensive problems in which the data being analyzed is already stored on the machine. By bringing data straight to the reconfigurable computer, its parallel processing capabilities can be used to perform real-time data processing.

Reconfigurable computers offer high performance because they can be customized to the problem and they are relatively fast due to their highly parallel and spatial execution [2]. Adding the ability to process large amounts of data in real-time gives reconfigurable computing the potential to evolve into efficient signal processors. Instead of having specialized gear for cryptographic analysis, radar processing, or electronic signal collection, a single SRC-6E, through its CHAIN port, can capture the requisite data and process it through hardware. This capability is very attractive in light of the ever increasing cost and complexity of signal processing equipment. Therefore, it was essential that this research use a valid real-world example to test the CHAIN port of the SRC-6E and determine its capabilities and limitations.

B. DESIGN OVERVIEW

The design illustrated in Figure 1 began by selecting a suitable real-world device that would produce real-time data to be processed by the SRC-6E. The U.S. Navy AN/SPS-65 search radar used by the Electrical Engineering Department at the Naval

Postgraduate School was selected to fulfill this role. The AN/SPS-65 provided access to its in-phase (I) channel, quadrature (Q) channel, and automatic gain control (AGC) voltage, as well as its pulse repetition frequency (PRF) timing reference signal which could be used to perform basic radar signal processing. Located on the tallest academic building on campus, the Naval Postgraduate School AN/SPS-65 could track a wide array of real targets, ranging from ships in Monterey Bay, the Santa Cruz Mountains, and aircraft on approach to the Monterey Airport. The real-world nature of the radar signals and the ease of access to them made the AN/SPS-65 a convenient and effective signal source for the project.

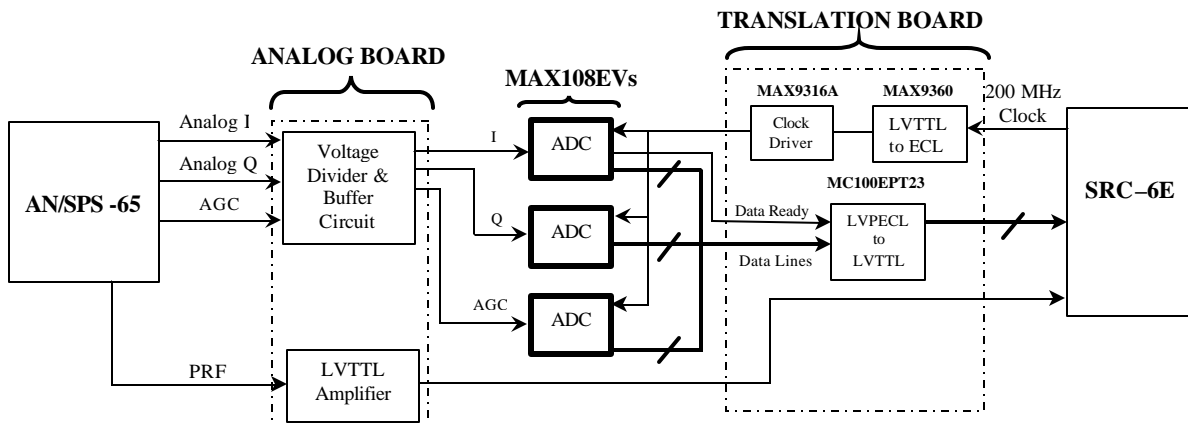


Figure 1. AN/SPS-65 to SRC-6E Hardware Interface Block Diagram

An analog board was designed and implemented to attenuate and buffer the I, Q, and AGC voltage signals from the AN/SPS-65 to a range of ± 250 mV for connection to the analog-to-digital converters. This analog board also amplified the pulse repetition frequency signal from a non-standard range of 0 to +1.1 V to the low-voltage transistor-transistor-logic (LVTTL) range of 0 to +3.3 V for direct connection to the SRC-6E.

Three MAX108 evaluation kits (MAX108EVKIT), each providing 8-bits of resolution, were then implemented to perform the analog-to-digital conversion (ADC) of the radar signals prepped by the analog board. Each MAX108EVKIT was to receive a 200-MHz sample clock generated by the SRC-6E. Each MAX108EVKIT would then demultiplex the output data to reduce the data rate into the SRC-6E to 100 MHz. This would create two sets of 8-bit data per MAX108EVKIT in differential low-voltage positive

emitter-coupled logic (LVPECL) format. Prior to connecting to the SRC-6E, these LVPECL outputs needed to be converted to the LVTTL logic standard of the SRC-6E.

To complete the interface, a translation board was designed and implemented to first translate the digitized radar signals from LVPECL to LVTTL. The board then connected the translated signals and the amplified pulse repetition frequency to the SRC-6E cabling through a surface mounted MICTOR™ connector. Finally, the translation board provided the necessary conversion of the LVTTL sample clock generated by the SRC-6E so that it could drive the emitter-coupled logic (ECL) clocks of the MAX108EVKITS.

C. THESIS OUTLINE

Each of the following chapters represents a major design area that needed to be addressed throughout the entire design process. The list below gives a brief synopsis of the remaining chapters:

- Chapter II describes the SRC-6E architecture, the CHAIN port interface, and external hardware requirements.
- Chapter III discusses the reasons for selecting the AN/SPS-65 radar, its basic operation, and how it was implemented in the design.
- Chapter IV discusses the selection, features, and design implementation of the MAX108 ADCs for the design.
- Chapter V covers the design, implementation, and testing of an analog printed circuit board designed to attenuate the three signals from the AN/SPS-65 to a level suitable for sampling by the MAX108s while also amplifying the pulse repetition frequency of the radar to LVTTL levels.
- Chapter VI covers the design, implementation, and testing of the printed circuit board responsible for providing the hardware interface between the SRC-6E and the MAX108 ADCs.
- Chapter VII discusses the complete interface testing and the overall results.
- Chapter VIII discusses the design conclusions and potential follow on work.

THIS PAGE INTENTIONALLY LEFT BLANK

II. SRC-6E ARCHITECTURE

A. INTRODUCTION

Reconfigurable computers could one day augment and possibly replace bulky and expensive specialized digital signal processing equipment. Studies have already proven that FPGA implementations are one to two orders of magnitude faster than typical embedded processors [3]. To harness this parallel processing power, reconfigurable computers must be successfully interfaced with already proven high-speed data sources. This design focused on interfacing the SRC-6E reconfigurable computer to an AN/SPS-65 radar using the high-speed CHAIN port of the SRC-6E. This chapter provides a brief system overview of the SRC-6E and describes the physical architecture and implementation of its high-speed CHAIN port.

B. SRC-6E SYSTEM ARCHITECTURE OVERVIEW

The SRC-6E is comprised of two microprocessor chassis and a reconfigurable MAP® chassis. Each microprocessor chassis consists of dual 1-GHz Intel® Pentium® III Xeon™ processors running the Linux operating system, 1.5 gigabytes of RAM, and a SNAP® port. The SNAP port connects the microprocessor chassis to one of the reconfigurable MAPs on the MAP chassis. Code is compiled and run on the Xeon processors, placing specialized functions on the MAP. These specialized functions are usually computationally intensive and can exploit the speedups afforded by hardware execution. Figure 2 illustrates the basic block diagram of the SRC-6E system configuration. [4]

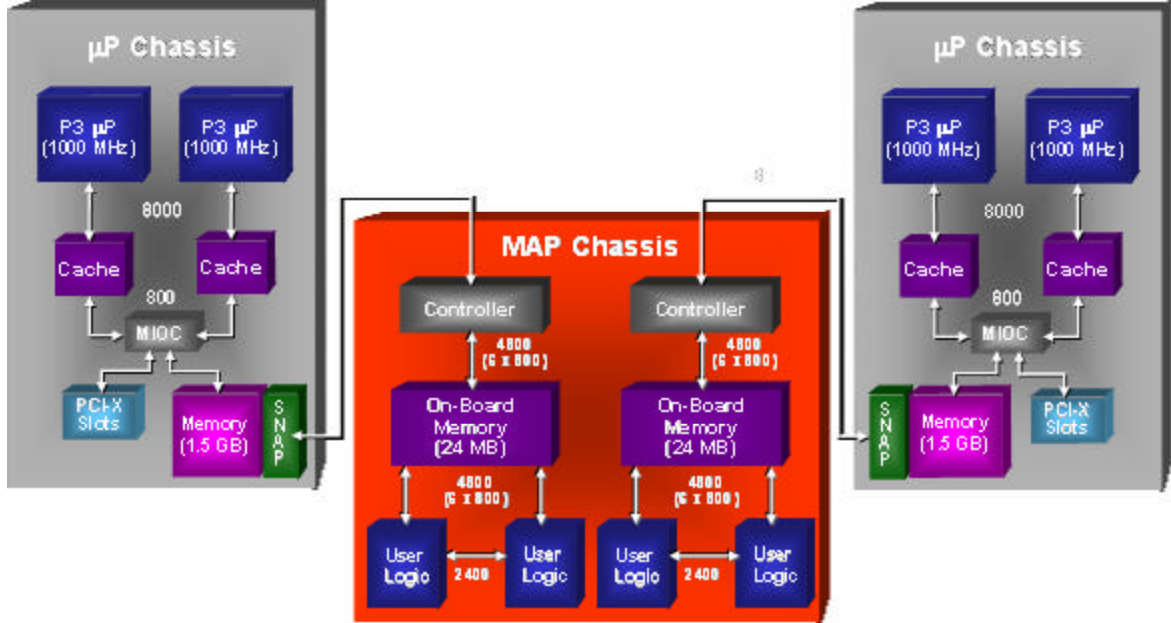


Figure 2. SRC-6E System Architecture Block Diagram (From Ref. 5.)

The MAP chassis contains two reconfigurable MAPs, each consisting of two Xilinx® Virtex-II FPGAs, a control processor, a total of 24 Mbytes of dual ported RAM, one SNAP port, and two CHAIN® ports. The two CHAIN ports (CHAIN In and CHAIN Out) are data ports that can be configured to connect the two MAPs together or be used as general input and output ports [6]. Figure 3 shows the actual layout of the MAP chassis. Most of the features inherent to the Virtex-II are available to the SRC-6E programmer, with a few exceptions. The two most notable are the FPGA clock frequency and the input and output levels. Though the Virtex-II FPGAs are capable of operating with a 420-MHz system clock [7], the MAPs on the SRC-6E restricts the system bus speed to 100 MHz. In addition, the internal voltage settings on the MAP set the input and output logic levels of the FPGAs to LVTTL.

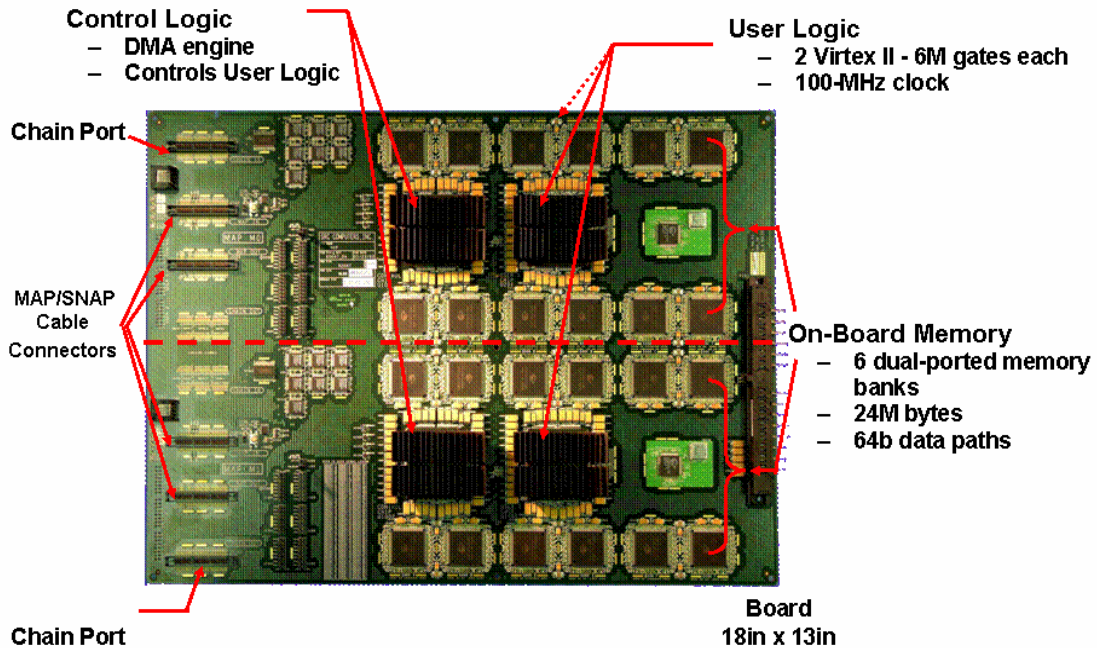


Figure 3. MAP Chassis Configuration (After Ref. 5.)

C. CHAIN PORT OVERVIEW

The CHAIN port is the dual-purpose high-speed parallel data port that allows either the interconnection of user logic between MAPs or the connection of user defined hardware to the SRC-6E. The CHAIN port supports user-defined data rates up to a maximum rate of 100 MHz in both single data rate (SDR) and double data rate (DDR) configurations. When in the SDR configuration, the CHAIN port can transfer data at 9,600 MBps. The data rate doubles to 19,200 MBps when the CHAIN port is used in the DDR configuration. The data flow onto the MAP through the CHAIN port must be source synchronous with a clock signal traveling with the data to indicate to the user logic when to latch the data. [6]

1. CHAIN Port Physical Configuration

Each CHAIN port has a total of 104 bi-directional signal lines that connect directly to the user logic FPGA input and output pins. The physical layout of the MAP separates these signals into four groups as listed in Table 1. The user is free to modify the groupings and functions of these bits as long as source synchronous data flow is maintained. Since the signals connect directly to the Virtex-II FPGAs, the user can define any signal to match its corresponding Virtex-II pin setting [6]. However, SRC took

extreme care to place the clock bits listed in Table 1 on the GCLK_x input and output pins of the Virtex-II FPGAs. These pins are specifically designed and optimized to distribute clock signals on and off the FPGA, but can be used for general input and output when not used for clock distribution purposes [7]. Appendix A lists the CHAIN port pin numbers, the corresponding Virtex-II pin numbers, and the Virtex-II pin descriptions.

Table 1. SRC-6E CHAIN Port Signal Groupings (From Ref. 6.)

Port Signal Group A	Port Signal Group B	Port Signal Group C	Port Signal Group D
36 Data Bits	36 Data Bits	20 Data Bits	6 Data Bits (SDR only)
1 Data Valid Bit	1 Data Valid Bit		
1 Clock Bit	1 Clock Bit		
1 Full Bit	1 Full Bit		

2. Implementation as a General Purpose Port

Since the user logic determines the function of the CHAIN port signals, the signals can be redefined to suit the particular needs of the user. When redefining the signals, the user must take care to ensure the correct Virtex-II input/output buffers are selected and that the signal levels are driven at LVTTL. Working within the confines of these two requirements, the user can fully customize the CHAIN port to interface with external hardware. [6]

The SRC-6E uses 114-pin AMP™ MICTOR surface mount connectors for all the SNAP and CHAIN port connections on the MAP board. A custom 50- Ω micro-coaxial cable with 114-pin push-in AMP connectors is then used to provide the necessary cabling between the surface mount connectors. SRC Computers highly recommends using the same micro-coaxial cables and surface mount MICTOR connector when connecting external hardware to the SRC-6E. This enables compatible high-speed connections between the user hardware and the MAP board. Appendix B lists the specific part numbers and manufacturer data of the parts required to establish a connection to the CHAIN port. [6]

To ensure proper signal transmission between the user hardware and the SRC-6E, the user hardware must pay particular attention to the trace impedance and signal termination. All transmission lines on the user hardware should be impedance matched as

closely as possible to the impedance of the micro-coaxial cable. Since the FPGAs have no termination resistors and the CHAIN port signals connect directly to the FPGA, the user hardware must handle all signal termination. For signals being transmitted to the SRC-6E, SRC Computers recommends implementing a source-series resistive termination on the data line. The resistive termination value, when summed with the driver output impedance, should match the $50 - \Omega$ impedance of the micro-coaxial cable as close as possible. For signals being transmitted by the SRC-6E, an RC shunt type termination should be implemented using a $50 - \Omega$ resistor in series with a $0.01 - \mu\text{F}$ capacitor. [6]

D. DESIGN IMPLEMENTATION

The design required that the CHAIN port be configured in SDR mode to interface with an external high-speed data source to perform real-time signal processing. This would allow the SRC-6E to capture data at the system speed of 100 MHz and was deemed fast enough to prove the viability of the SRC-6E as a real-time signal processor. Though DDR would have allowed for higher throughput, the technical risk and complexity it would add to the design exceeded the timeframe for this project.

To avoid any possible meta-stability issues and to implement the interface as a fully standalone configuration, the SRC-6E was used to generate the sample clock for the design. The clock signal would exit the SRC-6E on a designated clock pin to drive the ADCs on the interface hardware. The design sought to use a 200-MHz sampling clock as a result of the demultiplexing feature of the ADCs discussed in Chapter IV. This would allow the design to sample twice as fast while still staying within the maximum data rate of 100 MHz of the SRC-6E. To provide the possibility of DDR functionality for future work with the design, all signal lines were to be routed to DDR-capable signal groups.

E. CHAPTER SUMMARY

The CHAIN port of the SRC-6E is a high-speed data port that has the potential, when matched with the appropriate interface hardware, to allow the SRC-6E to receive and process data in real-time. The physical architecture of the SRC-6E creates the initial

requirements that this interface design has to meet to get data from the interface to the SRC-6E. The next chapter discusses the AN/SPS-65 selected to interface to the SRC-6E which defined the function and additional requirements of the interface design.

III. AN/SPS-65

A. INTRODUCTION

To prove the viability of reconfigurable computing as an alternative to specialized digital signal processing equipment, the SRC-6E needed to be connected to an already proven signal processing system. Military radars are such systems that have to process various high-speed digital signals to be able to accurately detect and track targets. Typically, these radars are very application specific and require massive, costly gear to transmit and process received signals. Using a reconfigurable computer to reduce the size, weight, and cost of just the signal processing equipment would greatly enhance the ability of the military to employ and maintain radars throughout the armed services. In addition, the ability to modify the signal processing algorithms in hardware while the system is in use could greatly enhance the operational capabilities of the radar. For these reasons, the design sought to interface the SRC-6E with a military radar.

B. RADAR SELECTION

The Electrical Engineering Department at the Naval Postgraduate School has access to several active military radars. With no other military emitters to compete with in the area, the only factors limiting the radar selected were its operating frequency and signal access. The AN/SPS-65(V)1 provided a 30-MHz received radio frequency (RF) signal that, at a Nyquist sampling rate of 60 MHz, was well within the design goal sampling rate of 200 MHz. In addition, the AN/SPS-65 provided direct access to the received signal channels internal to the radar. Thus, the AN/SPS-65 was selected as the signal source to be interfaced with the SRC-6E.

C. AN/SPS-65(V)1 OPERATIONAL OVERVIEW

The AN/SPS-65 is a modern master-oscillator, power-amplifier chain (MOPA), L-Band radar built by Westinghouse. Designed as a self-defense radar for large high value units, its primary purpose was to queue a ship fire control system to the approach

of high-speed, low-flying targets. Specifically, the AN/SPS-65 looked for targets traveling in excess of 80 knots but less than 1800 knots, with an effective range of 1 to 25 nautical miles. [8]

The AN/SPS-65 transmits a 1.3-GHz carrier frequency with a 7-**ms** pulse (with no pulse compression) and uses a PRF of 3,063 Hz. The transmitted and received pulses are steered to and from the antenna via a high speed circulator. Once a return is received and steered into the radar receiver, it is amplified by the receiver RF amplifier. The receiver amplifier either amplifies or attenuates the RF signal, based on the value of the sensitivity time control (STC) generated by the synchronizer. In addition, the receiver RF amplifier serves as the signal injection point for system test targets and performance analysis. The 1.3-GHz RF signal is then sent through a narrowband filter (NBF) centered on 1.3 GHz to remove any signal noise. Next, the receiver mixer uses a 1.269-GHz continuous wave stable local oscillator (CW STALO) input to down-convert the 1.3-GHz carrier to 30 MHz. The signal is then sent through an intermediate frequency (IF) amplifier. The IF amplifier amplifies the signal to its pre-filtered state, sends the signal through a bandpass filter (BPF) centered at 30 MHz to remove any additional noise, and then uses an AGC voltage to either attenuate or amplify the received signal to ensure that signal level at the amplifier output remains constant. The resulting IF signal is then processed by a phase detector that uses a continuous-wave coherent oscillator input (CW COHO) to split the IF signal into two channels, I and Q. The I and Q channels are identical signals except that the Q channel is 90 degrees out of phase with respect to I. These two channels are then sent to individual 12-bit ADCs prior to being routed to the signal processing hardware of the radar. Figure 4 depicts the block diagram of the AN/SPS-65 receiver and the path the signal takes from the antenna to the analog-to-digital converters. [8]

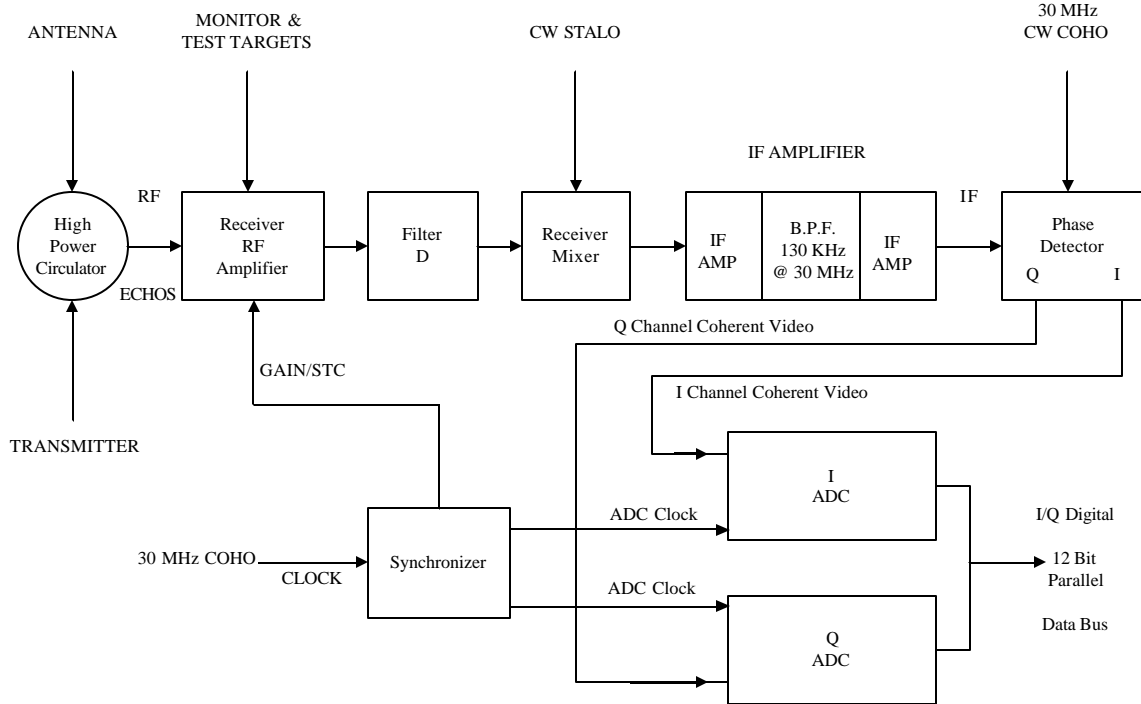


Figure 4. AN/SPS-65 Receiver Block Diagram (After Ref. 8.)

D. DESIGN IMPLEMENTATION

The design sought to provide the SRC-6E enough data to be able to determine the range of a target. The I, Q, and PRF timing reference signals summarized in Table 2 were required to perform this basic radar signal processing. The PRF timing reference signal is an impulse that establishes a time reference for the transmitter and receiver of the radar. Once the PRF timing reference triggers, the transmitter transmits the 1.3-GHz RF signal for 7 ms. After 7 ms, the transmitter turns off and the receiver turns on generating the I and Q channels. The I and Q channels carry the information obtained from a target reflection. The phase difference between them prevents the target from appearing during a zero-transition in the received signal [8]. The time from when PRF timing reference is triggered to the time a target is detected on I or Q represents the range of the target. The AGC voltage, though not required for this basic signal processing, was also desired to be brought into the SRC-6E for analytical purposes.

Table 2. AN/SPS-65 Channel Parameters

Channel	Voltage
I	± 5.8 V
Q	± 5.8 V
AGC	0–12 V
PRF Timing Reference	0–1.1V

The AN/SPS-65 has test points that allow easy access to the I, Q, AGC, and PRF timing reference signals. The I and Q channels are accessed just prior to the signals entering their respective 12-bit ADCs. The AGC voltage is tapped prior to it entering the third stage of the IF amplifier and the PRF timing reference is tapped just prior to it entering the transmitter. The red lines in Figure 5 depict the location of the signal taps for the I, Q, and AGC signals. The test points used high impedance probes to prevent the probe from distorting the signal. As a result, any external hardware desiring to extract the signal from the test points needed to provide a high-impedance input to prevent loading down the radar.

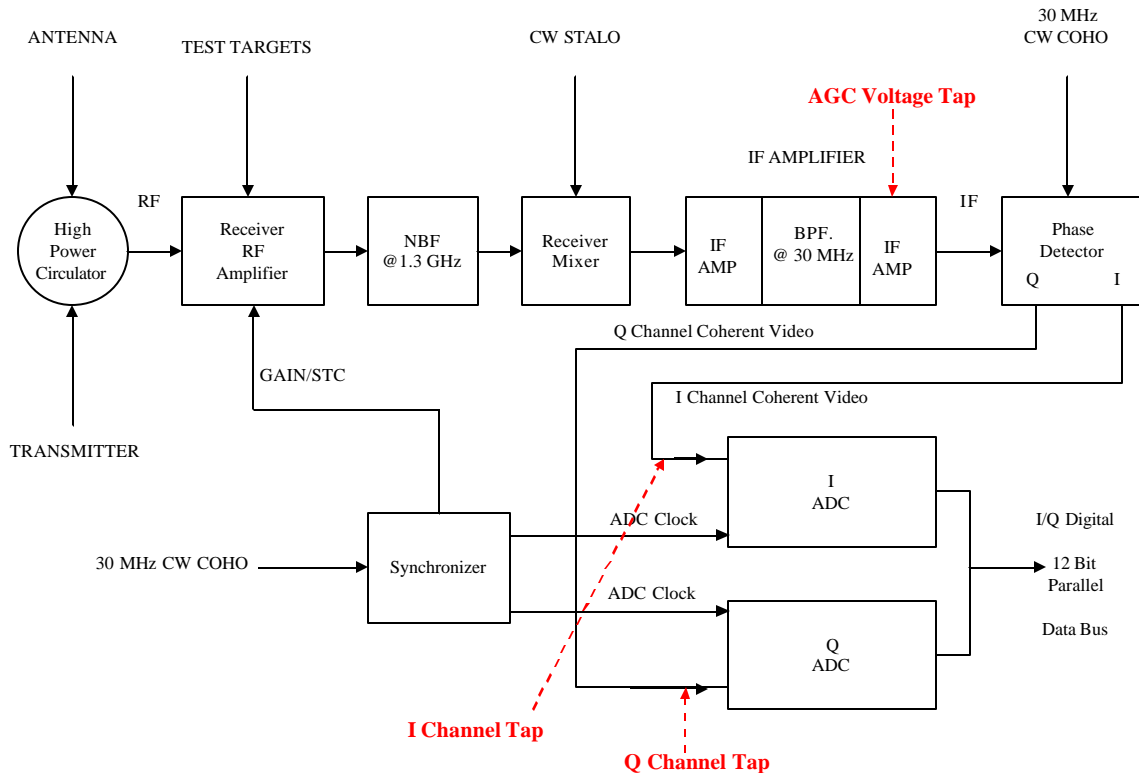


Figure 5. AN/SPS-65 Block Diagram Illustrating Test Point Taps (After Ref. 8.)

E. CHAPTER SUMMARY

The AN/SPS-65 proved to be a viable high-speed signal source to connect to the SRC-6E, providing convenient access to the required signals needed to conduct basic radar signal processing. However, the high impedance test points and the analog I, Q, AGC, and PRF timing reference signals could not be directly connected to the SRC-6E. The next chapter discusses the first part of the interface design which deals with the analog-to-digital conversion of the I, Q, and AGC signals.

THIS PAGE INTENTIONALLY LEFT BLANK

IV. MAXIM MAX108EVKIT 8-BIT ADC BOARD

A. INTRODUCTION

The design of the AN/SPS-65 radar allowed access to the I, Q, and AGC signals only in analog format. In order to perform any data processing and analysis of these signals on the SRC-6E, the signals first needed to be converted into the digital realm. For the purposes of this design, an 8-bit ADC would provide enough resolution to analyze and reconstruct the sampled radar data. It was also desired to sample the radar signals at 200 MHz, well over the Nyquist frequency of 60 MHz. Finally, the selected ADC needed to fit with the overall design in terms of power requirements, ease of implementation, and overall flexibility. After examining several potential ADCs, the MAXIM MAX108 was chosen for use in this project.

B. OVERALL CAPABILITIES OF THE MAX108

The MAX108 is a ± 5.0 V 8-bit flash ADC capable of performing 1.5 Gsps. It can accept either single-ended or differential inputs for both the sample clock and analog inputs and provides differential digital outputs [9]. To effectively harness the full capabilities of this high-speed ADC for testing and evaluation purposes, MAXIM provides the MAX108EVKIT, shown in Figure 6, that makes the MAX108 ready to run out of the box. The MAX108EVKIT mounts the MAX108 with a heatsink on a four layer board with an optimized layout for the MAX108. Test point connectors are provided for all required power supplies and side-launched SMA connectors are provided for connecting to the analog and sample clock inputs. For proper signal termination, the MAX108EVKIT terminates all input and output signals with precision $50 - \Omega$ termination resistors and has all the required circuitry to generate the proper termination voltages. To facilitate capturing the digital output for analysis, the MAX108EVKIT has each digital output connect to a 0.100 in 2 2-pin header to simplify the connection to a logic analyzer [10].

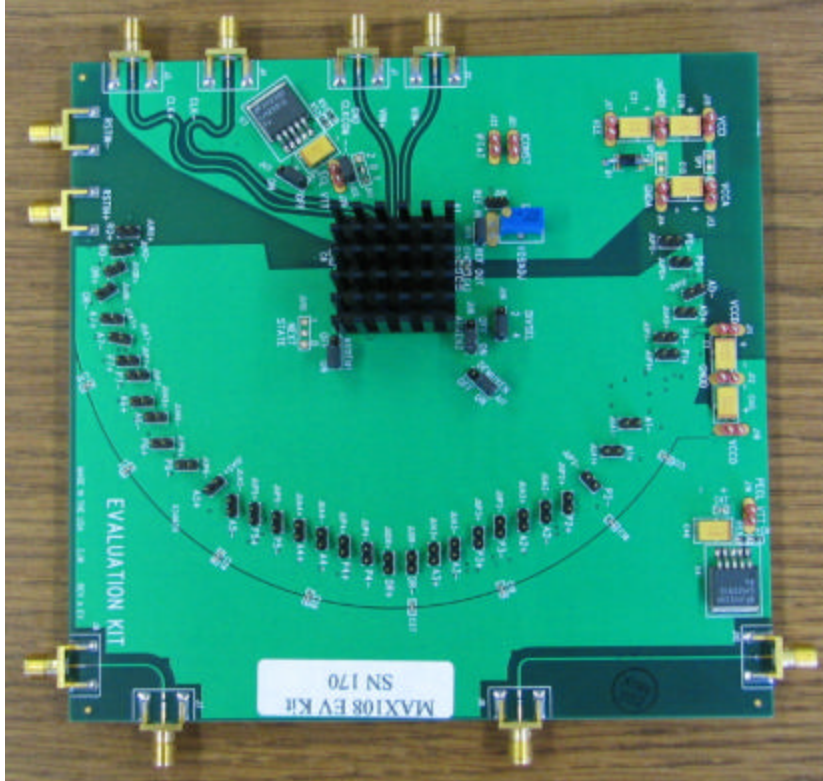


Figure 6. MAXIM MAX108EVKIT

Three MAX108s were needed to convert the analog I, Q, and AGC signals into digital form. Knowing that additional hardware needed to be developed and tested to allow the SRC-6E to interface with the converted data made the MAX108EVKIT an efficient way to fill the ADC requirement while reducing the overall technical risk of the design. The MAX108EVKITS eliminated the need for the development and testing of a custom circuit to implement the individual MAX108s, ensuring that each ADC performed at its maximum potential. Three MAX108EVKITS could be independently tested upon delivery and then connected to the additional SRC-6E interface hardware. This approach looked to simplify the overall design and allow for more time to be devoted to the testing and development of the additional hardware. Thus four MAX108EVKITS were purchased, providing one MAX108EVKIT for each channel (I, Q, and AGC) and the fourth one acting as a spare.

C. POWER REQUIREMENTS

With a maximum sample clock of 1.5 GHz with 8-bits of resolution, undesired digital crosstalk may couple through the analog input, power supply, and ground connections ultimately leading to a possible reduction in the dynamic performance of the ADC [9]. To avoid this, MAXIM provides very specific guidelines on how the MAX108 should be implemented on a printed circuit board (PCB). The MAX108EVKIT is designed with these specifications in mind and is optimized for minimizing crosstalk from developing on the board. However, the user must use separate power supplies for the analog and digital portions of the MAX108 and its accompanying logic to ensure that crosstalk does not propagate through the power supplies and into the MAX108.

To simplify the implementation and testing of the MAX108, the MAX108EVKIT reduces the number of individual power connections needed to drive the evaluation board. To power up the MAX108EVKIT requires two analog power supply connections (V_{EE} and V_{CCI}) and two digital supplies (V_{CCD} and V_{CCO}). Table 3 lists the power supply connections, their ground reference, the general circuitry each one is responsible for powering, and their current requirements. The V_{CCO} supply determines if the digital outputs are LVPECL or PECL. By setting V_{CCO} to +3.3V the digital outputs are LVPECL and by setting V_{CCO} to +5.0 V the digital outputs PECL. The power supply connections are made via several test points on the MAX108EVKIT. Figure 7 illustrates the general location of these test points on the MAX108EVKIT and demonstrates a proper power supply configuration. It is important to note that the analog and digital ground references, GNDI and GNDD, respectively, should only be tied together at the power supply. Once all the power supply connections are made power can be applied to the board to initiate its operation. [10]

Table 3. Power Supply Requirements [9]

Power Supply Connection	Ground Reference	Circuitry Driven	Current Requirements	Type
$V_{EE} = -5.0 \text{ V}$	GNDI	Analog circuits	-250 mA	Analog
$V_{CCI} = +5.0 \text{ V}$	GNDI	T/H amplifier, clock distribution, bandgap reference, reference amplifier, comparator array	600 mA	Analog
$V_{CCD} = +5.0 \text{ V}$	GNDD	All logic circuits of converter	250 mA	Digital
$V_{CCO} = +3.3 - +5.0 \text{ V}$	GNDD	Powers all PECL logic sections	600 mA	Digital

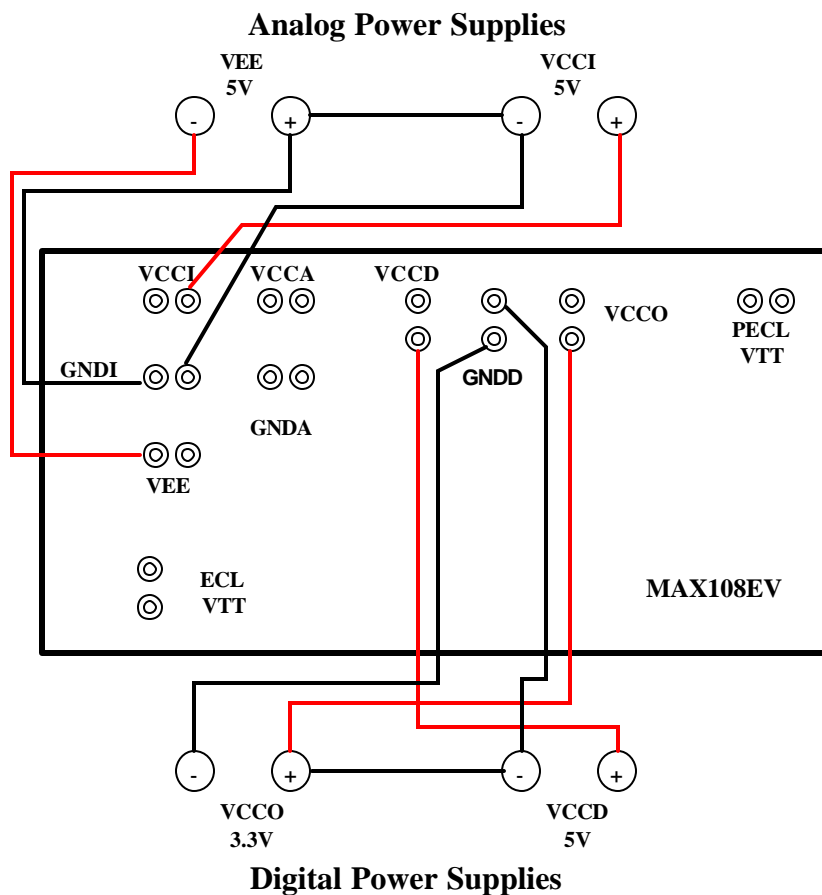


Figure 7. MAX108EVKIT Power Supply Connections

D. ANALOG AND CLOCK INPUTS

1. Sample Clock Inputs

The sample clock is brought onto the board via two SMA connectors (CLK and $\overline{\text{CLK}}$) and is distributed throughout the board via $50 - \Omega$ microstrip transmission lines. Each clock input is terminated by an on-chip $50 - \Omega$ termination resistor that is connected to a termination path designated as CLKCOM. The CLKCOM termination voltage can be connected between ground and -2.0V for compatibility with most standard ECL devices. The MAX108EVKIT provides an onboard bias generator that generates a -2.0 V termination voltage from the V_{EE} power supply for connecting the evaluation kit to ECL clock sources. In the event this onboard termination is not required, CLKCOM can be connected to ground by connecting the shorting jumper to JU2 and placing JU3 in its off position on the MAX108EVKIT. [10]

2. Analog Inputs

Two side-launched SMA connectors ($VIN+$ and $VIN-$) bring differential or single-ended analog signals onto the MAX108EVKIT. Like the clock inputs, the MAX108 provides on-chip $50 - \Omega$ termination to ground for each of the analog input lines. Sampling a differential analog input signal provides the best performance but limits the input signal amplitude to $\pm 125\text{ mV}$. When sampling a single-ended analog input, the input signal range increases to $\pm 250\text{ mV}$. To configure the MAX108EVKIT to accept a single-ended analog input, the undriven input ($VIN+$ or $VIN-$) needs to be externally reverse terminated to GNDI to ensure proper DC balance. [10]

E. DIGITAL OUTPUTS

The MAX108 produces data in offset binary format and routes it to differential LVPECL/PECL outputs. The output codes vary depending on whether the analog input is differential or single-ended [10]. Tables 4 and 5 show the input voltage values and the generated output codes for differential and single-ended inputs, respectively.

The step size for each input configuration was calculated by the following equation [11]

$$\text{Step Size} = \frac{\text{Full-Scale Voltage}}{2^{n-1}}, \quad (4.1)$$

where full-scale voltage is the maximum voltage swing of the input signal and n is the number of bits. Substituting 8 for n and 125 mV for the full-scale voltage yielded a step size of 0.976 mV for differential inputs. For the single-ended input configuration, the full scale voltage was increased to 250 mV yielding a step size of 1.95 mV. The output codes could be converted to the decimal voltage value by converting the unsigned binary output to decimal and then applying the following equation

$$\text{Signed Voltage Value} = (\text{Converted Decimal} - 128) \times \text{Step Size}. \quad (4.2)$$

This binary-to-decimal conversion process worked with either analog input configuration and was essential in testing various components of the interface design for proper operation.

Table 4. Ideal Input Voltage and Output Code Results for Single-ended Operation
(From Ref. 10.)

VIN+	VIN-	OVERRANGE BIT	OUTPUT CODE
+125 mV	-125 mV	1	11111111 (full scale)
+125 mV - 0.5LSB	-125 mV + 0.5LSB	0	11111111
0 V	0 V	0	01111111 toggles 10000000
-125 mV + 0.5LSB	+125 mV - 0.5LSB	0	00000001
-125 mV	+125 mV	0	00000000 (zero scale)

Table 5. Ideal Input Voltage and Output Code Results for Single-ended Operation
(From Ref. 10.)

VIN+	VIN-	OVERRANGE BIT	OUTPUT CODE
+250 mV	0 V	1	11111111 (full scale)
+250 mV - 1LSB	0 V	0	11111111
0 V	0 V	0	01111111 toggles 10000000
-250 mV + 1LSB	0 V	0	00000001
-250 mV	0 V	0	00000000 (zero scale)

All the PECL digital outputs are routed on equal-length $50-\Omega$ microstrip traces in an arc pattern from the MAX108 to the 2-pin headers as evident in Figure 6. This layout allowed MAXIM to keep the trace lengths to within 0.050 inches of each other greatly reducing the layout-induced skew amongst the data bits. As Figure 8 demon-

strates, the outputs are terminated to the PECL termination voltage just prior to the 2-pin headers. This places the terminators as close to the receiver as possible before leaving the board. [10]

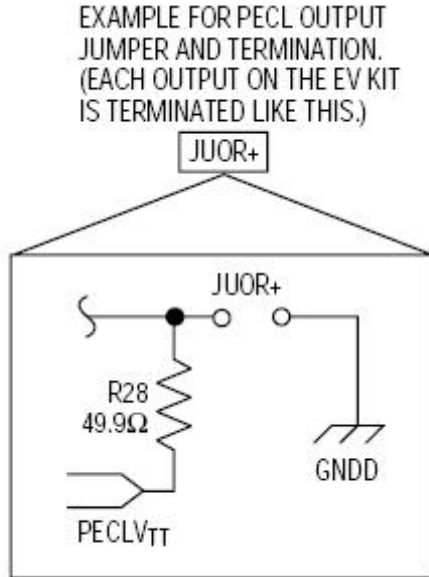


Figure 8. MAX108EVKIT Digital Output Termination (From Ref. 10.)

The value of the PECL termination voltage determines if the digital outputs are PECL or LVPECL providing connection flexibility with +3.3 V and +5.0 V devices. The LVPECL/PECL termination voltage (PECLV_{TT}) is generated from the V_{CCO} power supply. Setting V_{CCO} to +5.0 V generates a +3V PECL V_{TT} providing compatibility with standard PECL devices and setting V_{CCO} to +3.3 V generates a +1.3 V PECL V_{TT} which allows the outputs to connect to LVPECL devices. [10]

1. Demultiplexer Operation

The MAX108 has an 8-bit primary output port and an 8-bit auxiliary output port. The converted data is routed to these ports via an internal demultiplexer with three modes of operation. Table 6 lists the MAX108EVKIT jumpers and the settings required to utilize each mode.

Table 6. MAX108EVKIT Demultiplexer Jumper Settings [10]

Jumper	Mode		
	DIV1	DIV2	DIV4
DEMUXEN	OFF	ON	ON
AUXEN2	OFF	ON	ON
AUXEN1	OFF	ON	ON
DIVSELECT	OPEN	Position 2	Position 4

a. Non-Demultiplexed Mode

When the demultiplexer is in non-demultiplexed or DIV1 mode, the output is only placed on the primary output port at a maximum sample clock rate of 750 MHz. The sampled data will be repeated on the auxiliary port, but it will be delayed by one clock cycle. To save power, the auxiliary port can be shut down by connecting the jumpers AUXEN1 and AUXEN2 to ground. Figure 9 illustrates the timing relationship between the sample clock, data ready (DREADY), and the output data ports. The DREADY signal lags the sample clock by half a clock cycle. Data is loaded into the primary and auxiliary output ports on the falling edge of DREADY 7.5 clock cycles after the sample was captured. [9]

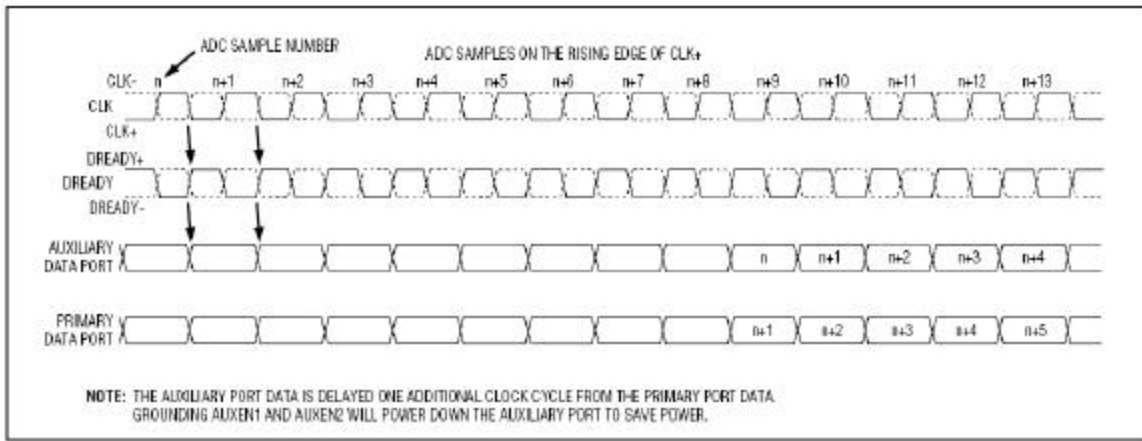


Figure 9. Non-Demuxed, DIV1 Timing Diagram (From Ref. 9.)

b. Demultiplexed Mode

The de-multiplexed or DIV2 mode reduces the output data rate to one-half the rate of the sample clock. Two consecutive samples are presented on the primary and auxiliary output ports in a dual 8-bit format. On the rising edge of the data ready clock,

the most recent sample is placed on the primary port and the previous sample is placed on the auxiliary port. The timing for this mode is illustrated in Figure 10. The most current data is placed on the primary output port and the previous sample is placed on the auxiliary port. However, the primary output is only delayed 7.5 clock cycles where the auxiliary port is delayed 8.5 clock cycles [9]. The timing diagram also clearly shows how DREADY operates at half the sample clock rate. By using the DIV2 mode to demultiplex the sampled data, the MAX108 is able to sample data at a maximum rate of 1.5 GHz.

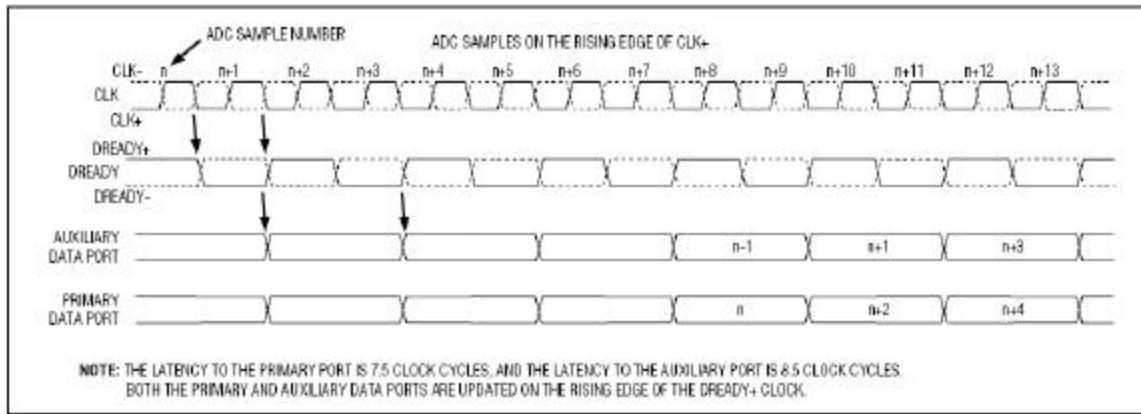


Figure 10. Demuxed, DIV2 Timing Diagram (From Ref. 9.)

c. Decimation Mode

The decimation mode or DIV4 mode is a special mode of the MAX108 primarily intended for debugging purposes. When in this mode, every other sample is discarded as data is placed on the primary and auxiliary output ports at one-fourth the sample clock rate. A sample clock of 1.5 GHz would place data into each output port at 375 MHz for an effective sampling rate of 750 MHz. Figure 11 shows how DREADY and the data output rate is reduced to one-fourth the sample clock rate. [9]

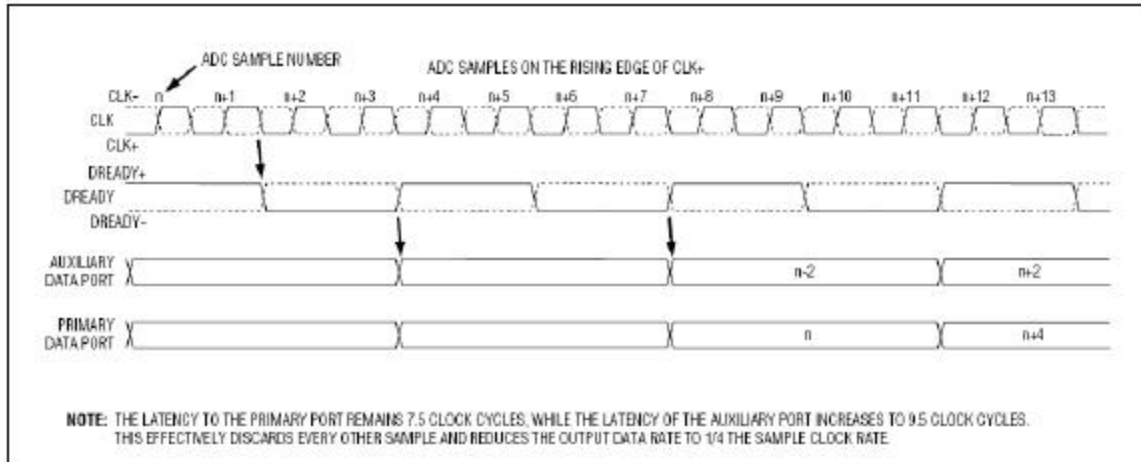


Figure 11. Decimation, DIV4 Mode Timing Diagram (From Ref. 9.)

2. Data Ready

The MAX108 produces a differential DREADY signal to indicate when the data in the primary and auxiliary ports is valid. As a digital output, its termination resistor and termination voltage are exactly the same as the primary and auxiliary output ports. Data is loaded into the primary and auxiliary output ports on the rising edge of DREADY. The DREADY signal and the data outputs are internally time aligned by the MAX108, placing the falling edge of DREADY+ in the center of the valid data window. Triggering off of the falling edge of DREADY+ in a single-ended configuration or the falling edge of DREADY in a differential configuration will yield the maximum setup and hold time for the devices receiving the data. [10]

The data ready clock comes directly from the demux clock generator that creates the appropriate clocks for the non-demultiplexed and multiplexed modes of operation using a divide by two circuit. When the MAX108 is powered up, the phase relationship between the CLK/CLK inputs and the DREADY+/DREADY– outputs is random. As a result, there is no way to tell if the DREADY clock is in phase with the sample clock or 180 degrees out of phase of the system clock as Figure 12 illustrates. When a single MAX108 is being used, the phase of DREADY is irrelevant. The most current data will be on the primary output port and the older data will be on the auxiliary port. However, when two or more MAX108 are used together to achieve higher sampling rates the order of samples between devices is critical. Therefore DREADY must be set to a known state in each MAX108 device. To provide this functionality the MAX108 has a differential

PECL reset input (RSTIN) and differential PECL reset output (RSTOUT). The MAX108EVKIT provides access to these reset pins via 2-pin headers and again handles the proper LVPECL/PECL termination. To achieve synchronization, a one is applied to the RSTIN input on the first MAX108 device. The RSTOUT pin of this device is then connected to the RSTIN of the second device. When the RSTIN signal returns to zero the phase of the DREADY clock will be reset. [9]

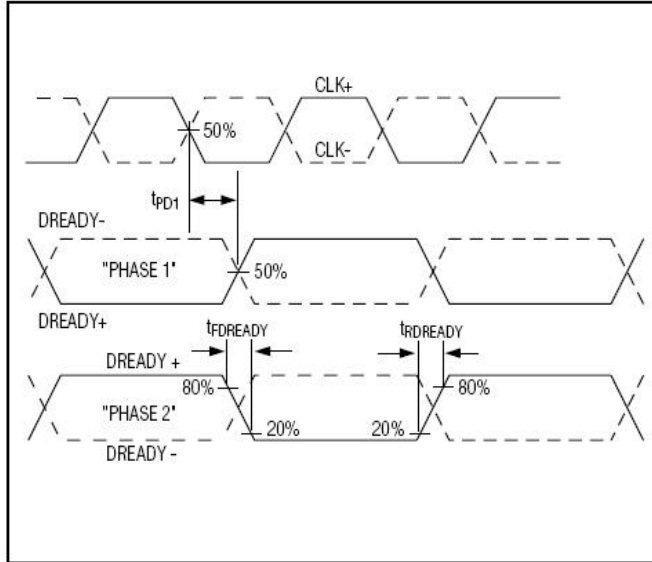


Figure 12. CLK and DREADY Timing in DIV2 mode Showing the Two Possible Phases of DREADY (From Ref. 9.)

F. DESIGN IMPLEMENTATION

1. Input Configuration

The design called for sampling the I and Q channels from the AN/SPS-65 along with its AGC voltage. Each signal was given its own MAX108EVKIT to facilitate the analog-to-digital conversion. Since the radar signals were only accessible from single-ended taps, each MAX108EVKIT was configured to accept single-ended inputs. This was accomplished by bringing the analog signal in on VIN+ and reverse terminating VIN- to GNDI via a $50 - \Omega$ terminator attached to the VIN- SMA connector.

2. Sample Clock and Demux Operation

One of the design goals was to sample the 30-MHz I and Q channels from the AN/SPS-65 using a 200-MHz sample clock generated by the SRC-6E. The MAX108 was more than capable of handling the 200-MHz clock generated by the SRC-6E. However, the SRC-6E in the SDR mode is limited to accepting data at its system bus speed of

100 MHz. To resolve this issue, the MAX108EVKITS were configured to the DIV2 mode of the MAX108 in order to reduce the sampling rate to 100 MHz by placing data on both the primary and auxiliary output ports. Once captured by the SRC–6E, the data would be recombined prior to processing.

3. Data Ready

To facilitate a source synchronous data flow into the CHAIN port, the sample clock generated by the SRC–6E to drive the MAX108s needed to follow with the data back into the SRC–6E. In addition to having the clock with the data, the SRC–6E needs a data valid bit to inform it when to latch the data on the CHAIN port. The MAX108-EVKIT does not have a clock output pin, and to complicate the issue, the 200-MHz sample clock was twice as fast as the output clock.

To implement source synchronous data flow with the MAX108EVKIT, the DREADY output from one MAX108EVKIT was used to facilitate the need of a data valid bit and serve as the source synchronous clock. Since the falling edge of DREADY+ is time aligned to be in the center of the data valid window, all three boards would be within their valid data window. Any phase delay between the outgoing sample clock generated by the SRC–6E and the data ready clock would be compensated for by the DCMs internal to the SRC–6E.

4. Termination and Power Supplies

The SRC–6E does not have onboard termination resistors, thus any signal generated or received by the CHAIN port needs to be terminated by the external hardware. With regards to the differential sample clock inputs, the MAX108EVKIT was configured to use its onboard –2.0 V bias generator and $50 - \Omega$ termination resistors properly terminate the ECL sample clock. This placed the termination for the differential sample clock as close to the receiver as possible. With regards to the digital PECL outputs, the initial design called for using the termination resistors that were provided on the MAX108-EVKIT and using the onboard generated PECL V_{TT} . In the event that distance from the 2-pin header to the chain port proved to be too great for the MAX108EVKIT termination resistors to be effective, the design could be modified to have the output termination resistors moved from the MAX108EVKIT and placed closer to the CHAIN port. The V_{CCO} voltage was set to +3.3 V to generate LVPECL outputs.

G. INITIAL TESTING AND FAMILIARIZATION

To ensure the MAX108EVKIT would function as the design implementation anticipated, one MAX108EVKIT was connected to the requisite power supplies as shown in Figure 7. The digital outputs for the primary and auxiliary ports were connected to an HP 16500B logic analyzer with the clock input connected to DREADY+. The logic analyzer was then configured to trigger on the falling edge of DREADY+ and the switching threshold was set to +2.0 V to be compatible with the LVPECL outputs.

The -2.0 V bias generator was left enabled for the clock inputs and the MAX108EVKIT was placed in DIV2 mode by setting the correct jumpers in accordance with Table 6. An HP 8082A pulse generator was used to generate a 100-MHz differential-ECL sample clock and an HP 3312A function generator was used to generate a single-ended 1-MHz, 200-mV_{PP} sine wave. With the MAX108EVKIT fully powered up and both the sample clock and sine wave running into the board, the logic analyzer captured the demultiplexed digital output and saved it to an ASCII file. The first 600 samples from this capture are listed in Appendix C and show the DIV2 functioning correctly. These demultiplexed samples were then recombined in the correct order, converted to the correct voltage value using Equation 4.2, and then plotted using the MATLAB script listed in Appendix D. The resulting plot in Figure 13 shows the reconstructed sine wave. The slight DC offset was a function of the HP 3312A being slightly out of calibration. This test, though not fully flexing the full capabilities of the MAX108EVKIT, proved the correct operation of the onboard bias generators, terminators, and correct operation of the MAX108.

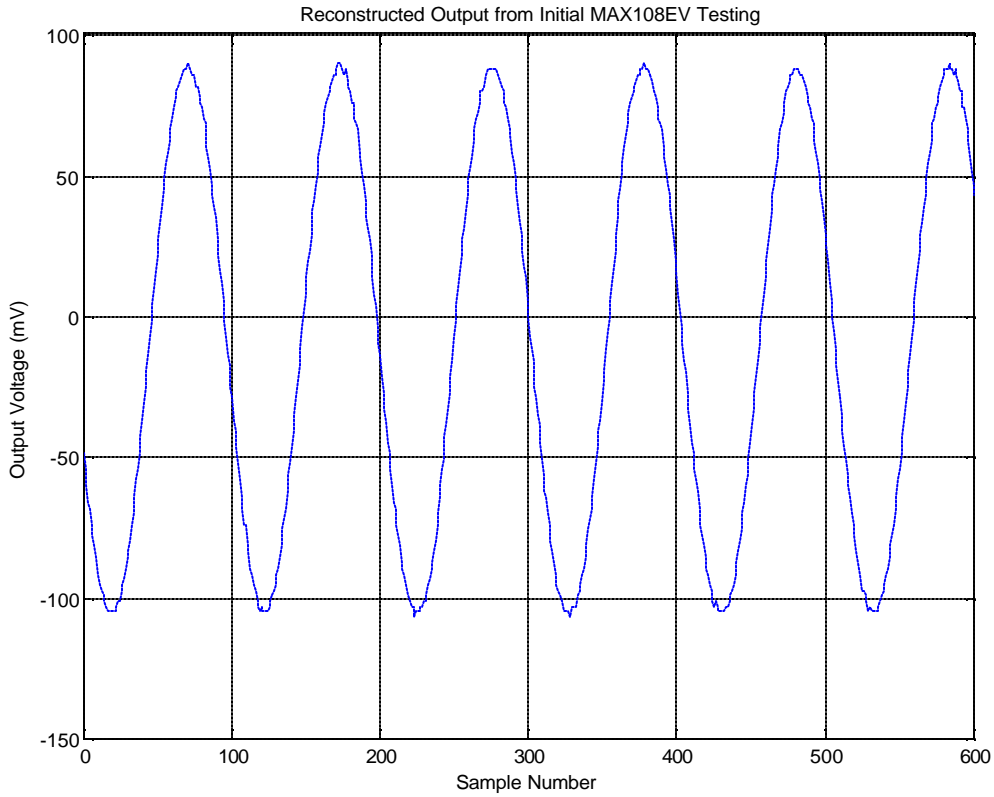


Figure 13. Reconstructed Output from MAX108EVKIT Testing

H. ADDITIONAL HARDWARE REQUIRED

Though the MAX108EVKITS made maximizing the performance of the MAX108 fairly straightforward, they were not capable of connecting directly to either the AN/SPS-65 or the SRC-6E. First, the I, Q and AGC signals could only drive a high impedance load, making the $50-\Omega$ input of the MAX108EVKIT inadequate. In addition, the ± 5.8 V maximum swing of I and Q plus the 0–12 V range of the AGC voltage were well above the ± 250 -mV input range of the MAX108. Therefore to get the input signals to the MAX108EVKITS, an analog board needed to be developed to provide the high impedance needed for the input signals while simultaneously attenuating the three signals to within the ± 250 mV range.

Next, to be able to get the data from the differential LVPECL outputs into the SRC-6E, the outputs needed to be translated to single-ended LVTTL. In addition to translating the signals, a method for connecting the MAX108EVKIT 2-pin headers to the

MICTOR connector used by the SRC-6E CHAIN port needed to be developed. Finally, the LVTTL sample clock generated by the SRC-6E needed to be translated to ECL and driven properly to the three MAX108EVKITS.

I. CHAPTER SUMMARY

The MAX108EVKITS provided an efficient and effective way to implement the required analog-to-digital converters for the design. However, as the previous section discussed, additional hardware was required to complete the interface between the AN/SPS-65 and the SRC-6E. The next two chapters discuss the design, development, and testing of these additional hardware interfaces.

THIS PAGE INTENTIONALLY LEFT BLANK

V. ANALOG PCB DESIGN

A. INTRODUCTION

The I, Q, and AGC signals from the AN/SPS-65 were well outside the maximum analog input voltage swing allowed by the MAX108. They also needed to be connected to a high impedance load whereas the analog inputs of the MAX108EVKITS only offered a $50-\Omega$ load. Therefore, all three signals needed to be buffered and attenuated prior to being routed to their respective MAX108EVKITS for analog-to-digital conversion. In addition to having to attenuate the I, Q, and AGC channels, the PRF timing reference signal needed to be amplified to LVTTL before being sent to the SRC-6E. To help contain the design to as few boards as possible and reduce the number of power supply connections, it was decided to perform the attenuation, buffering, and amplification on one single board.

B. ATTENUATION DESIGN OPTIONS

1. Inline RF Attenuator and Buffer

The first option pursued to attenuate the I, Q, and AGC signals was to run the signals through a buffer and through an RF attenuator. This method appeared to be the simplest to implement and would provide the best overall frequency response. To see if this was a feasible option, the attenuation level required to reduce the AGC voltage from its range of 0 to 12V was calculated using

$$\text{Attenuation level [dB]} = 20\log\left(\frac{V_{in}}{V_{out}}\right). \quad (5.1)$$

Substituting 12 V for V_{in} and 0.250 V for V_{out} yielded an attenuation level of 33.62 dB. A 30-dB RF attenuator in series with 6 dB attenuator would efficiently attenuate the signal to 190 mV which was well within the ± 250 mV input range of the MAX108.

Due to the large difference between the input and output voltages, the power dissipated was also examined using

$$P = \frac{(V_{in} - V_{out})^2}{R}. \quad (5.2)$$

This yielded 2.76 W in dissipated power which exceeded most RF attenuator power ratings of 1.0 W. RF attenuators that could handle 3.0 W of power were extremely cost prohibitive. Due to this substantial cost and the desire to implement the same attenuation scheme on the I, Q, and AGC signals, the RF attenuator option was deemed unacceptable for this design.

2. Op–Amp Attenuation Circuit

The next attenuation design considered was to again run the signals into a high-speed buffer and then into a high-speed op–amp circuit with a gain less than one. The buffer would provide the required high input impedance while the fractional gain would attenuate the signal to the appropriate level and drive the low load impedance. Again, the design goal was to use the same overall circuit design for the I, Q, and AGC signals.

Though the signal bandwidth of I and Q was 30.13 MHz, the attenuation circuit was designed to have at least 200 MHz of analog signal bandwidth for the possibility of interfacing with radars other than the AN/SPS–65. In addition, the minimum slew rate (S) required to drive the ± 250 –mV outputs at 200 MHz was determined from [11]

$$S = 2p f_{SR} V_o. \quad (5.3)$$

Substituting 200 MHz for the slew rate limiting frequency (f_{SR}) and 250 mV for the maximum output voltage (V_o) yielded a minimum slew rate of 315 V/ μ s.

The gain required for the I and Q channels was -0.043 and the gain required for the AGC voltage was -0.021 . The power supply rails needed to be greater than 7.8 V and greater than 14 V for the AGC voltage to avoid saturation for the I and Q channels. Several high-speed op–amps could provide the needed slew rate and analog bandwidth. However, no high-speed op–amp could be found to drive a negative gain of less than one and at the same time drive a $50 - \Omega$ load with power rails in excess of ± 5.8 V. To be able to use the commercially available high-speed op–amps, the I, Q, and AGC signals needed to be attenuated prior to being buffered.

3. Voltage Divider to High-Speed Buffer

To achieve high input impedance attenuation, each signal was routed through a simple two-resistor voltage divider prior to entering a high-speed buffer. Figure 14 illustrates the general voltage divider and buffer circuit implemented in the design.

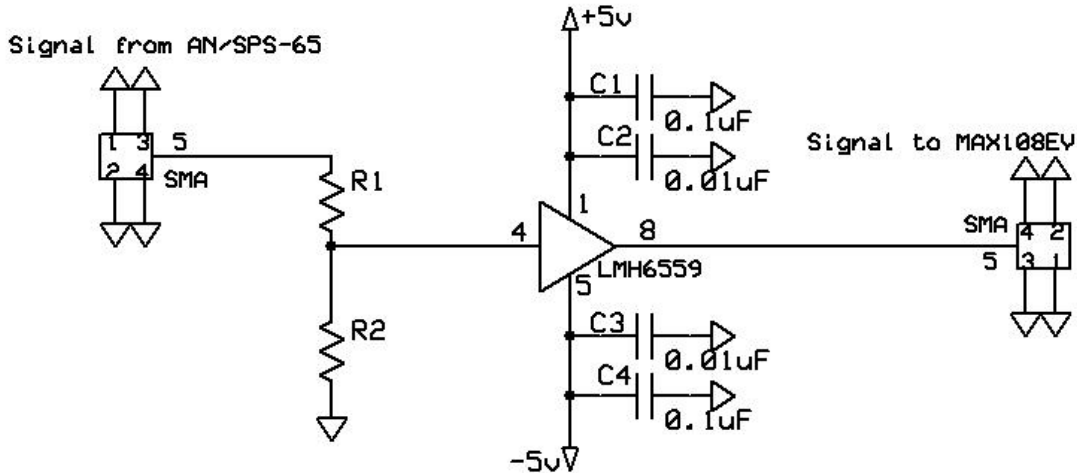


Figure 14. Two-Resistor Voltage Divider and Buffer Circuit

The resistor $R1$ was set to $10\text{ k}\Omega$ to provide the requisite high input impedance for the AN/SPS-65 signals. As an added measure of safety, the I, Q, and AGC signals were attenuated to $\pm 225\text{ mV}$ to ensure that the analog inputs of the MAX108 were not overdriven. The resistor $R2$ was then calculated to provide the appropriate attenuation for the I, Q, and AGC signals using

$$R2 = \frac{V_{out} R1}{V_{in} - V_{out}}. \quad (5.4)$$

Table 7 lists the calculated and selected $R2$ resistors values for the I, Q, and AGC voltage dividers.

Table 7. Resistor Values for Voltage Divider

Signal	V_{in} (V)	V_{out} (V)	Selected $R1$ Value (k Ω)	Calculated $R2$ Value (Ω)	Selected Standard $R2$ Value (Ω)
I	± 5.8	0.225	10.0	403.59	402.0
Q	± 5.8	0.225	10.0	403.59	402.0
AGC	12.0	0.225	10.0	191.08	191.0

With the I, Q, and AGC voltage signals attenuated to ± 225 mV, an appropriate buffer needed to be selected to drive the $50 - \Omega$ analog inputs of the MAX108EVKITS. The power rails for this high-speed buffer were set to ± 5 V in an effort to reduce the number of power supplies employed in the overall interface design. Since a positive and negative power rail was required to handle the voltage swing of the analog signals, the analog board could easily connect to the ± 5 V supplies already needed to power the three MAX108EVKITS.

The LMH6559 high-speed closed loop buffer was the only buffer at the time of design that could meet the analog signal bandwidth, slew rate, and power supply requirements. The LMH6559 offered a small-signal bandwidth of 1750 MHz, a 4580 V/ μ s slew rate, and could be powered by ± 5 V. It also had a $200 - k\Omega$ input impedance and a $1.2 - \Omega$ output impedance, making it ideal for driving the analog inputs of the MAX108EVKITS. [12]

To verify that the buffer would perform as expected driving a $50 - \Omega$ load, the LMH6559 performance was simulated using Silvaco® SmartSpice®. The LMH6559 spice model was downloaded from the National Semiconductor website and implemented in the SPICE deck shown in Appendix E. The source signal was a 0.225-V AC signal that was swept from 0 to 500 MHz. To simulate driving the MAX108EVKIT analog inputs, the output of the LMH6559 was connected to a $50 - \Omega$ resistor to ground. The results of the simulated AC sweep are shown in Figure 15.

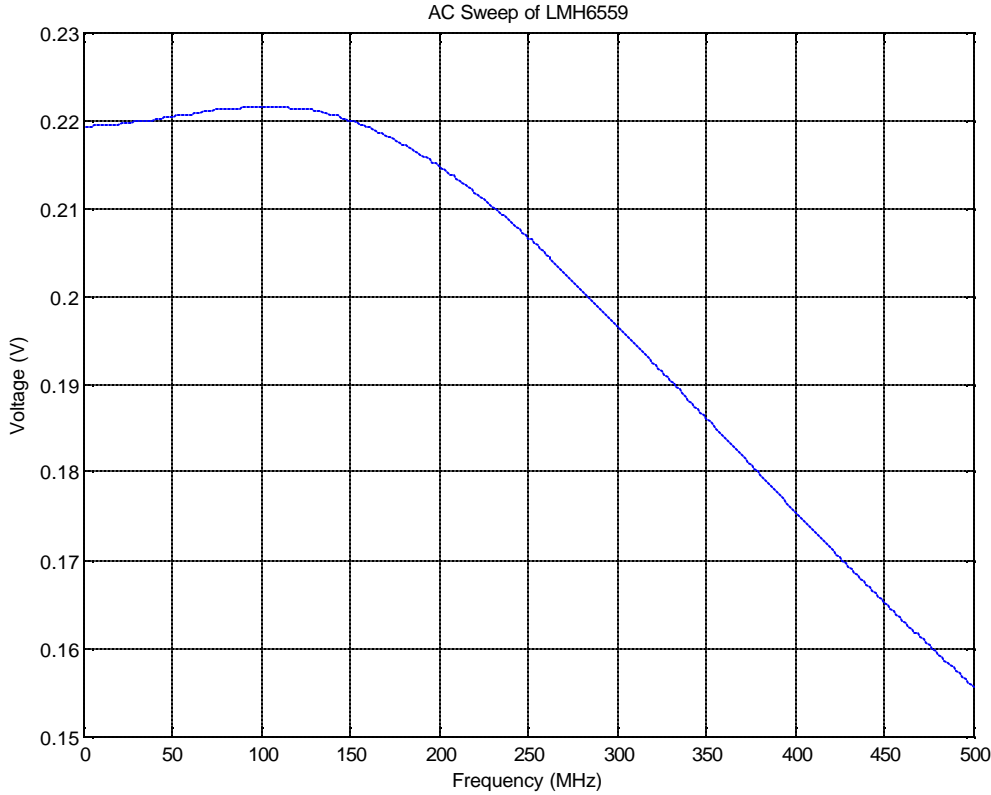


Figure 15. AC Sweep Analysis of the LMH6559

The results depicted in Figure 15 show the frequency response degrading linearly as the frequency exceeds 150 MHz. Since 150 MHz was still well above the 30.13 MHz bandwidth of the AN/SPS-65, it was determined that the LMH6559 would provide the desired performance. In addition, the accuracy of the model with a small load resistance was questioned since the LMH6559 has a 1750-MHz small-signal bandwidth and gain flatness up to 200 MHz when the output voltage is less than 0.5 V_{pp}. Therefore, the design went forward with using the LMH6559 high-speed buffer. [12]

C. PRF TIMING REFERENCE AMPLIFICATION DESIGN

At the time of the analog board design, the PRF timing reference signal was thought to be a square pulse signal that ranged from 0 to 1.0 V. To amplify the 1.0 V signal to the 3.3 V level of LVTTL, a non-inverting op-amp with a gain of 3.3 was used. Once amplified to LVTTL, the PRF timing reference signal only required source-series

termination prior to connecting to the SRC-6E. Therefore, the design placed a $50\text{-}\Omega$ resistor in series with the output of the amplifier circuit to properly terminate the signal. Figure 16 shows the PRF timing reference amplification circuit implemented in the design.

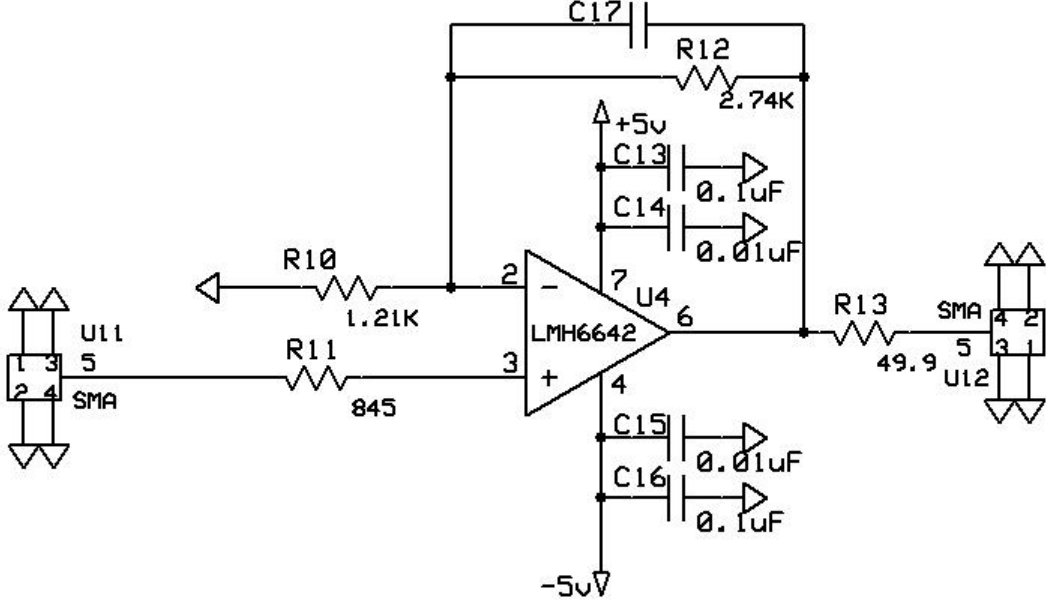


Figure 16. PRF Timing Reference LVTTL Amplification Circuit

The design of the attenuation and buffering circuit for the I, Q, and AGC signals set the power rails to ± 5 V and most op-amps operating with these power supplies could handle the 3063-Hz analog bandwidth of the PRF timing reference signal. The deciding factor for the op-amp to place in this circuit was its ability to source 66 mA continuously over the source-series termination resistor. The LMH6642 operational amplifier selected for the design provided rail-to-rail performance capable of driving 75 mA to the load. It also provided analog signal bandwidth of 15 MHz with a gain of +5 making it capable of interfacing to radars with much higher PRFs [13].

Using

$$A_V = 1 + \frac{R_{12}}{R_1}, \quad (5.5)$$

standard resistor values were selected to provide a nominal gain of 3.3 (A_V). With R_{12} set to $2.74\text{ k}\Omega$ and R_{10} set to $1.21\text{ k}\Omega$, the circuit produced a gain of 3.26 which was

adequate enough for the LVTTL requirements of the SRC-6E. The resistor R11 was placed to ensure proper DC biasing. Its value was determined by calculating the equivalent parallel resistance of R12 and R10. The capacitor C17 was inserted as a place holder in the event the circuit needed to be stabilized [13].

The circuit was simulated in SmartSpice using the SPICE deck in Appendix F. A 1.0-V 3063-Hz signal representing the PRF timing reference was connected to the input of the circuit and the output was connected to a $50 - \Omega$ resistor to ground to represent the source-series termination resistor. Figure 17 plots both the simulated PRF timing reference signal and the resulting output waveform illustrating the correct operation of the circuit.

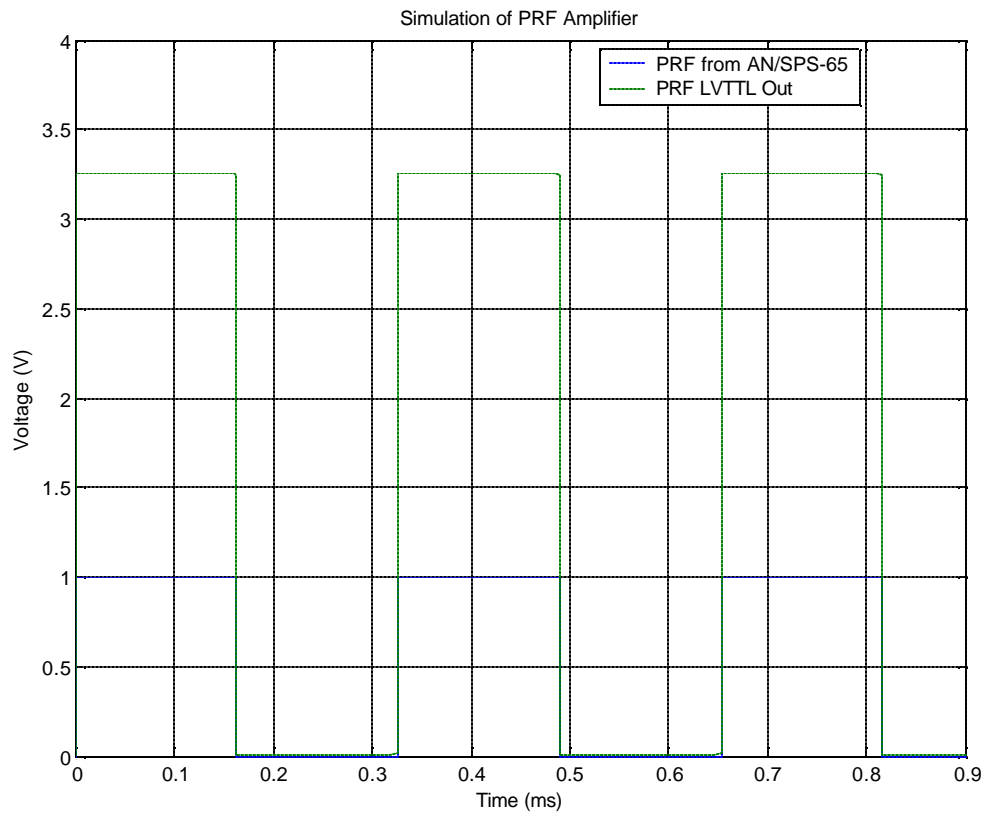


Figure 17. Simulation of PRF Timing Reference Amplifier Circuit

D. PCB DESIGN AND LAYOUT

Initially, the design sought to assemble all the necessary components for any custom built hardware by wire-wrapping them to a protoboard. This would allow for rapid assembly and allow the design to be easily modified to rectify design errors. However, the components selected for the analog board and the translation board discussed in the following chapter only came in surface-mount packages. The number of test sockets required for the design became cost prohibitive and the parasitic capacitance that the test sockets would have induced could have degraded the quality of the high-speed data signals being analyzed. Ultimately, the MICTOR connector used to connect the radar interface to the SRC-6E made wire-wrapping impossible, driving the design to use printed circuit boards.

1. PCB Software Selection

The circuit boards needed for the design were not extremely complex, requiring power and ground planes with all signal traces running along the surface. Several evaluation or free versions of PCB software were examined to see if they would meet the needs of the design. However, most were limited to a maximum size of 3" by 5", supported no more than 30 components and allowed no more than two layers. The exception to these limitations was the software available from ExpressPCB™. The ExpressPCB free software, downloadable from www.expresspcb.com, offered a schematic editor that was linkable to their printed circuit board CAD drawing tool. The CAD program allowed two and four layer boards up to 12" by 14" in size. There was no limitation on the number of components implemented and the manufacturing specifications listed in Appendix G were adequate to facilitate the components implemented in the design [14]. The only tradeoff to using the software from ExpressPCB was that the printed circuit boards had to be manufactured through them. The cost to fabricate a board through ExpressPCB was comparable to other PCB fabrication houses. Thus, it was decided to use ExpressPCB to design and fabricate the required PCBs for the interface design.

2. Analog Board Schematic Layout

Using the ExpressSCH schematic editor from ExpressPCB, the circuits in Figure 14 and Figure 16 were drawn. In accordance with the application notes for the LMH6643 and LMH6659, both power supply rails were connected to two bypass capacitors. The

capacitors used were a $0.01 \mu\text{F}$ and a $0.1 \mu\text{F}$ with the $0.01 \mu\text{F}$ being placed closest to the device. The input and output of each circuit along with the +5 V and -5V supplies were connected to $50 - \Omega$ SMA connectors to provide clean and flexible connections. A separate SMA connector wired to ground was also provided to provide an accessible test point to connect probe ground leads. Figure 18 shows the complete analog board schematic.

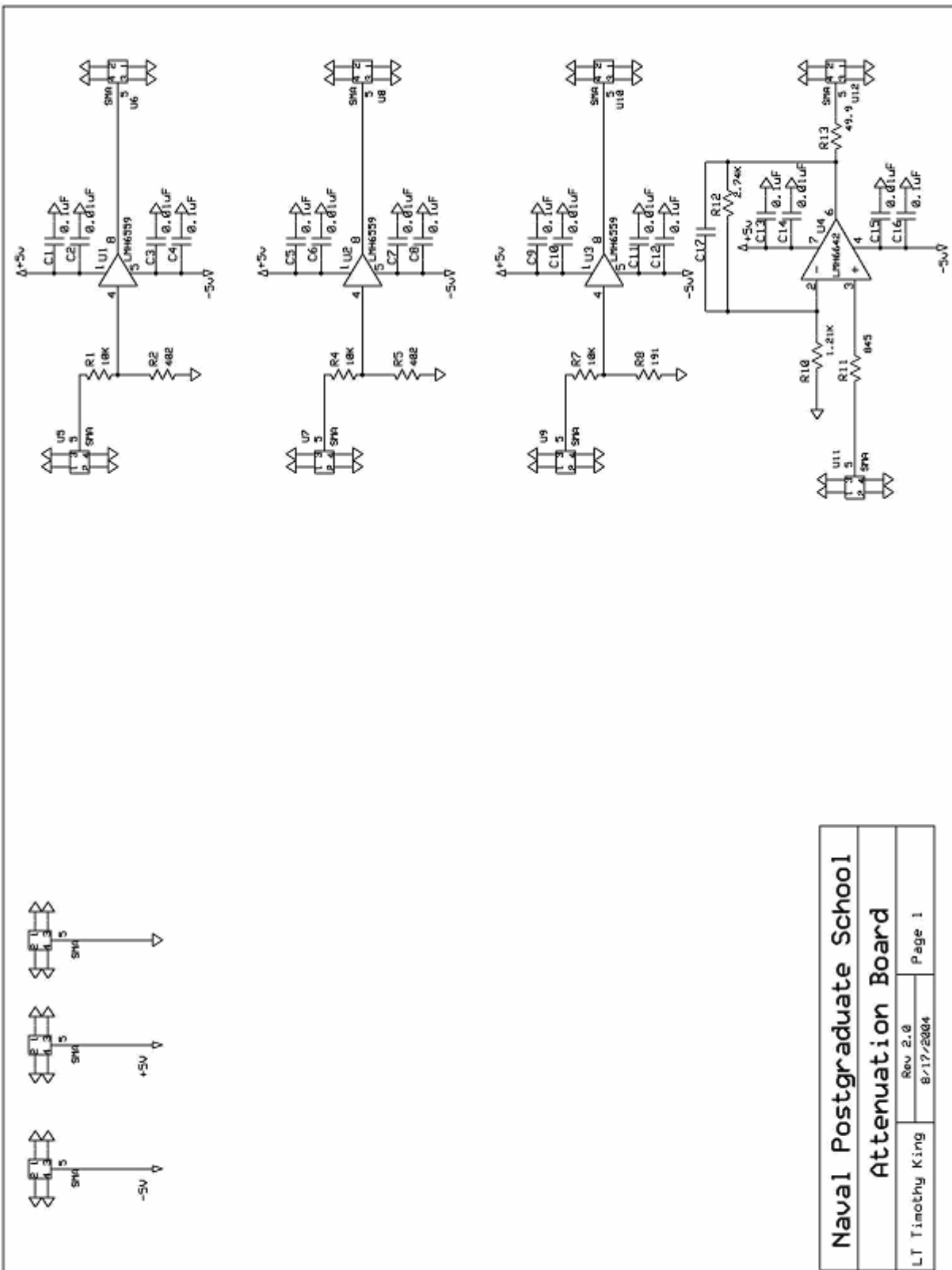


Figure 18. Complete Analog Board Schematic

3. Analog Board PCB Design

The analog board was implemented on a four-layer board for two reasons. First, since the ground plane and one power plane would be placed on the two inner layers, the top surface layer would be free to route the input, output, and feedback signals. Second, the four-layer board offered trace widths with impedances of about $50\ \Omega$.

Both the MAX108EVKITS and SRC-6E CHAIN port interface require $50-\Omega$ termination and $50-\Omega$ transmission lines, therefore it was extremely important for the PCBs used in the interface design to implement traces as close to $50\ \Omega$ as possible. Prior to conducting any component and trace placement, the impedances of various trace widths for four layer boards from ExpressPCB were calculated using [15]

$$Z_o = \frac{87 \ln \left[\frac{5.98d}{(0.8w+t)} \right]}{\sqrt{\epsilon_r + 1.41}}. \quad (5.6)$$

In Equation 5.6, d represents the distance to the ground plane, w represents the trace width, t is the trace thickness, and ϵ_r is the dielectric constant of the material used in the circuit board. From Appendix G, d was determined to be $0.012"$, t was $0.014"$, and ϵ_r was 4.6 ± 0.02 . These values were substituted into Equation 5.6 and solved for various trace widths. Table 8 lists the trace widths and their corresponding impedances.

Table 8. Trace Impedance Calculation Results

Trace Width (Mils)	Z _o Impedance (Ohms)
7	82.6
8	78.8
10	72.1
12	66.6
15	59.6
20	50.28
25	42.9
30	36.9

After calculating the trace impedances, the analog board schematic was linked to the ExpressPCB CAD software. All traces were implemented with a 20-mil trace to maintain a $50-\Omega$ trace impedance. Care was taken to place the circuits as close as possible to minimize the overall board size. Any vias needed to connect a device to power or ground were placed within the surface pad of the device. For ease of soldering purposes, the smallest resistor and capacitor deemed usable in the design was surface mount (SMT) size 0805. When placing resistors, care was taken to ensure the appropriate sized resistor was used that could handle the power dissipated across it. Table 9 lists the surface mount sizes, their power handling capability, and their physical dimensions. For the analog board, all but the source-series termination resistor on the output of the PRF timing reference amplifier was a size 0805 SMT resistor. Because the termination resistor would be required to dissipate 217 mW of power, it was implemented with a 1210 SMT resistor capable of handling 250 mW of power. To route power through the board, the power plane was set to carry the +5 V and the -5 V supply was routed to the devices through a 60 mil trace along the bottom layer. Figure 19 shows the complete PCB CAD drawing of the analog board.

Table 9. Resistor Size and Power Handling Comparison

Size Code	Power Rating (W)	L (mm)	W (mm)	L (mils)	W(mils)
0201	1/20	0.60	0.30	23.62	11.81
0402	1/16	1.00	0.50	39.37	19.69
0603	1/16	1.60	0.80	62.99	31.50
0805	1/10	2.00	1.25	78.74	49.21
1206	1/8	3.20	1.60	125.98	62.99
1210	1/4	3.20	2.50	125.98	98.43
2010	1/2	5.00	2.50	196.85	98.43
2512	1	6.40	3.20	251.97	125.98

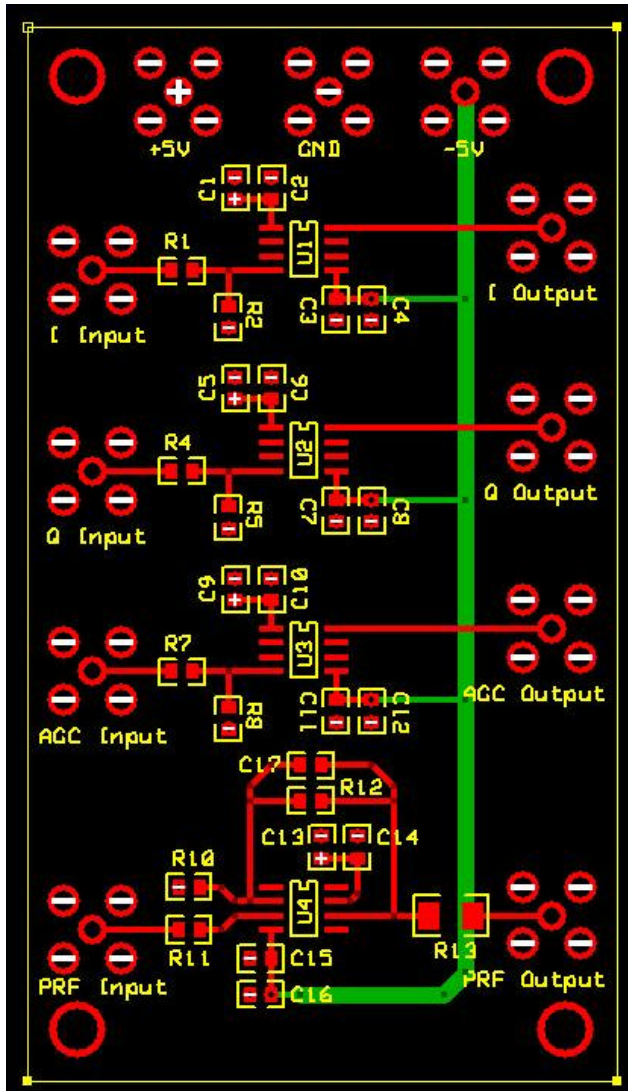


Figure 19. PCB CAD Drawing for Analog Board

E. TESTING

Prior to assembling the board, all traces were tested with an ohm meter to ensure trace continuity and to test for possible shorts on the board. After all traces and power planes appeared error free, the components were soldered to the board. Once assembled, power was applied to the board to verify that no shorts were present between the power and ground connections. Figure 20 shows the fully assembled analog board.

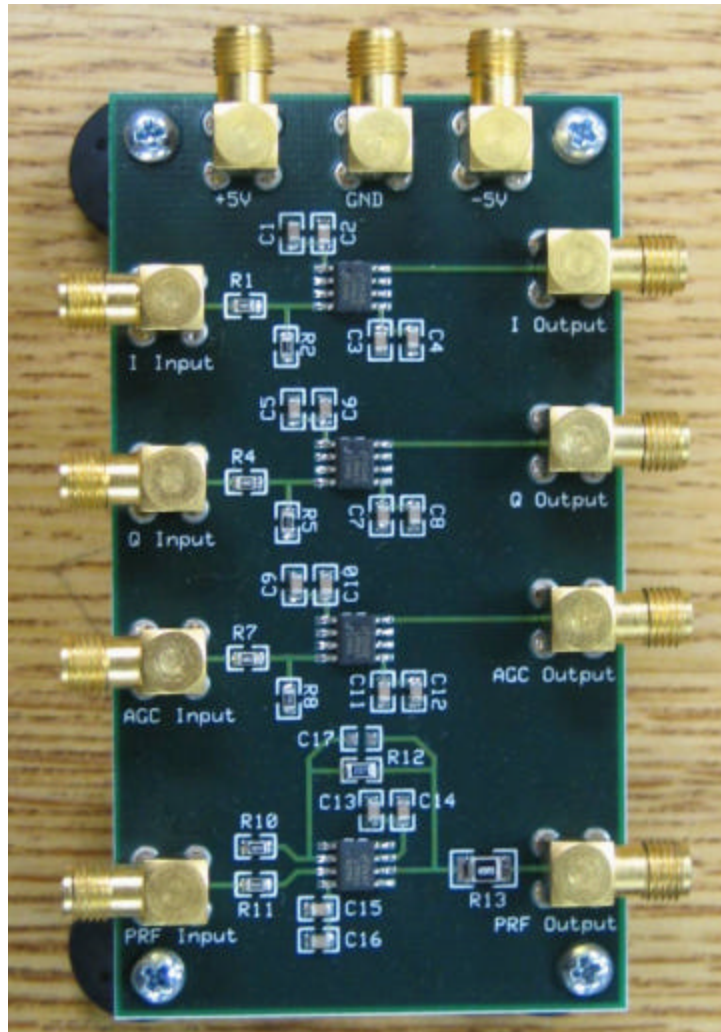


Figure 20. Assembled Analog Board

1. I and Q Channel Testing

With the power-up test complete, each channel of the board was tested independently. The I and Q channels from the AN/SPS-65 were connected to the appropriate inputs on the analog board and the attenuated outputs were connected to a digital oscilloscope. The outputs of the I, Q, and AGC buffers would normally drive $50 - \Omega$ termination resistors on the MAX108. Therefore, the oscilloscope input impedance was set to 50Ω to simulate this load. To generate sizable signals for I and Q, the AN/SPS-65 was pointed directly across the Monterey Bay to face the Santa Cruz Mountains. Channel 1 of the oscilloscope monitored the actual signal that the AN/SPS-65 was sending to the analog board and Channel 2 displayed the attenuated output. For the I and Q channels, the input was designed to be reduced by a ratio of 1:25.88. Figures 21 and 22 illustrate

the proper attenuation of the I and Q channels, respectively. The maximum voltage peak on the input for both channels was 250 mV which was correctly attenuated to 10 mV on both circuits. In addition, Figures 21 and 22 illustrate that the I and Q circuits have the needed frequency response as the output data tracks the input data exactly.

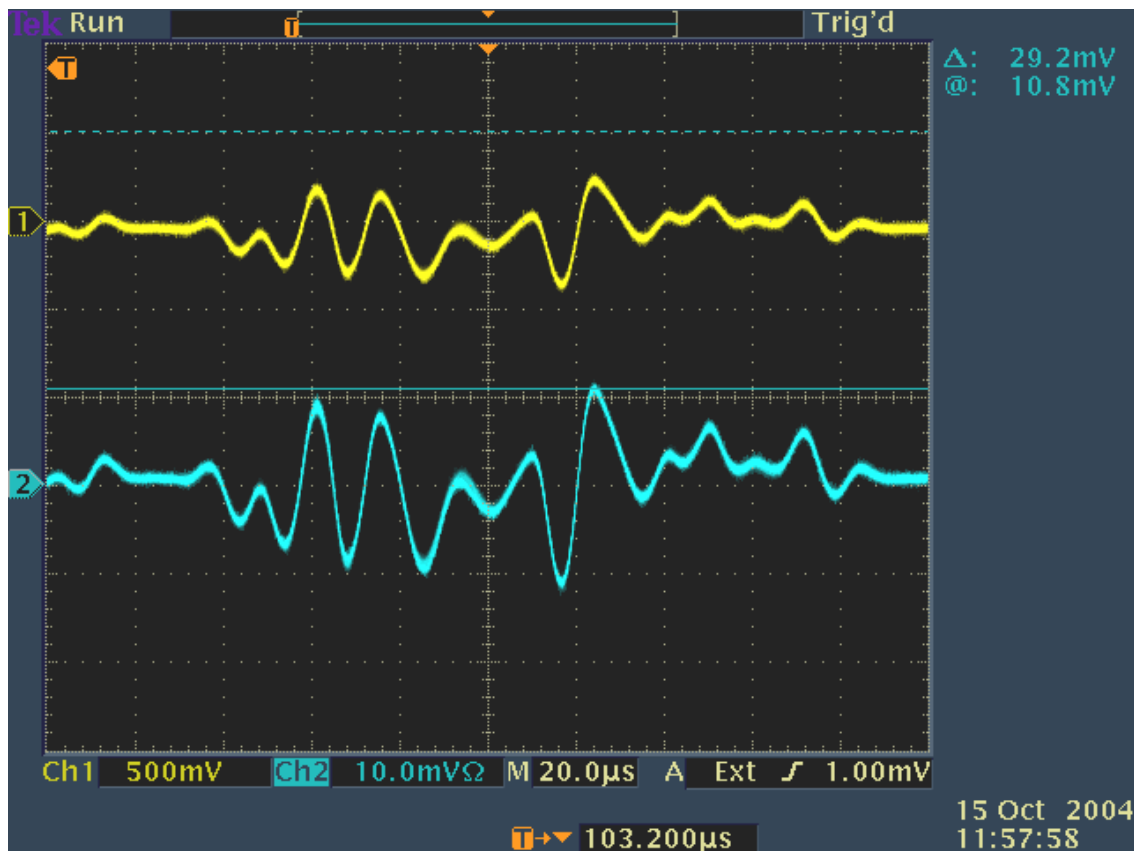


Figure 21. Test of I Channel Attenuation Circuit

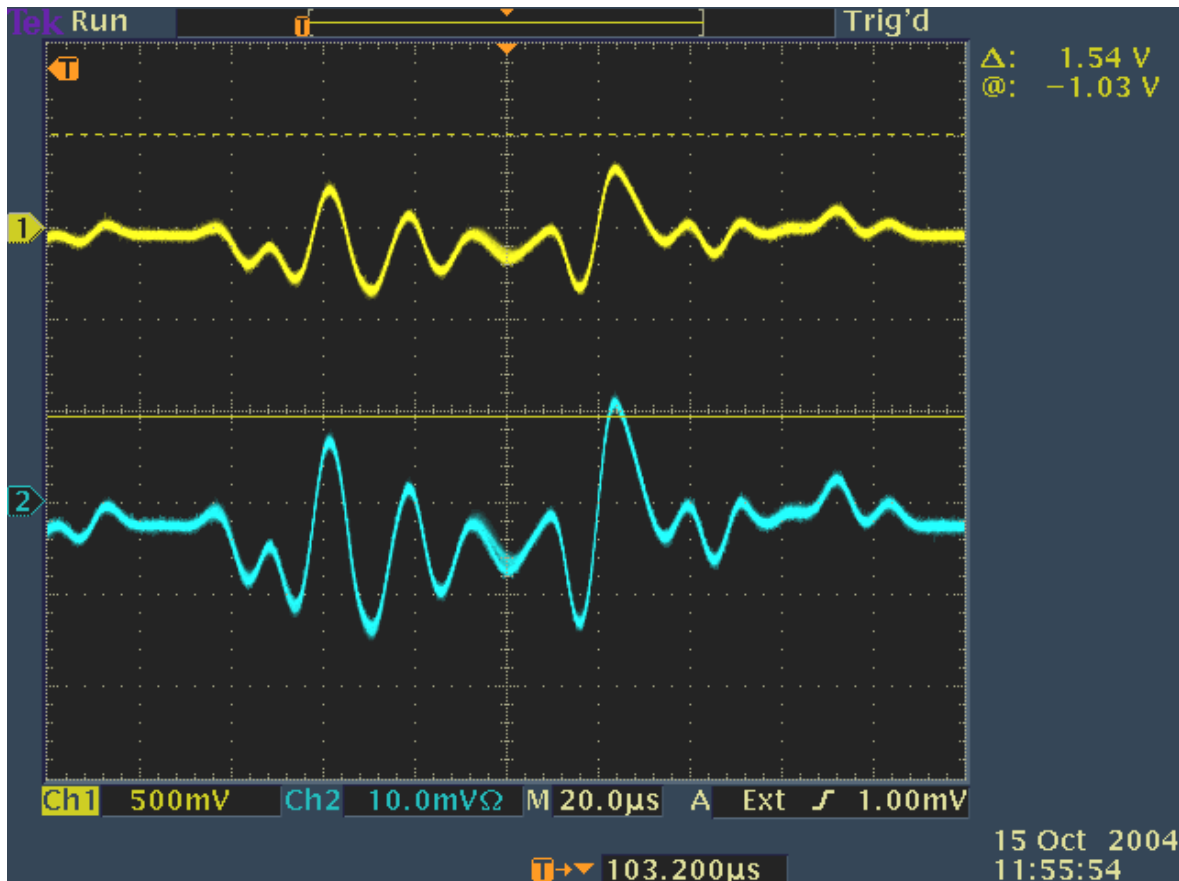


Figure 22. Test of Q Channel Attenuation Circuit

2. AGC Voltage Testing

The AGC voltage on the AN/SPS-65 used by the Naval Postgraduate School is set a fixed value of 10.0 V. It was connected to the appropriate input on the analog board and the oscilloscope input impedance remained set at 50Ω to simulate the termination resistor on the MAX108. Figure 23 shows the AGC voltage was correctly scaled by a ratio of 1:55.36 from 10 V down to 186 mV.

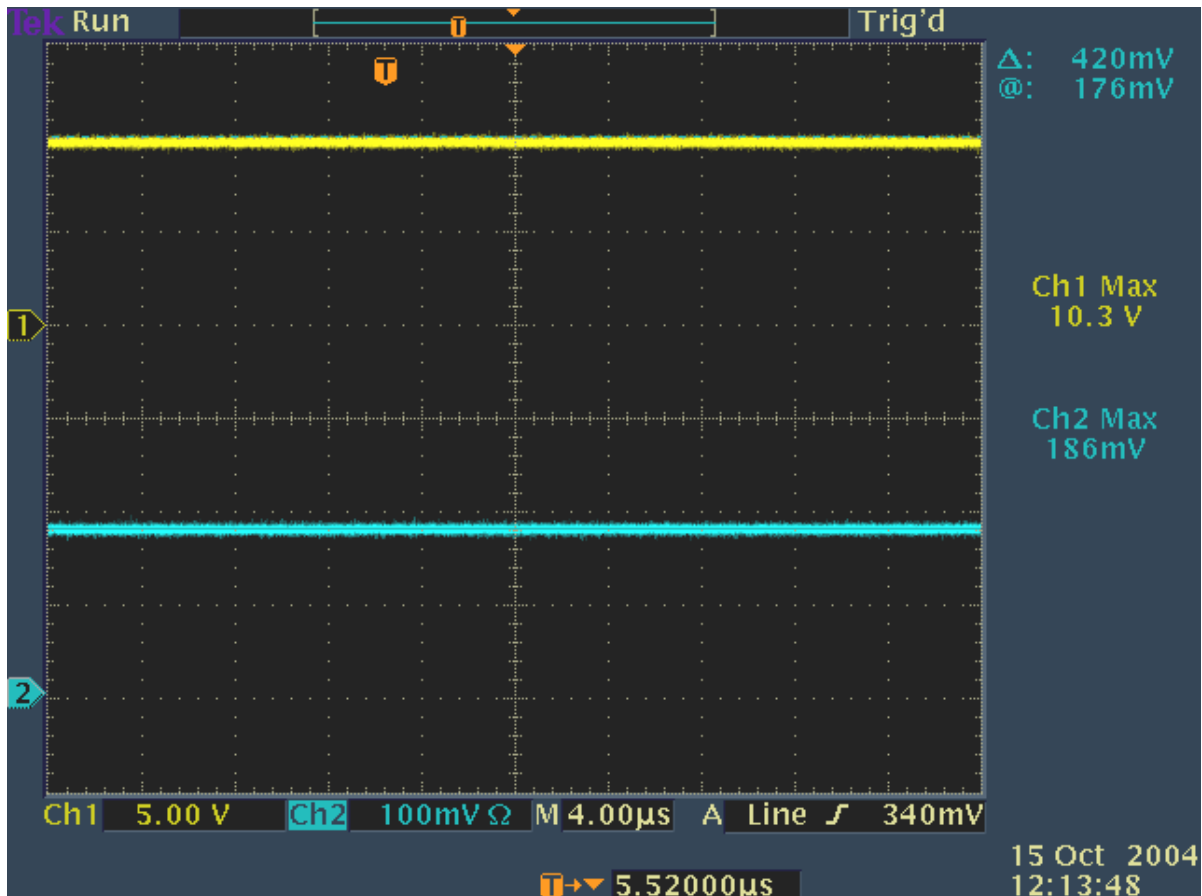


Figure 23. Test of AGC Voltage Attenuation Circuit

3. PRF Timing Reference Testing

The PRF timing reference signal testing was conducted in the same manner as the previous three signals except the oscilloscope input impedance was set to $1\text{ M}\Omega$. This was necessary because the output of the PRF timing reference amplifier was already connected to a $50 - \Omega$ load. As Figure 24 illustrates, the PRF timing reference was amplified by a factor of 3.3. However, the amplified PRF timing reference output was 3.56 V instead of 3.26 V as designed. This was a result of the PRF timing reference signal actually having a maximum value of 1.1 V instead of the 1.0 V the design anticipated. Not wanting to overdrive the LVTTL logic in the SRC-6E, the amplifier was modified to reduce the overall gain from 3.26 to 2.9. This was accomplished by replacing the $2.74 - \text{k}\Omega$ feedback resistor with a $2.3 - \text{k}\Omega$ feedback resistor. With a gain of 2.9, the resulting amplified PRF timing reference signal was 3.19 V, which is still a valid LVTTL signal.

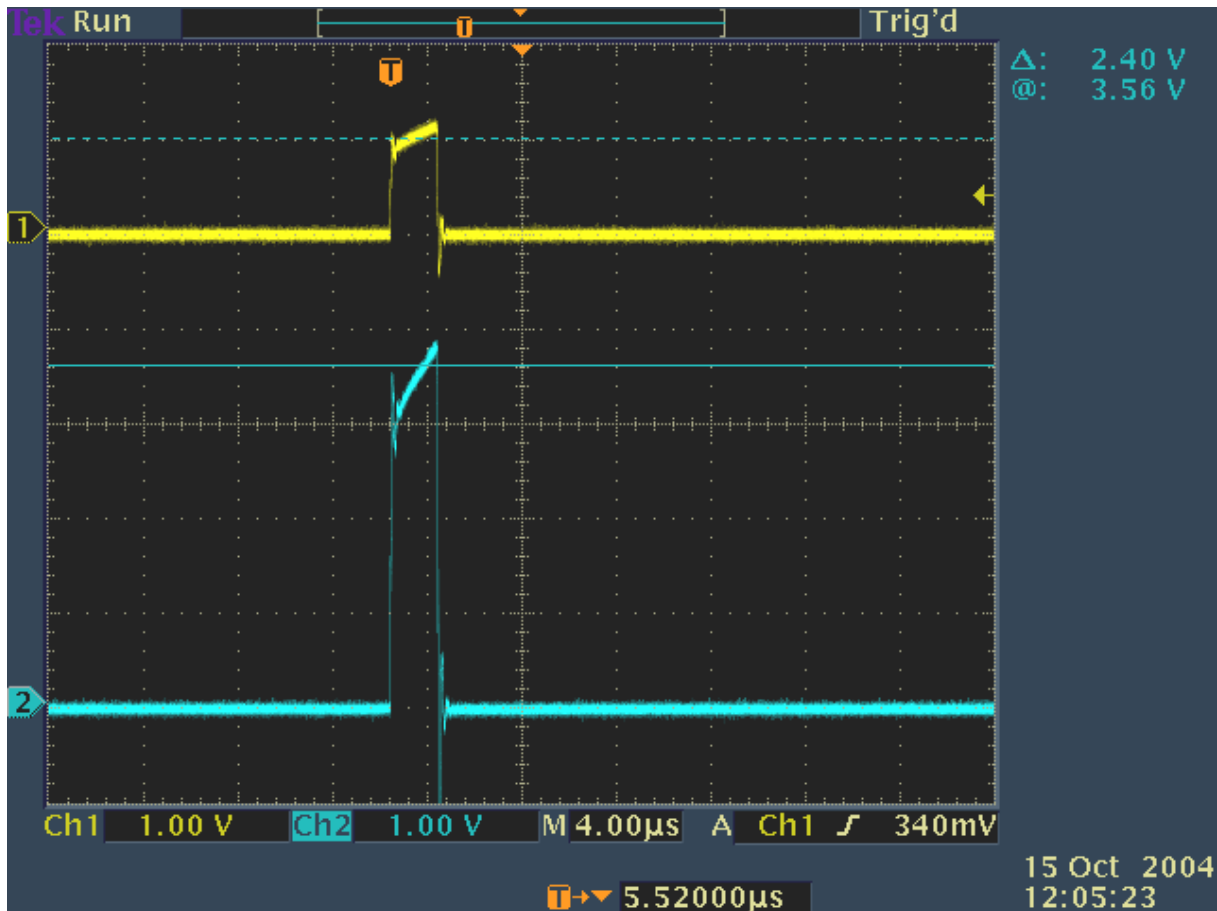


Figure 24. Test of PRF Timing Reference Amplification Circuit

F. CHAPTER SUMMARY

The analog board facilitated the connection of the AN/SPS-65 to the MAX108-EVKITs by attenuating the signals to within the $\pm 250\text{-mV}$ analog input range of the MAX108. The board also buffered the signals appropriately so they could drive the $50\text{-}\Omega$ inputs of the MAX108s. The PRF timing reference signal was also amplified and source terminated so it could connect directly to the SRC-6E. The design now needed a way to connect all the data outputs from the three MAX108EVKITs and the amplified PRF timing reference to the SRC-6E. The design also needed a method to distribute the sample clock generated by the SRC-6E to the MAX108EVKITs. The next chapter details the design, development, and testing of this last piece of hardware required to complete the interface design.

VI. TRANSLATION BOARD DESIGN

A. INTRODUCTION

The MAX108EVKITS converted the analog I, Q, and AGC voltage signals into digital form and presented the data using LVPECL logic levels onto 2–pin headers. For the SRC–6E to use these signals, they needed to be connected to a 114–pin MICTOR connector and converted from LVPECL to LVTTL. The amplified PRF timing reference signal from the analog board also needed to be connected to the MICTOR connector while the sample clock generated by the SRC–6E needed to be converted from LVTTL to ECL to drive the MAX108EVKITS. To facilitate this signal translation and mate the signal lines to the MICTOR connector, a single translation board was developed.

B. SIGNAL TRANSLATION

1. LVPECL-to-LVTTL Translation

To effectively convert the 49 differential LVPECL data outputs of the three MAX108EVKITs to LVTTL for use in the SRC–6E, it was decided to use commercial–off–the–shelf LVPECL–to–LVTTL translator ICs. The use of a translator IC would increase the propagation delay of the signal, so care was taken to select a translator chip that had an extremely small propagation delay. In addition, the translator needed to be capable of handling a 200–MHz signal to allow future work with the interface using the DDR capability of the SRC–6E.

Though multiple LVTTL–to–LVPECL translators could be found, only On Semiconductor produced LVPECL–to–LVTTL translators that met the design requirements. The MC100EPT21 and MC100EPT23 provided an operating frequency in excess of 275 MHz, used a single 3.3–V power supply, and only imposed a typical propagation delay of 1.5 ns. The difference between the two 8– pin translators was that the MC100EPT21 could only handle a single differential pair, while the MC100EPT23 came in a dual differential configuration. The MC100EPT23 was selected for the design because the ability to translate two differential pairs cut the number of chips required in half and greatly reduced the surface area required for the translation board.

2. LVTTL-to-ECL Translation

Having handled the translation from LVPECL to LVTTL for the data inputs into the SRC-6E, the next design step was to select an adequate LVTTL-to-ECL translator to convert the LVTTL sample clock generated by the SRC-6E to the ECL clock required by the MAX108EVKITS. As with the selection of the LVPECL-to-LVTTL translators, the design looked to maintain compatibility with the DDR mode of the SRC-6E. Therefore, the clock translator needed to be capable of translating a 400-MHz sample clock which was twice the design frequency of 200 MHz. Once translated, the clock signal needed to pass through a clock driver to effectively distribute the clock to all three MAX108-EVKITS.

The MAXIM MAX9360 LVTTL-to-ECL translator, designed for high-speed clock and data distribution, was selected to perform the sample clock translation. With a maximum frequency of 3 GHz, the MAX9360 converts a single-ended LVTTL input to a differential-ECL output with a typical propagation delay of 440 ps. A +3.3 V and a -5 V are required to facilitate the translation between the two logic standards. Though the internal circuitry of the MAX9360 is capable of being a clock driver, it can only drive one clock. Therefore an additional clock driver was still needed. [17]

A clock driver with at least three differential outputs was required to ensure that a clean and low-skew clock signal was delivered to the three MAX108EVKITS. The MAX9316A 1:5 differential clock driver solved the clock distribution problem. Using a single -5-V supply, it can drive a 1.5-GHz differential clock to five separate devices while imposing only a 365-ps delay. With two extra outputs available, the design used one to provide a test clock and the other was terminated to ground. [18]

C. MICTOR CONNECTOR ALTERNATIVES

As discussed in Section D of Chapter V, the design sought to assemble all custom hardware on a proto-board and then wire-wrap the components together. Though the surface-mount ICs selected for the design could be implemented with test sockets, the AMP MICTOR connector used by the SRC-6E could not. The 114 pins of the connector had 0.025-inch centerlines with the ground pins protruding from the center of the con-

nection with no known test socket available [19]. In order to wire-wrap the data lines to a connector, the connector pins needed to have 0.100-inch centerlines. Before leaving the wire-wrap implementation for PCB design, two other alternatives to the surface-mount MICTOR connector were pursued.

1. Custom Micro-Coaxial Cable

SRC Computers, Inc. provided the project with four 48-inch-long micro-coaxial cables with the requisite push-in connector for the MICTOR connector on each end. The micro-coaxial cable mates to the push-in connector through an extremely small PCB that connects the 114 pins of the connector to the individual signal lines. Precision Interconnect manufactured the cables used by SRC Computers and was contacted to see if they could make a custom cable with a push-in MICTOR connector on one end and a 0.100-inch header connector on the other. A custom cable of this type was possible, but due to the automated process involved a small run of a few cables would cost well over \$2,000.00. The simplicity of implementation that this custom cable would have provided was not enough to justify the cost and was eliminated as a possible alternative.

2. MICTOR Connector Breakout Adapter

The next alternative considered was an adapter that would breakout the 114 pins of the MICTOR connector from their 0.025-inch spacing to individual pins with 0.100-inch spacing. This would allow the design to utilize the micro-coaxial cable provided by SRC Computers while still affording the capability to wire-wrap the requisite connections on a proto-board. Again the need for only one breakout adapter and the cost of the surface-mount MICTOR connector itself prevented this from being a viable alternative.

3. Printed Circuit Board Implementation

Without a cost effective method to wire-wrap a connector capable of connecting to the micro-coaxial cable of the SRC-6E, the surface-mount MICTOR connector needed to be implemented on a PCB. The manufacturing specifications provided by ExpressPCB in Appendix G were sufficient to handle the pitch of the surface-mount MICTOR connector. In addition, the ExpressPCB software discussed in Chapter V allowed the design of custom device footprints. Using the data from Reference 19 and the schematic shown in Appendix H, the appropriate device footprint was constructed for the surface-mount MICTOR connector for use in the translation board PCB layout.

As with the breakout adapter alternative, the cost of an individual MICTOR connector was still an issue. At the time of design, no supplier could be located that would sell a low volume order of less than 35 connectors. At an average price of \$50.00 per connector, the design budget could not afford to purchase a large number of connectors. To avoid incurring this sizable cost, a sample MICTOR connector was obtained from Tyco Electronics for implementation in the design.

D. MAX108EVKIT–TO–TRANSLATION BOARD CABLING

The design implementation of the three MAX108EVKITS produced 49 differential pairs of LVPECL outputs for a total of 98 individual signals that needed to be connected to the translation board. To interface the MAX108EVKITS to the translation board, the design used 34–position 0.1" by 0.1" low-profile headers from 3M Interconnect to provide a compact arrangement of 2–pin headers on the translation board. The I, Q, and AGC voltage signals each used two of these headers to handle the demultiplexed data coming from the MAX108EVKITS.

To maintain a $50 - \Omega$ signal path from the 2–pin headers on the MAX108EVKITS to the headers on the translation board, the design sought to implement shielded $50 - \Omega$ coaxial cables terminated at each end by 2–pin connectors. However, no cable manufacturer could be found that offered pre–made coaxial cable in this configuration. Custom cables could have been fabricated, but again the cost for such cables outweighed the convenience they would provide. Since coaxial cable was not a feasible option, the design selected shielded controlled impedance (SCI) cables manufactured by 3M Interconnect. Designed specifically to connect to standard 2–pin headers, these cables were offered in two $50 - \Omega$ variations and one $75 - \Omega$ variation with user specified lengths. Table 10 lists the electrical properties for each type. To keep the transmission path as short as possible yet still be able to connect all three MAX108EVKITS to the translation board, a cable length of 10 inches was selected. The cost per cable for type 017 was \$15.31 and it was \$16.61 for the type 027. Since the type 027 was only \$1.30 more than the type 017 and provided better performance, the type 027 cable was selected for the design. Figure 25 illustrates the cable implemented in the design. Though these cables

were still relatively expensive, they were the most cost-effective option available to meet the design requirements. [20]

Table 10. Shielded Controlled Impedance Cable Electrical Properties (From Ref. 20.)

Electrical Properties (TYP)					
Cable Type		Capacitance	Propagation Delay	Attenuation	Conductor Resistance
017	50 Ω $\pm 5 \Omega$	32 pf/ft max (105 pf/m)	1.46 ns/ft nom (4.8 ns/m)	33 dB Max/100 ft @ 400 MHz (108 dB/100 m)	0.24 Ω /ft at 68° F (0.8 Ω /m at 20° C)
027	50 Ω $\pm 2 \Omega$	23 pf/ft nom (75 pf/m)	1.15 ns/ft nom (3.77 ns/m)	20 dB Max/100 ft @ 400 MHz Nom (65 dB/100 m)	0.041 Ω /ft at 68° F (0.15 Ω /m at 20° C)
041	75 Ω $\pm 3 \Omega$	16 pf/ft max (52 pf/m)	1.22 ns/ft nom (4.0 ns/m)	10 dB Max/100 ft @ 100 MHz (33 dB/100 m)	0.09 Ω /ft at 68° F (0.3 Ω /m at 20° C)

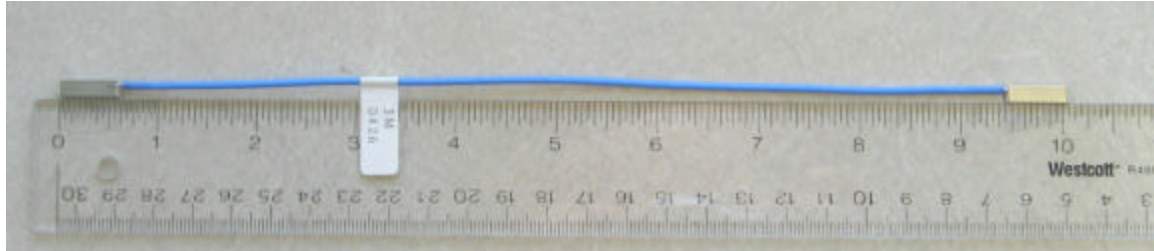


Figure 25. Shielded Controlled Impedance Cable

E. PCB DESIGN AND LAYOUT

1. Initial Design Considerations

Due to the number of signal traces involved and the need to maintain a trace impedance of 50Ω , the translation board was designed on a four-layer PCB. As Table 8 in Chapter V illustrated, trace widths of 15 mils and 20 mils on a four-layer board have an impedance of 60Ω and 50Ω , respectively. Keeping the trace impedance of the data lines as close as possible to 50Ω was essential to minimizing reflections that can distort the data. The four-layer board also allowed the primary voltage source to be implemented as a power plane and thus greatly increased the amount of board area available for device placement and trace routing.

To provide clean connections to the board all power supply inputs, clock outputs, and the PRF timing reference input were implemented using right-angle SMA connectors. The SMA connectors provided a reliable $50 - \Omega$ connection to the translation board and required a relatively small footprint on the PCB. In an attempt to keep all traces to the MICTOR connector the same length, the MICTOR connector was located in the center of the translation board. As Figure 26 illustrates, the data lines connect to the MICTOR connector from both sides keeping all the traces on the top layer of the board. The signals from one side of the connector could have been routed to the other side by using vias to traverse the layers of the board. However, each via induces a small amount of parasitic capacitance onto the trace, slowing down the signal. Keeping the traces on the top layer ensured that the cleanest signal path was achieved.

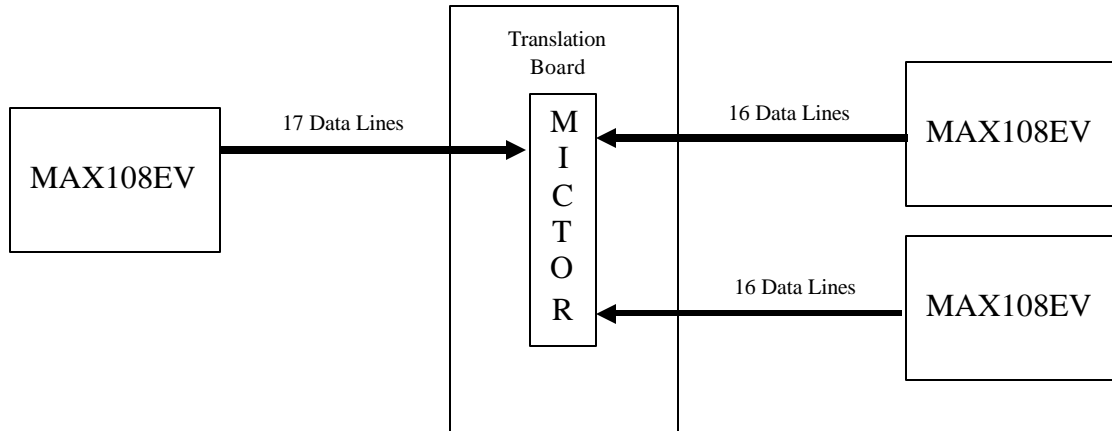


Figure 26. Block Diagram of Translation Board and MAX108EVKIT Arrangement

2. Device Termination

All of the signal paths in the design between the analog board and the MICTOR connector had to be properly terminated. The PRF timing reference signal was already source-series terminated on the analog board and the MAX108EVKITS provided on-board termination for both its inputs and outputs. The translation board thus needed to provide the appropriate termination for the implemented devices on the translation board itself. In addition, the translation board needed to provide for termination for both the LVPECL inputs and ECL clock outputs in the event that the terminators of the MAX108-EVKIT were ineffective.

The LVPECL-to-LVTTL translators on the translation board needed to be source-series terminated to $50 - \Omega$ terminations prior to connecting to the MICTOR connector. Since the output impedance of a TTL circuit varies depending if it is transmitting a high or low, a $50 - \Omega$ resistor could not just be simply placed in series with the output. The MC100EPT23 has an output impedance of 5Ω when transmitting a logic high and an output impedance of 15Ω when transmitting a logic low [21]. The average output impedance of 10Ω was assumed to be the output impedance of the device. Therefore, a $40 - \Omega$ resistor was placed in series with the output to produce the 50Ω source-series termination.

The RC shunt termination required for the SRC-6E sample clock was implemented as recommended by SRC Computers. A $50 - \Omega$ resistor in series with a $0.01 \mu\text{F}$ capacitor was tied to ground prior to the LVTTL clock entering the MAX9360 LVTT-to-ECL translator. The differential output of the MAX9360 was terminated to -2V through $50 - \Omega$ resistors. All of the outputs of MAX9316A clock driver had pads placed for terminating the outputs to -2V through $50 - \Omega$ resistors with the intent of only terminating the unused output. The additional pads were placed in the event that testing showed the termination resistors for the clock inputs on the MAX108EVKITS were ineffective. This was highly unlikely because having the terminators on the MAX108EVKIT clock inputs placed them as close to the receiver as possible which is the ideal termination configuration.

Similarly, pads for $50 - \Omega$ resistors connected to $+1.3 \text{ V}$ were placed on the inputs to the MC100EPT23 translators in case the signal path between the outputs of MAX108-EVKITS and inputs on the translation board was too long for the termination resistors on the MAX108EVKITS to effectively terminate the signal. If this was the case, the termination resistors could be removed from the MAX108EVKITS and placed on the translation board. This would then place the terminators as close to the receiver as possible, creating an optimum termination configuration.

To ensure the correct size of the SMT termination resistor was selected, the power dissipated over each termination resistor was calculated as

$$P = \frac{(V_{Ox} - V_{ref})^2}{R_{term}}. \quad (6.1)$$

The value V_{Ox} represents the largest output voltage seen at the resistor, V_{ref} is the reference voltage, and R_{term} is the termination resistor value. Table 11 lists the power dissipated over each termination resistor and the size of resistor selected.

Table 11. Termination Resistor Power Calculations

Terminator	V_{Ox}	V_{ref}	R_{term}	Power	Resistor Size
LVPECL to LVTTL Input	2.5 V	1.3 V	50Ω	0.029 W	0805
LVTTL to MICTOR	3.3 V	0.0 V	45 Ω	0.242 W	1210
ECL DeviceTermination	-0.865 V	-2.0 V	50Ω	0.026 W	0805

3. Power Distribution

To determine what voltage to assign to the power plane, the power requirements for all the devices to be implemented on the translation board were tabulated in Table 12. In addition to the individual device requirements, the table also includes the -2.0 V and +1.3 V termination voltages needed on the board using the total number of termination resistor pads implemented to calculate the total possible required current.

Table 12. Translation Board Voltage and Current Requirements

Device	Quantity	Voltage	Max Current	Total Current
MC100EPT23	25	3.3 V	33 mA	825 mA
MAX9360	1	3.3 V	7 mA	7 mA
MAX9360	1	-5.0 V	20 mA	20 mA
MAX9316A	1	-5.0 V	40 mA	40 mA
-2.0V ECL Termination Voltage	12	-2.0 V	23 mA	276 mA
1.3 V LVPECL Termination Voltage	98	1.3 V	24 mA	2.352 A

The initial testing of the design intended to use the onboard termination resistors of the MAX108EVKITS, which would eliminate the immediate need to have a power plane dedicated to either the -2.0 V or 1.3 V termination voltages. Also, the termination resistors were concentrated at the edges of the board allowing the use of a wide trace

along the bottom layer of the board. The power required by the two -5.0-V devices was dwarfed by the large number of devices requiring 3.3 V . The 26 3.3-V devices were to be located throughout the board and required a significant amount of current. Therefore, the power plane was set to 3.3 V and traces of sufficient width were used to route power to the devices requiring -5.0 V .

4. Translation Board Schematic Layout

The ExpressSCH schematic editor was used to lay out the circuitry of the translation board. The devices were arranged in the schematic as close as possible to how they would be placed on the actual printed circuit board. This was done to resolve any potential layout problems prior to investing time in the actual PCB layout. As with the analog board, all device power connections were implemented with two bypass capacitors. The $0.01\text{ }\mu\text{F}$ and $0.1\text{ }\mu\text{F}$ capacitors were placed in parallel using separate vias with the $0.01\text{ }\mu\text{F}$ being placed closest to the device. Figure 27 illustrates the schematic of the translation board.

When routing the I, Q, and AGC voltage signals to the MICTOR connector, care was taken to ensure that they were connected to DDR capable pins to maintain the DDR functionality of the design while attempting to minimize trace length. In addition, the DREADY signal was connected to pin 39 of the MICTOR connector. This pin connects to a GCLKx pin on the FPGAs on the MAP board. Since DREADY was implemented as a source-synchronous clock, this ensured the cleanest clock signal into the SRC-6E. Similarly, the sample clock from the SRC-6E was routed from the GCLKx signal line located on pin 79 of the MICTOR connector. This was imperative to allow the SRC-6E to generate the 200-MHz sample clock to drive the MAX108EVKITS.

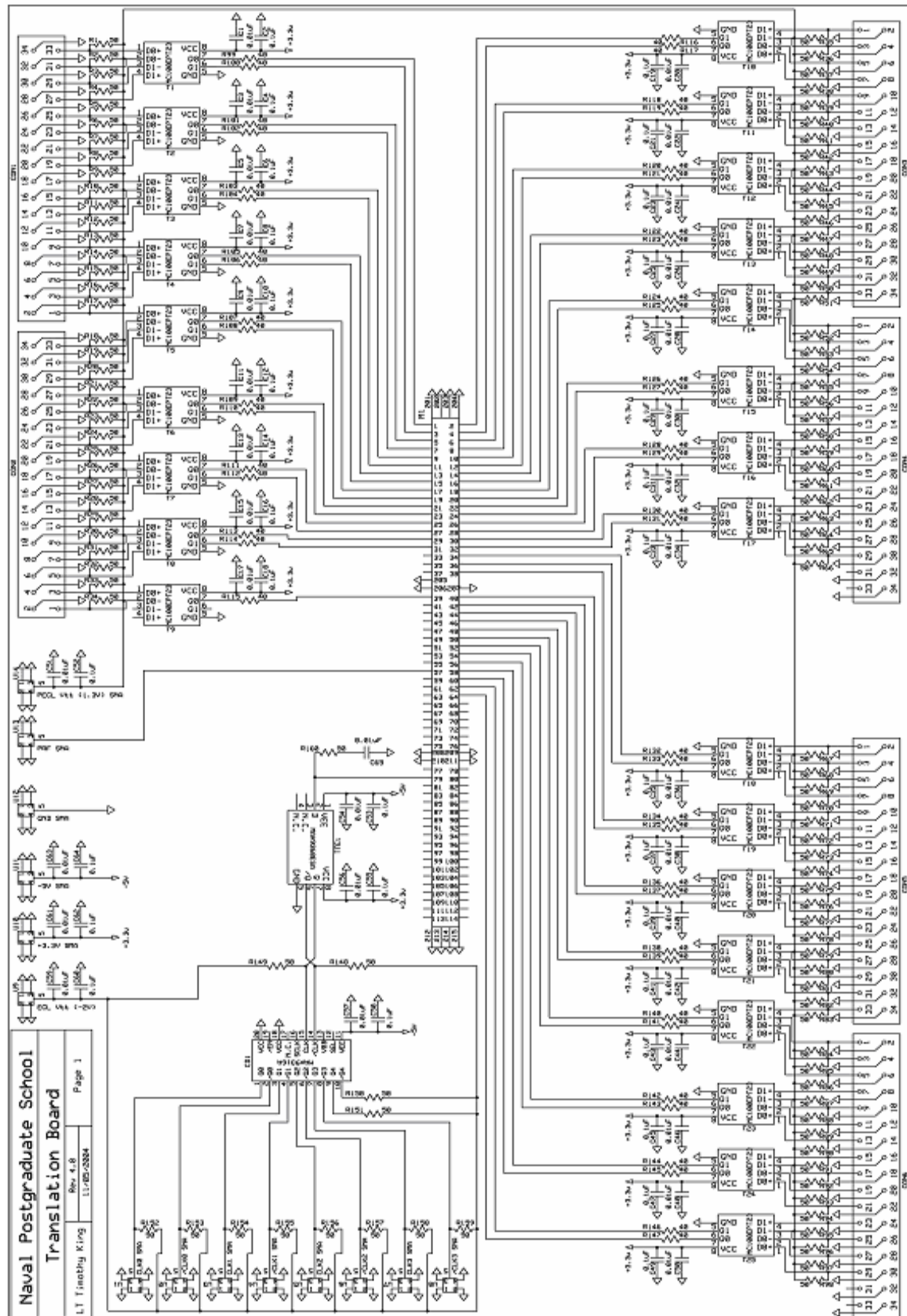


Figure 27. Translation Board Schematic

5. Translation Board PCB Layout

The translation board schematic was linked to the ExpressPCB software to aid in the layout process. All signal traces and devices were placed on the top layer of the board. The termination resistors and the -5.0V , -2.0 V , and 1.3 V power supply traces were placed on the bottom layer of the board. This arrangement provided the most freedom for trace routing and device placement on the top layer. A trace width of 15 mils was the largest trace that could be routed to the MICTOR connector. This was due to the minimum spacing requirement of 7 mils between traces set by ExpressPCB. The 25-mil centerline spacing of the MICTOR connector in conjunction with 15-mil traces provided 10 mils of spacing between the individual traces. If 20-mil traces were used, the trace spacing would be reduced to 5 mils which exceeded the ExpressPCB manufacturing specifications. Therefore, 15-mil traces were used for all signal lines on the board providing 60Ω of impedance. The only exception to this was the PRF timing reference signal trace which was 20 mils from the SMA connector to just before the MICTOR connector where the trace was reduced to 15 mils. This was done to minimize reflections in the PRF timing reference signal since it was terminated on the analog board.

The devices were placed as close as possible to minimize the overall board size while still maintaining the ability to manually solder the components to the board. Table 13 was referenced to determine the appropriate width for the power supply traces implemented on the bottom layer of the board. As Table 12 illustrated, the LVPECL termination voltage trace could possibly need to handle 2.342 A. Since the finished external copper traces produced by ExpressPCB were determined to be 1.25 ounces from Appendix G, a minimum trace of 30 mils was required. To provide an adequate margin of safety and to minimize trace resistance, a 60-mil trace was selected for all the power supply traces. Figure 28 illustrates the final translation board printed circuit layout that was implemented.

Table 13. Trace Width Current Capacity (From Ref. 22.)

Temp Rise	10 C			20 C			30 C		
	1/2 oz.	1 oz.	2 oz.	1/2 oz.	1 oz.	2 oz.	1/2 oz.	1 oz.	2 oz.
Trace Width	Maximum Current Amps								
0.010	0.5	1.0	1.4	0.6	1.2	1.6	0.7	1.5	2.2
0.015	0.7	1.2	1.6	0.8	1.3	2.4	1.0	1.6	3.0
0.020	0.7	1.3	2.1	1.0	1.7	3.0	1.2	2.4	3.6
0.025	0.9	1.7	2.5	1.2	2.2	3.3	1.5	2.8	4.0
0.030	1.1	1.9	3.0	1.4	2.5	4.0	1.7	3.2	5.0
0.050	1.5	2.6	4.0	2.0	3.6	6.0	2.6	4.4	7.3
0.075	2.0	3.5	5.7	2.8	4.5	7.8	3.5	6.0	10.0
0.100	2.6	4.2	6.9	3.5	6.0	9.9	4.3	7.5	12.5
0.200	4.2	7.0	11.5	6.0	10.0	11.0	7.5	13.0	20.5
0.250	5.0	8.3	12.3	7.2	12.3	20.0	9.0	15.0	24.5

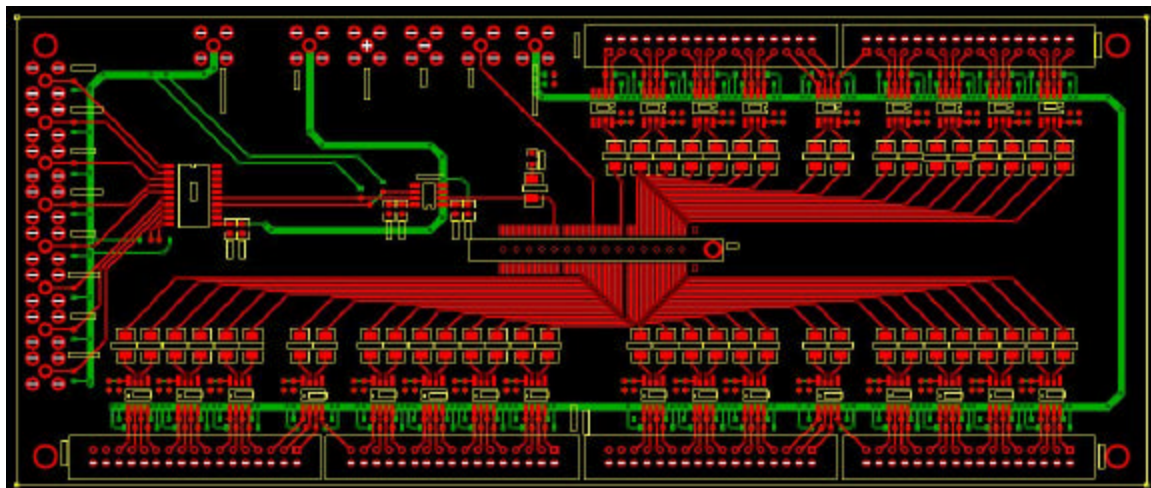


Figure 28. PCB CAD Drawing of Translation Board

F. TRANSLATION BOARD TESTING

As with the analog board, all traces were tested with an ohm meter to test for possible shorts on the board and to ensure trace continuity. This testing revealed two errors in the PCB layout sent to ExpressPCB for fabrication. The pads for the terminating resis-

tors for pin 1 on translators T11 and T17 were not connected to 1.3-V termination voltage trace as shown by the light blue circles in Figure 29. This was not a catastrophic issue for the board for, in the event that the LVPECL terminators were moved to the translation board, a jumper wire could be used to connect the resistor to the termination voltage trace. The components were then soldered to the board and power was applied to all power supply inputs to verify that there were no shorts present between the power and ground connections. The fully assembled translation board is depicted in Figure 30.

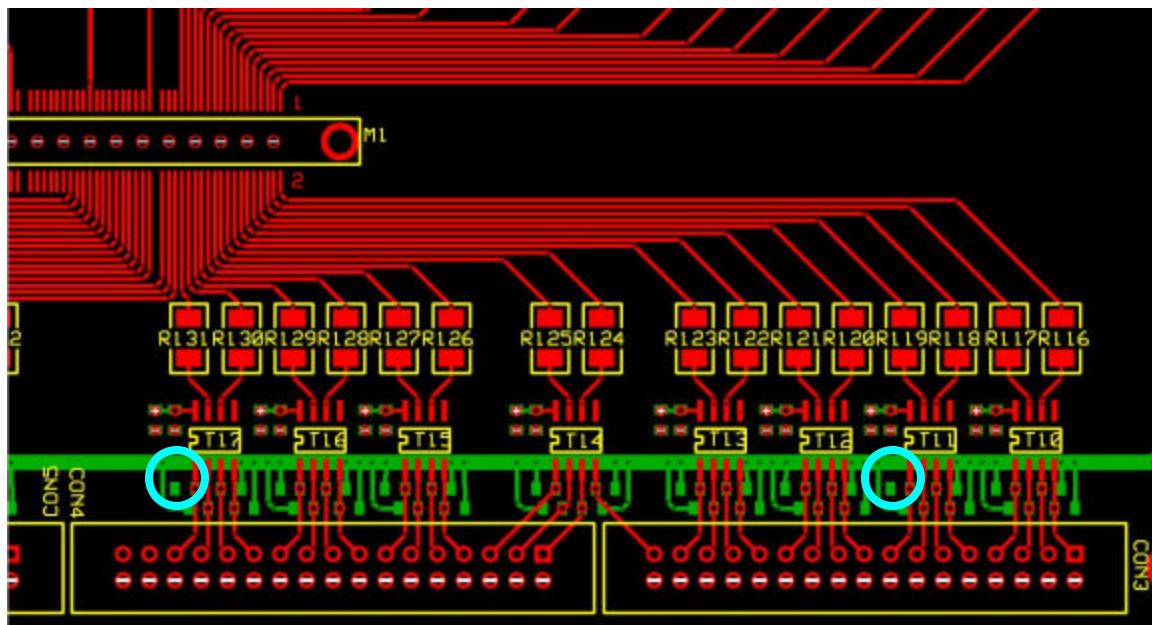


Figure 29. Translation Board Trace Errors

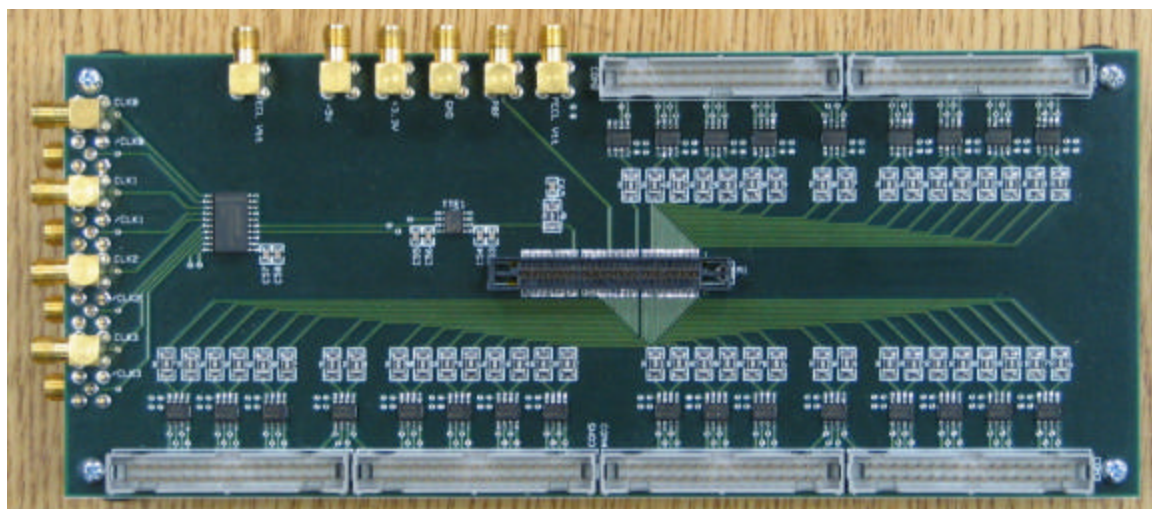


Figure 30. Assembled Translation Board

1. Sample Clock Translation Testing

With the translation board assembled, the first circuit tested was the translation of the LVTTL sample clock to differential ECL. Without connecting the board to the SRC–6E, there was no way to connect a clock signal directly to the translation board to perform lab bench testing. To facilitate the required bench testing, SRC Computers provided the design with a breakout board designed to connect a logic analyzer to the CHAIN port of the SRC–6E. The breakout board had two surface-mounted MICTOR connectors on each end with 2–pin headers to each of the individual 114 pins of the MICTOR connectors located in the center of the board. Using this breakout board a small piece of RG174A/U coaxial cable with an SMA connector on one end was soldered to the 2–pin header that connected to pin 79 on the MICTOR connector. The translation board was then connected to the breakout board via the 48–inch micro-coaxial cable and a function generator capable of producing a 200–MHz LVTTL square wave was connected to pin 79 via the coaxial cable soldered to the breakout board. With the function generator on and the translation board powered up, the output of the ECL clock driver was probed to ensure a valid ECL clock was being generated. The circuit was first tested at 10 MHz and then at 200 MHz. Figures 31 and 32 show the resulting ECL clocks generated by the translation board.

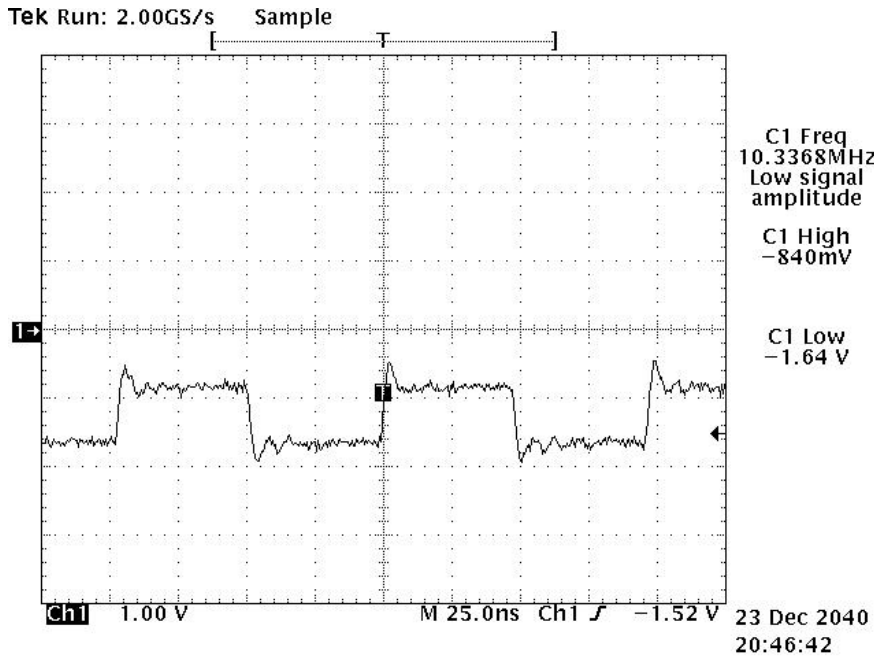


Figure 31. 10–MHz LVTTL Clock Translated to ECL

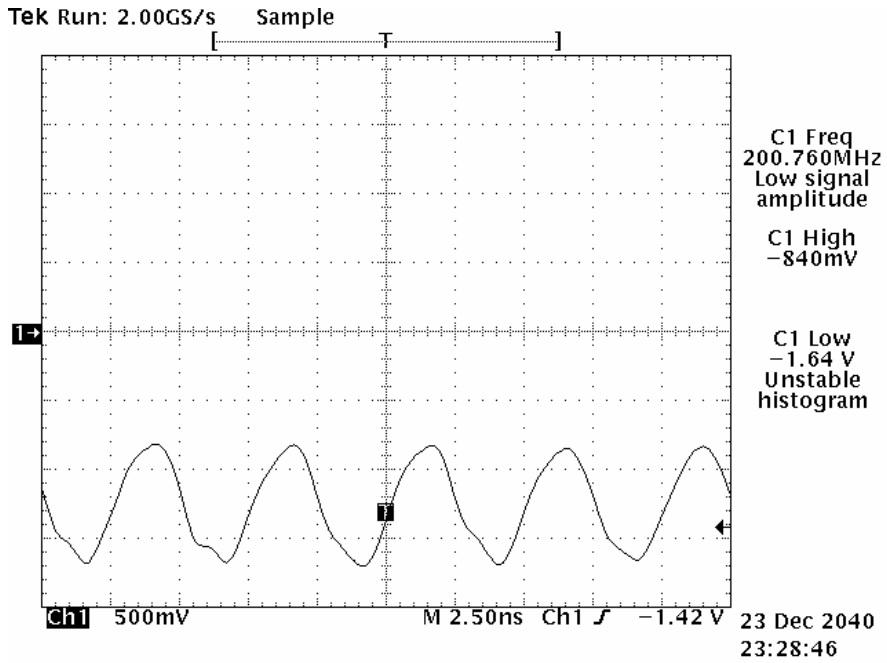


Figure 32. 200–MHz LVTTL Clock Translated to ECL

The clock signal in Figure 31 shows a nice 10–MHz square wave at the appropriate ECL voltage values of -0.840 V and -1.64 V . Figure 32 shows the 200–MHz ECL clock but it is not as clean as the 10–MHz clock. This distortion was attributed to the method in which the clock signal was being sent to the translation board. The 2–pin headers on the breakout board had a high impedance relative to the $50-\Omega$ impedance of the cables and traces that were implemented in the design and caused severe reflections to occur in the clock signal path. At 10 MHz the reflections were minimal, but as the frequency increased the constructive and destructive effects of the reflections caused by the connection to the 2–pin header became more evident. As a result, the clock signal entering the translation circuitry on the translation board was distorted resulting in the waveform shown in Figure 32. With this in mind it was determined that the LVTTL-to-ECL translation circuitry was functioning correctly.

2. LVPECL-to-LVTTL Translation Testing

To verify that the clock driver on the translation board could drive the MAX108EVKITS and that the data from the MAX108EVKITS was being properly translated, the translation board was connected to one MAX108EVKIT. One differential clock output pair from the translation board was connected to the differential clock inputs

of one MAX108EVKIT. The outputs of the MAX108EVKIT were connected to the translation board using the SCI cables. The sample clock was routed to the translation board in the same manner as the previous test and an HP16500B logic analyzer was connected to the breakout board to capture the data as if it were the SRC-6E. The same 1-MHz, 200-mV_{PP} sine wave used to individually test the MAX108EVKIT was connected to the analog input of the MAX108EVKIT. With all the components connected, everything was powered up and data was collected for a 10-, 100-, and 200-MHz sample clock. Using the same MATLAB script in Appendix D, the logic analyzer data was plotted for each different sample clocks. The results of the data collected by the logic analyzer for the 200-MHz sample clock are shown in Figure 33.

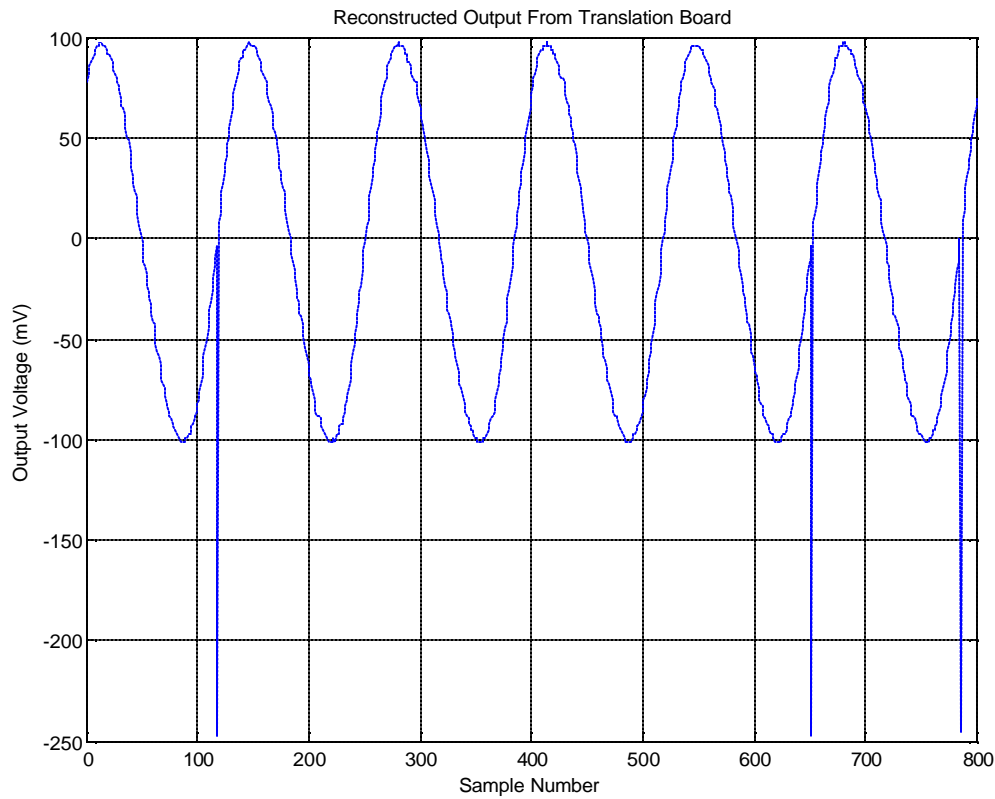


Figure 33. Translation Board Output with a 200-MHz Sample Clock

The reconstructed output from the translation board in Figure 33 mirrored the output generated by the MAX108EVKIT shown in Figure 13. The only item of note was the

-250 mV spikes that occurred at random when the analog signal transitioned from negative to positive. In the offset binary encoding that the MAX108 employs, a 0111111 toggles to 10000000 when representing zero. It was likely that the most significant bit was slow to change relative to the other seven bits. When the data was latched, the logic analyzer saw 00000000 instead of 1000000 and thus produced the erroneous value. Another possibility was that all the trace lengths on the translation board were not exactly the same length delaying the simultaneous arrival of all the bits at the logic analyzer. However, the issue was with the most significant bit not flipping from 0 to 1 which had a shorter trace length than the other bits. Thus, if the trace length was the issue, the erroneous value should have been $+250$ mV and not -250 mV. In either case, the random erroneous data was not deemed detrimental to the design in that when the data was processed the outliers would be filtered out. As a result, the design from the lab bench perspective was operating correctly.

3. LVPECL Termination Resistor Analysis

Though the translation board appeared to be functioning correctly, the LVPECL output path from the MAX108EVKIT to the translation board was examined to see if the signal path could be improved by moving the termination resistors from the MAX108EVKIT to the translation board. Continuing with the test setup used in the previous section, the DREADY signal was probed to determine the termination resistor location effectiveness. DREADY was chosen because it would always have a frequency of one-half the sample clock frequency in DIV2 mode or the clock frequency in DIV1 mode. Therefore it was probed prior to translation from LVPECL to LVTTL, immediately following translation but before the series termination resistor, and just before the signal connected to the MICTOR connector. This probing was conducted for 10-, 100-, and 200-MHz sample clocks with the termination resistors on the MAX108EVKIT and with the termination resistors on the translation board. The most noticeable change was with a 100-MHz sample clock and examining the signal on the output of the translator. The DREADY frequency was approximately 50 MHz and Figure 34 illustrates how the reflections in the signal path severely distorted the waveform when the termination resistor was located on the MAX108EVKIT. Moving the termination resistor made a tremendous improvement which Figure 35 demonstrates. With such a dramatic improvement in

the signal quality, the design moved all the LVPECL termination resistors off the MAX108EVKITs and onto the translation board.

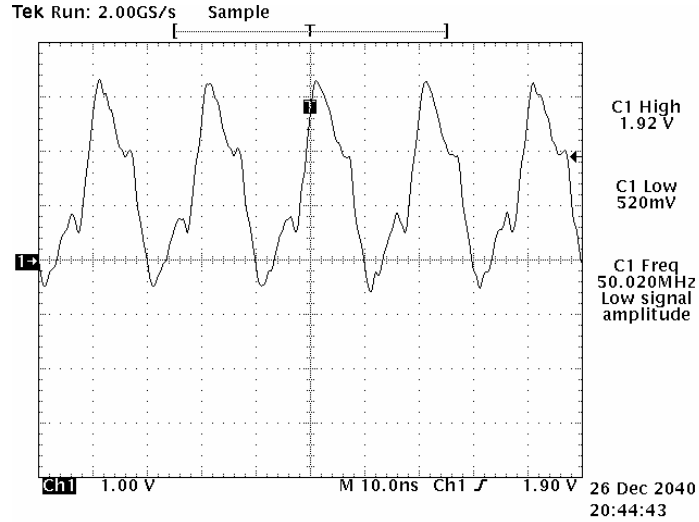


Figure 34. DREADY Immediately Following Translation (Terminator Located on MAX108EVKIT)

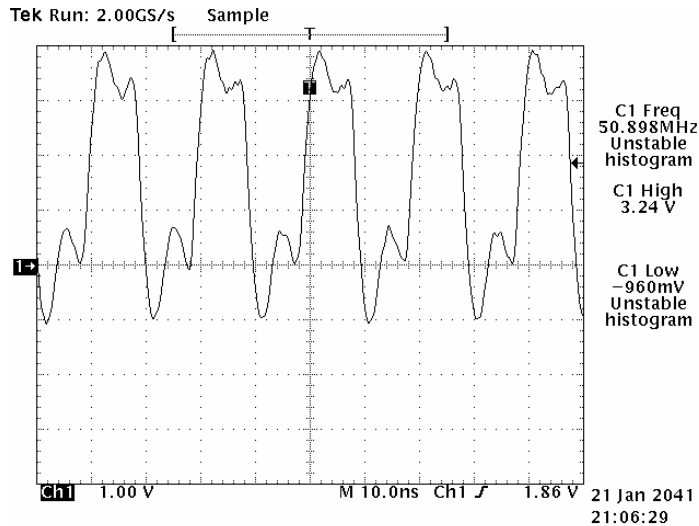


Figure 35. DREADY Immediately Following Translation (Terminator Located on Translation Board)

G. CHAPTER SUMMARY

The translation board facilitated the interfacing of the SRC-6E to the MAX108EVKITs and the PRF timing reference signal. It properly translated and terminated the digital LVPECL outputs from the MAX108EVKITs to the LVTTL levels re-

quired by the SRC-6E. The translation board also provided the necessary translation and distribution mechanism for the sample clock generated by the SRC-6E to effectively drive the MAX108EVKITS. To make the digital output lines as clean as possible, the LVPECL termination resistors were removed from the MAX108EVKITS and placed on the translation board. Having been successfully proven in lab bench testing, each of the individual components of the interface needed to be connected together and tested as one complete unit. The next chapter discusses the final testing of the design.

THIS PAGE INTENTIONALLY LEFT BLANK

VII. COMPLETE INTERFACE TESTING

A. INTRODUCTION

Up to this point in the design, each element of the hardware interface had been independently tested to prove their correct operation. To prove the overall functionality of the interface, the analog board, the MAX108EVKITS, and the translation board needed to be connected to the AN/SPS-65 and to the SRC-6E.

B. DESIGN MODIFICATION

Prior to connecting the interface to the radar and SRC-6E, it was discovered that to ensure that the I and Q channels maintained the correct phase relationship, the phase of sample clock on each of the respective MAX108EVKITS needed to be identical. As Chapter IV discussed, the phase of the sample clock and that of DREADY will be random at startup. The MAX108EVKITS can be synchronized by using the RSTIN inputs and therefore ensure each MAX108EVKIT is running with the same phase sample clock and DREADY. However, the design did not account for this and did not provide any method to implement the reset operation. Therefore, the design lowered the sample clock to 100 MHz and placed the MAX108EVKITS in DIV1 mode. This removed the DREADY phase issue between the individual MAX108EVKITS and allowed the interface to sample the I, Q, and AGC voltage signals at roughly 2.3 times the Nyquist frequency.

C. INTERFACE TEST

The I and PRF timing reference channels from the AN/SPS-65 were connected to the respective inputs on the analog board. The PRF timing reference output from the analog board was then connected directly to the translation board while the attenuated I channel output was connected to the analog input of a MAX108EVKIT. The digital outputs of the MAX108EVKIT, including DREADY, were then connected to the headers on

the translation board. Finally, the translation board was connected to the CHAIN port of the SRC–6E using a 48 inch micro-coaxial cable. Figure 36 illustrates the complete interface configuration.

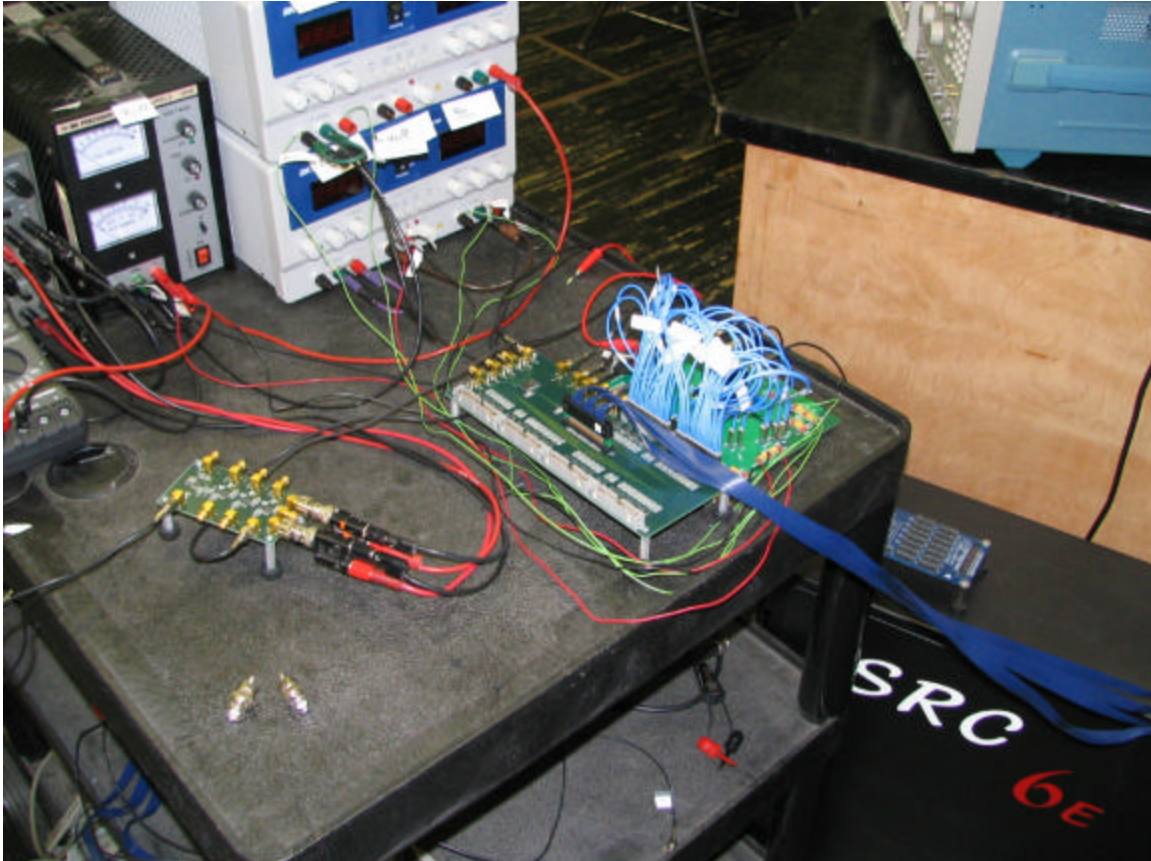


Figure 36. Complete Hardware Interface Configuration

With all components power up, the AN/SPS–65 was directed across Monterey Bay to point at the Santa Cruz mountains. The SRC–6E then captured several of the AN/SPS–65 pulses along a single access. The data stored in the SRC–6E was then manipulated and plotted in MATLAB to produce the plot depicted in Figure 37. The plot shows the range that the radar returned for the Santa Cruz Mountains, which corresponds directly with the actual range of the mountains from the AN/SPS–65. This real-world test proved that design effectively interfaced the AN/SPS–65 radar to the SRC–6E [23].

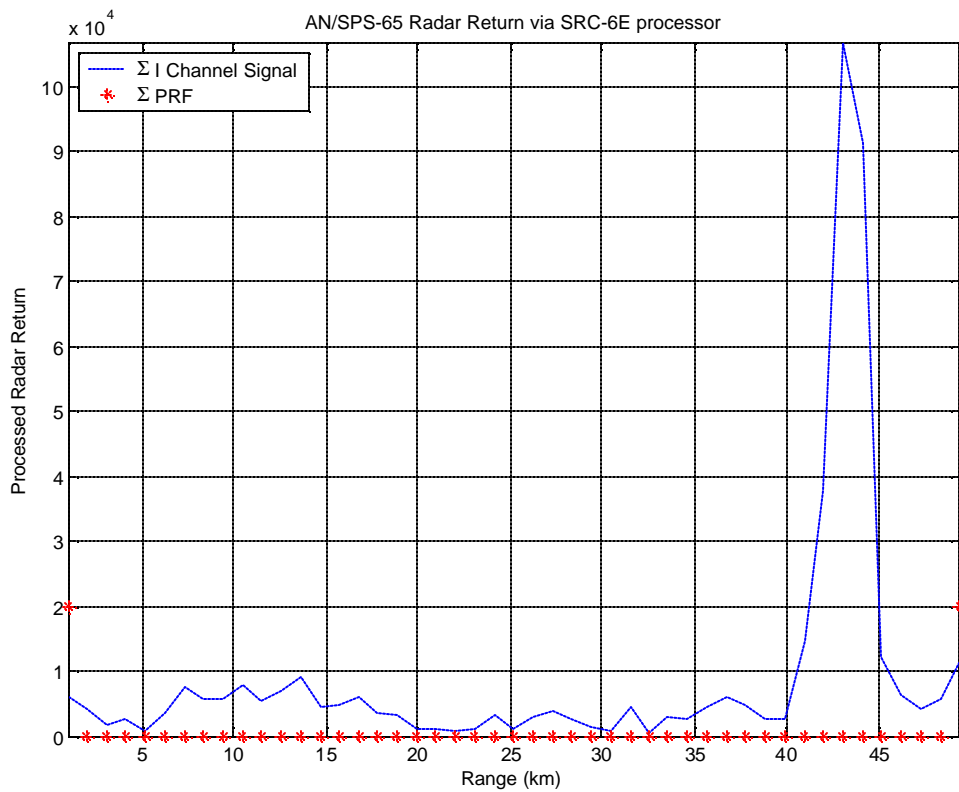


Figure 37. Reconstructed Radar Data Collected by the SRC-6E (From Ref. 23.)

D. CHAPTER SUMMARY

This real-world testing proved that the hardware interface design effectively allowed the SRC-6E to interface with a high-speed data source and effectively process the data. Time constraints permitted testing only the I channel and PRF timing reference signals from the AN/SPS-65. However, enough data was captured to perform basic range analysis on a known target which was the overall goal of the design.

THIS PAGE INTENTIONALLY LEFT BLANK

VIII. CONCLUSIONS

A. DESIGN SUMMARY

The entire purpose of the hardware interface design was to interface the SRC-6E reconfigurable computer at the Naval Postgraduate School to a high-speed data source. To prove the real-world applicability of such an interface, the AN/SPS-65 radar was selected as the data source. The goal of the hardware interface design was to implement, develop, and test the requisite hardware needed to permit the SRC-6E to process the data received by the AN/SP-65 to calculate the range of a target.

The data received by the AN/SPS-65 is carried on the $\pm 5.8\text{-V}$ I and Q channels while the internal amplification value of these two channels is carried on the separate 0–12 V AGC voltage signal. The AN/SPS-65 also produced a 0 to 1.0-V pulse repetition frequency signal to generate a timing reference for the received RF signals. The signals were connected to a custom-built analog board which buffered each signal and either amplified or attenuated the signal for proper compatibility with other parts of the design. The I, Q, and AGC voltage signals were attenuated to $\pm 225\text{ mV}$ to be compatible with the MAX108 ADC analog inputs and the PRF timing reference signal was amplified to LVTTL to be compatible with the SRC-6E.

The I, Q, and AGC voltage signals were connected to individual MAX108-EVKITs where they were sampled at 100 MHz by the MAX108 ADCs. The LVPECL outputs of each MAX108EVKIT were routed via shielded controlled impedance cables to a custom built translation board. On the translation board, the LVPECL signals were translated to LVTTL and routed, along with the PRF timing reference signal from the analog board, to a 114-pin MICTOR connector. Micro-coaxial cable was then used to connect the MICTOR connector of the translation board to the MICTOR connector of the CHAIN port on the SRC-6E, completing the interface between the radar and the SRC-6E. The translation board also took the 100-MHz sample clock generated by the SRC-6E from the MICTOR connector and translated it into a differential ECL clock. This differential ECL clock was then routed through a clock driver for distribution to the three MAX108EVKITS.

B. DESIGN ACCOMPLISHMENT

The complete interface testing conducted in Chapter VII proved that the SRC–6E and the hardware interface were fully capable of interfacing to the AN/SPS–65 radar.

Though time constraints only allowed for complete interface testing of the I channel, the use of the I channel provides enough information to calculate the range of a target. The Q channel is identical to the I channel except for a 90 degree phase shift induced to eliminate the possibility of “phase blindness” [8]. Also, the AGC voltage is not required for processing the I or Q channel. Therefore, limiting the testing to the I channel does not detract from the ability of the interface to bring data from an external high-speed device into the SRC–6E through its CHAIN port.

The initial design goal was to drive the MAX108EVKITS with a 200-MHz sample clock and to utilize the MAX108 demultiplexing feature to reduce the output data rate to the 100-MHz system bus speed of the SRC–6E. The initial testing of the I channel on the lab bench and in the complete interface configuration proved that the interface design was capable of implementing this configuration. However, it was discovered that there was no way to ensure that the I channel and Q channel samples were in phase with each other. This was due to the random phase relationship between the sample clock and DREADY on startup in DIV2 mode. Since no reset signal path was incorporated in the translation board design, there was no method to use the RSTIN inputs on the MAX108-EVKIT to synchronize all three MAX108EVKITS. To avoid redesigning the translation board, it was decided to place the MAX108EVKITS in DIV1 mode and to use a 100-MHz sample clock. This would ensure that all three MAX108EVKITS outputs remained in-phase and still allowed the design to sample over 1.5 times the Nyquist frequency of 60 MHz. Though the sampling rate was cut in half, the 100-MHz sampling rate provided more than enough resolution to effectively process the data coming from the AN/SPS–65.

The design met the established goal of interfacing the AN/SPS–65 radar to the SRC–6E reconfigurable computer. The design tested focused only on the SDR mode of the SRC–6E, but engineered all aspects of the design to be capable of exploiting the DDR capability of the SRC–6E allowing room for future speed-ups. To provide flexibility of implementation, the bandwidth of the analog board and the MAX108EVKITS allows the design to be capable of interfacing with other radars with similar output signals to the

AN/SPS-65. Ultimately, the design proved that the CHAIN port of the SRC-6E is a very capable high-speed port that can be effectively interfaced with external devices through user-defined hardware.

C. RECOMMENDATIONS FOR FUTURE WORK

The design only utilized the SDR mode of the SRC-6E, which limited the data rate into the CHAIN port to a maximum of 100 MHz. Using the DDR mode of the SRC-6E in the final design configuration with the MAX108s set in DIV1 mode would allow the input signals to be sampled at 200 MHz. Combining the DDR mode with a RSTIN capability on the translation board would allow the use of the DIV2 mode of the MAX108 and would increase the maximum sampling rate to 400 MHz. This would provide for greater resolution of sampled signals as well as allow the SRC-6E to sample signal sources with frequencies in excess of its 100-MHz system bus.

The final form of the design used five different printed circuit boards of devices between the analog board, three MAX108EVKITS, and the translation board. If more robust PCB CAD software was used, all five boards could be consolidated onto one. This would reduce the amount of cabling required for power and signal transmission. Signal transmission would also be greatly improved due to shorter transmission lengths between devices and the ability to match transmission line impedances. In addition, the number of power supplies required for the interface could be reduced if onboard voltage regulators were implemented to generate the requisite termination voltages.

The CHAIN port interface of future SRC designs would benefit greatly from allowing the user to implement any of the input and output signal levels supported by Virtex-II FPGAs. This would increase the overall flexibility of the CHAIN port by allowing it to directly interface to a broader range of hardware without the need for costly and potentially bandwidth limiting translator chips. If the input and output signal settings need to be configured at the factory, the user should have the option to choose the logic level implemented. If production constraints limit the logic level setting to only one input and output logic standard, then either (LV)ECL or (LV)PECL should be implemented instead of LVTTL. More and more modern data and signal processing devices are re-

quiring data rates in the gigahertz range. To effectively process and transmit these signals, the overall propagation delay needs to be reduced while simultaneously reducing the effect of noise on the signal itself. The logic families of (LV)ECL and (LV)PECL in differential format offer propagation delays under 500 ps and are very noise resistant [24]. In addition to being able to set the logic levels to (LV)ECL or (LV)PECL, removable or selectable termination resistors on the CHAIN port signal lines would simplify the interface implementation. By making the CHAIN port compatible with these logic levels, the SRC-6E would be even more useful for real-time high-speed signal processing purposes.

APPENDIX A CHAIN PORT PIN LISTING (AFTER REFS. 6 & 7.)

This appendix provides a listing of the CHAIN port pins, the corresponding Vitrex-II pins, the Virtex-II pin description, and the bank the pin is located in.

Port A				
Chain Port Pin	Virtex-II Pin	Virtex-II Pin Description	Bank Number	Notes
IN.1	U12	IO_L53P_2	2	
IN.2	T12	IO_L53N_2	2	
IN.3	M2	IO_L52P_2	2	
IN.4	N2	IO_L52N_2	2	
IN.5	R11	IO_L51P_2	2	
IN.6	T11	IO_L51N_2	2	
IN.7	P8	IO_L50P_2	2	
IN.8	N8	IO_L50N_2	2	
IN.9	M3	IO_L49P_2	2	
IN.10	N3	IO_L49N_2	2	
IN.11	M5	IO_L48P_2	2	
IN.12	N5	IO_L48N_2	2	
IN.13	R10	IO_L47P_2	2	
IN.14	P10	IO_L47N_2	2	
IN.15	K1	IO_L46P_2	2	
IN.16	L1	IO_L46N_2	2	
IN.17	L4	IO_L45P_2	2	
IN.18	M4	IO_L45N_2	2	
IN.19	P9	IO_L44P_2	2	
IN.20	N9	IO_L44N_2	2	
IN.21	L3	IO_L43N_2	2	
IN.22	L6	IO_L36P_2	2	
IN.23	M6	IO_L36N_2	2	
IN.24	R12	IO_L35P_2	2	
IN.25	P12	IO_L35N_2	2	
IN.26	J2	IO_L34P_2	2	
IN.27	K2	IO_L34N_2	2	
IN.28	J4	IO_L33P_2	2	
IN.29	K4	IO_L33N_2	2	
IN.30	M8	IO_L32P_2	2	
IN.31	L8	IO_L32N_2	2	
IN.32	H1	IO_L31P_2	2	
IN.33	J1	IO_L31N_2	2	
IN.34	L7	IO_L30P_2	2	
IN.35	M7	IO_L30N_2	2	
IN.36	P11	IO_L29P_2	2	
IN.37 (Valid)	N11	IO_L29N_2	2	
IN.38 (Full)	D1	IO_L21P_2	2	
IN.39 (Clock)	F19	IO_L96N_1/GCLK3P	1	

Port B				
Chain Port Pin	Virtex-II Pin	Virtex-II Pin Description	Bank Number	Notes
IN.41	K5	IO_L28N_2	2	Mate is J5, not on port
IN.42	J6	IO_L27P_2	2	
IN.43	K6	IO_L27N_2	2	
IN.44	N10	IO_L26P_2	2	
IN.45	M10	IO_L26N_2	2	
IN.46	H3	IO_L25P_2	2	
IN.47	J3	IO_L25N_2	2	
IN.48	G4	IO_L24P_2	2	
IN.49	H4	IO_L24N_2	2	
IN.50	M9	IO_L23P_2	2	
IN.51	L9	IO_L23N_2	2	
IN.52	G2	IO_L22P_2	2	
IN.53	H2	IO_L22N_2	2	
IN.54	J7	IO_L21P_2	2	
IN.55	K7	IO_L21N_2	2	
IN.56	L10	IO_L20P_2	2	
IN.57	K9	IO_L20N_2	2	
IN.58	F1	IO_L19P_2	2	
IN.59	G1	IO_L19N_2	2	
IN.60	G5	IO_L12P_2	2	
IN.61	H5	IO_L12N_2	2	
IN.62	K8	IO_L11P_2	2	
IN.63	J8	IO_L11N_2	2	
IN.64	F3	IO_L10P_2	2	
IN.65	G3	IO_L10N_2	2	
IN.66	H7	IO_L09P_2	2	
IN.67	H6	IO_L09N_2	2	
IN.68	N12	IO_L08P_2	2	
IN.69	M12	IO_L08N_2	2	
IN.70	E2	IO_L07P_2	2	
IN.71	F2	IO_L07N_2	2	
IN.72	F5	IO_L06P_2	2	
IN.73	G6	IO_L06N_2	2	
IN.74	M11	IO_L05P_2	2	
IN.75	L12	IO_L05N_2	2	
IN.76	E4	IO_L03P_2	2	
IN.77 (Valid)	F4	IO_L03N_2	2	
IN.78 (Full)	E1	IO_L04N_2	2	
IN.79 (Clock)	F20	IO_L96P_1/GCLK2S	1	

Port C				
Chain Port Pin	Virtex-II Pin	Virtex-II Pin Description	Bank Number	Notes
IN.81	D2	IO_L01P_2	2	
IN.82	E3	IO_L01N_2	2	
IN.83	B4	IO_L01P_1	1	
IN.84	C4	IO_L01N_1	1	
IN.85	C6	IO_L04P_1	1	
IN.86	C5	IO_L04N_1	1	
IN.87	E8	IO_L06P_1	1	
IN.88	F8	IO_L06N_1	1	
IN.89	A5	IO_L07P_1	1	
IN.90	A4	IO_L07N_1	1	
IN.91	B6	IO_L10P_1	1	
IN.92	B5	IO_L10N_1	1	
IN.93	H11	IO_L11P_1	1	
IN.94	H12	IO_L11N_1	1	
IN.95	C8	IO_L19P_1	1	
IN.96	C7	IO_L19N_1	1	
IN.97	E7	IO_L20P_1	1	
IN.98	D8	IO_L20N_1	1	
IN.99	E10	IO_L21P_1	1	
IN.100	E9	IO_L21N_1	1	

Port D				
Chain Port Pin	Virtex-II Pin	Virtex-II Pin Description	Bank Number	Notes
IN.103	J10	IO_L02P_1	1	
IN.104	H10	IO_L02N_1	1	
IN.105	J11	IO_L05N_1	1	
IN.106	G10	IO_L09P_1	1	
IN.107	G9	IO_L09N_1	1	
IN.108	F9	IO_L12N_1	1	

THIS PAGE INTENTIONALLY LEFT BLANK

APPENDIX B SRC-6E PART NUMBERS

This appendix lists the specific part numbers of the devices used by SRC Computers, Inc. in the SRC-6E.

A. USER LOGIC FPGAS [6]

Description: Xilinx Virtex-II
Part Number: XC2V6000-4FF1517C

B. MICRO-COAXIAL CABLE [6]

Description: Cable, AMP, 47" 50 - Ω 114 Pos. Straight/Straight
SRC Part Number: 2500-0007
Manufacturer Part 0138501141119JM20
Number:
Manufacturer Precision Interconnect

C. 114-PIN AMP MICTOR CONNECTOR [6]

Description: Connector, MICTOR 114 Pin
SRC Part Number: 0400-0018
Manufacturer Part 767054-3
Number:
Manufacturer AMP

THIS PAGE INTENTIONALLY LEFT BLANK

APPENDIX C LOGIC ANALYZER DATA

This appendix provides a listing of the data captured by the HP16500B logic analyzer from the MAX108EVKIT testing.

Label > CLK PRI AUX

		Base	> Hex	Hex	Hex
0	1 100 103				
1	1 094 097				
2	1 090 093				
3	1 086 088				
4	1 081 084				
5	1 079 081				
6	1 077 078				
7	1 075 076				
8	1 074 074				
9	1 074 074				
10	1 074 074				
11	1 076 075				
12	1 078 076				
13	1 080 079				
14	1 084 082				
15	1 087 085				
16	1 092 090				
17	1 098 095				
18	1 103 100				
19	1 109 106				
20	1 115 112				
21	1 121 118				
22	1 127 124				
23	1 133 130				
24	1 139 136				
25	1 145 142				
26	1 151 148				
27	1 156 153				
28	1 160 158				
29	1 164 162				
30	1 168 166				
31	1 170 169				
32	1 172 171				
33	1 173 172				
34	1 174 173				
35	1 173 174				

36	1 172 172
37	1 170 172
38	1 168 170
39	1 166 167
40	1 163 164
41	1 157 159
42	1 152 155
43	1 148 150
44	1 142 146
45	1 136 139
46	1 131 134
47	1 124 127
48	1 119 121
49	1 113 115
50	1 107 109
51	1 101 104
52	1 095 098
53	1 090 093
54	1 086 090
55	1 082 085
56	1 079 081
57	1 078 079
58	1 075 076
59	1 075 074
60	1 074 074
61	1 074 074
62	1 075 074
63	1 077 076
64	1 079 078
65	1 082 081
66	1 086 084
67	1 091 089
68	1 096 093
69	1 101 099
70	1 107 104
71	1 113 110
72	1 119 116
73	1 126 122
74	1 132 129
75	1 138 135
76	1 143 140
77	1 149 147
78	1 154 152
79	1 159 157
80	1 163 161
81	1 167 165

82	1 169 168
83	1 171 170
84	1 172 172
85	1 174 173
86	1 173 174
87	1 172 173
88	1 171 173
89	1 169 170
90	1 167 167
91	1 163 164
92	1 158 162
93	1 154 157
94	1 149 152
95	1 144 146
96	1 139 142
97	1 132 135
98	1 126 130
99	1 121 123
100	1 114 117
101	1 109 111
102	1 103 105
103	1 097 100
104	1 093 094
105	1 088 090
106	1 083 086
107	1 081 082
108	1 077 079
109	1 076 077
110	1 075 075
111	1 074 073
112	1 074 074
113	1 075 075
114	1 076 076
115	1 079 077
116	1 082 080
117	1 085 083
118	1 090 087
119	1 095 092
120	1 100 097
121	1 106 102
122	1 111 108
123	1 117 114
124	1 124 120
125	1 130 127
126	1 136 133
127	1 142 139

128	1 147 144
129	1 153 150
130	1 157 155
131	1 162 160
132	1 165 164
133	1 169 167
134	1 170 169
135	1 172 172
136	1 173 173
137	1 173 173
138	1 173 173
139	1 172 172
140	1 170 171
141	1 167 169
142	1 164 166
143	1 161 162
144	1 156 158
145	1 151 153
146	1 145 148
147	1 140 143
148	1 135 137
149	1 128 131
150	1 122 124
151	1 115 120
152	1 110 113
153	1 105 108
154	1 099 102
155	1 095 096
156	1 090 092
157	1 085 087
158	1 081 083
159	1 078 079
160	1 076 077
161	1 074 076
162	1 074 074
163	1 073 074
164	1 075 075
165	1 075 075
166	1 078 077
167	1 081 079
168	1 084 082
169	1 089 086
170	1 093 091
171	1 098 095
172	1 104 101
173	1 109 107

174	1 116 112
175	1 122 118
176	1 128 125
177	1 134 131
178	1 140 137
179	1 146 143
180	1 151 149
181	1 156 154
182	1 161 159
183	1 165 163
184	1 168 167
185	1 170 169
186	1 172 171
187	1 173 172
188	1 174 173
189	1 173 173
190	1 172 173
191	1 171 171
192	1 168 169
193	1 164 166
194	1 162 163
195	1 157 159
196	1 152 155
197	1 148 150
198	1 142 145
199	1 136 138
200	1 129 132
201	1 123 126
202	1 118 120
203	1 111 114
204	1 105 108
205	1 100 103
206	1 096 098
207	1 090 093
208	1 086 088
209	1 082 084
210	1 079 081
211	1 076 078
212	1 076 075
213	1 074 075
214	1 074 074
215	1 074 074
216	1 075 075
217	1 077 076
218	1 079 078
219	1 083 081

220	1 087 085
221	1 092 089
222	1 097 094
223	1 102 099
224	1 108 105
225	1 114 111
226	1 120 117
227	1 126 123
228	1 132 129
229	1 138 135
230	1 144 141
231	1 150 147
232	1 155 152
233	1 159 157
234	1 163 162
235	1 167 165
236	1 170 169
237	1 172 171
238	1 173 172
239	1 173 173
240	1 173 173
241	1 172 172
242	1 171 172
243	1 168 170
244	1 166 167
245	1 163 164
246	1 158 160
247	1 153 156
248	1 149 151
249	1 143 146
250	1 138 141
251	1 131 134
252	1 125 128
253	1 119 122
254	1 113 116
255	1 107 110
256	1 102 104
257	1 097 099
258	1 092 095
259	1 088 090
260	1 083 085
261	1 081 081
262	1 078 078
263	1 076 077
264	1 075 074
265	1 074 074

266	1 074 074
267	1 075 074
268	1 077 076
269	1 079 078
270	1 082 081
271	1 086 084
272	1 090 088
273	1 095 093
274	1 100 098
275	1 106 103
276	1 112 109
277	1 118 115
278	1 124 121
279	1 131 127
280	1 137 134
281	1 143 140
282	1 148 145
283	1 153 150
284	1 158 156
285	1 163 160
286	1 166 164
287	1 168 167
288	1 171 170
289	1 173 172
290	1 173 173
291	1 173 174
292	1 172 173
293	1 172 173
294	1 169 171
295	1 166 169
296	1 164 166
297	1 160 162
298	1 154 157
299	1 150 152
300	1 145 148

THIS PAGE INTENTIONALLY LEFT BLANK

APPENDIX D MATLAB LOGIC ANALYZER PLOTTING SCRIPT

This appendix lists the MATLAB script used to reconstruct and plot the data captured by the HP16500B logic analyzer.

```
%testplot.m
%
%MATLAB script designed to load a test file containing data
%captured from a MAX108EVKIT using a HP16500B logic analyzer.
%captured data is demultiplexed and needs to be recombined prior
%to plotting.

%request file to load and number of points to plot
fid = input('Enter file name: ','s');
points_to_plot = input('Enter number of points to plot: ');

data_array = load(fid); %assign loaded text file a variable name
final_array_length = length(data_array)*2; %calculate required array
length

i=1;
for n=1:length(data_array)      %loop for number of requested points
    A(i,1)= data_array(n,4);   %store auxiliary port data
    A(i+1,1)= data_array(n,3); %store primary port data
    i=i+2;
end

A = A - 128;                  %subtract out binary offset
A = A * 1.95;                 %multiply value by 1.95 mV to get voltage
value

plot(A(1:points_to_plot)); %plot points
grid;                         %display grid
```

THIS PAGE INTENTIONALLY LEFT BLANK

APPENDIX E SPICE MODEL OF ATTENUATION CIRCUIT

This appendix lists the SPICE model used to simulate the LMH6559 high-speed buffers.

Test of LMH6559 SPICE Model

```
.include LMH6559.mod

* Power Supplies
Vcc    1    0    5.0
Vee    2    0   -5.0

* Input Signals
*vin 10 0 sin(0.0 .225 200E6)
vin 10 0 AC 0.225

* Instance LMH6559
* input, positive power supply, negative power supply, output.
XBuffer 10 1 2 12 LMH6559
Rload 12 0 50

* Simulation Parameters
.tran 2E-8 4E-6 0
.ac lin 300 1E6 500E6
*.TF V(12,0) vin
.plot v(12) v(10)

.END
```

THIS PAGE INTENTIONALLY LEFT BLANK

APPENDIX F SPICE MODEL OF PRF TIMING REFERENCE AMPLIFIER

This appendix lists the SPICE model used to simulate the LMH6643 operational amplifier.

LMH6643 SPICE Model PRF

```
.include LMH6643.mod

* Power Supplies
Vcc    1    0    5.0
Vee    2    0   -5.0

* Input Signals
vin 10 0 PULSE(0.0 1.0 2ns 1ns 1ns 163.24us 326.48us)

* Instance LMH6643
* PINOUT ORDER -IN +IN VCC VEE OUT
XOpAmp1 13 11 1 2 12 LMH6643
Rin 0 13 1.2K
Rf 13 12 2.7K
R1 10 11 820
Rload 12 0 50

* Simulation Parameters
.tran 1us 900us 0
.plot v(12) v(10)

.END
```

THIS PAGE INTENTIONALLY LEFT BLANK

APPENDIX G EXPRESSPCB MANUFACTURING SPECIFICATIONS

The following manufacturing specifications were obtained from the ExpressPCB website [14].

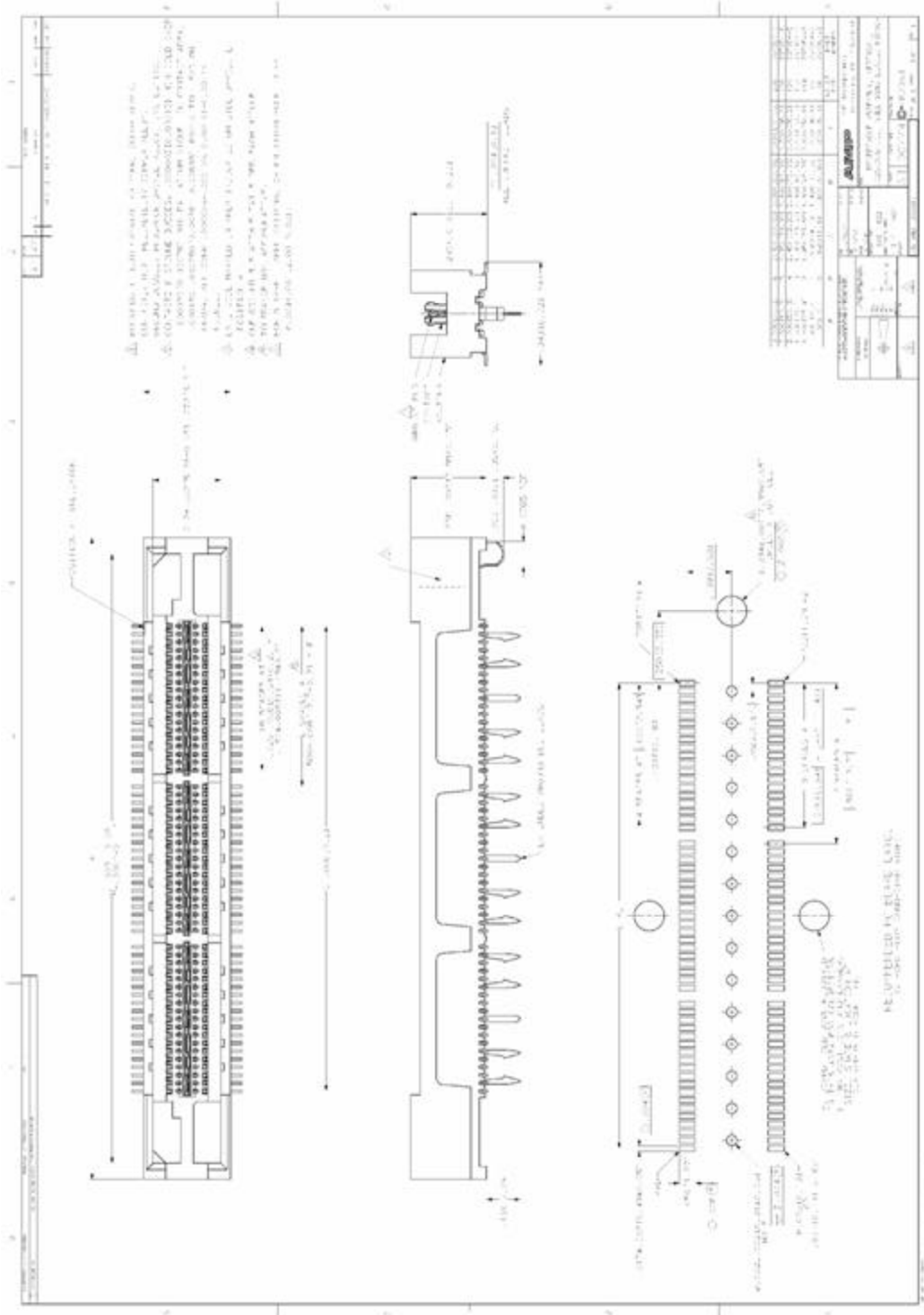
Manufacturing Specs

- > Boards are manufactured with 4 copper layers and plated-through holes.
- > Our laminate is FR-4 with an overall thickness of 0.062". The two inner layers have a copper weight of 1 ounce. The outer copper layers have a finished copper weight of ~1.25 ounce.
- > The final finish of the outer layers is tin-lead reflow.
- > The top and bottom solder mask layers are green LPI.
- > Pads on the solder mask layers are grown by a minimum of 0.004" on all sides. As a result, very fine pitch surface mount components may not include any solder mask between the pins.
- > The board finish is the industry standard of SMOBC.
- > The maximum board size we manufacture is 12 x 14 inches.
- > The minimum board dimension in height or width is 0.35 inches, however the total board area must be greater than 0.4 square-inches. (i.e. smallest square board we can make is 0.64 x 0.64 inches)
- > Etching resolution is: 0.007" minimum trace width, 0.007" minimum space width.
- > A white silkscreen is applied to the top side of the board.
- > Text placed on a board can be written in copper on the outer layers or drawn in ink on the silkscreen layer. Component outlines will be printed on the silkscreen layer.
- > Board perimeters are cut to shape using a 0.093" router bit. Slots in the perimeter must be larger than 0.124". Narrower slots will not be milled correctly. Routing slots or holes in the interior of the board are not offered.
- > Sixteen hole sizes are available: 0.008", 0.020", 0.025", 0.029", 0.035", 0.040", 0.046", 0.052", 0.061", 0.067", 0.079", 0.093", 0.110", 0.125", 0.150", 0.192". These sizes are the finished hole diameters after plating. The tolerance for the 0.008" hole is +0.003 / -0.008 (the 0.008" hole may be filled with solder and can only be used as a via). The tolerance for the 0.020" hole is +0.003 / -0.005. The tolerance for the other hole sizes is +/- 0.004". Hole sizes other than those listed are not offered.
- > A minimum of 0.021" space must remain between adjacent holes. For example, the center-to-center distance between two pads with 0.020" holes must be 0.041" or greater.
- > The dielectric spacing between the top layer and the "Ground" inner layer is 0.012" with a dielectric constant of 4.6 +/-0.2. The dielectric spacing between the bottom layer and the "Power" inner layer is 0.012" with a dielectric constant of 4.6 +/-0.2. The dielectric spacing between the "Power" and "Ground" inner layers is 0.028" with a dielectric constant of 4.7 +/-0.2.
- > The two inner layers are solid copper planes. Through-hole pads can either be connected to or isolated from these copper planes. The planes are inset 0.025" from each edge of the board.
- > The maximum operating temperature is 125 degrees C.

THIS PAGE INTENTIONALLY LEFT BLANK

APPENDIX H MICTOR CONNECTOR SCHEMATIC

This appendix illustrate the MICTOR connector schematic used in the translation board design.



THIS PAGE INTENTIONALLY LEFT BLANK

LIST OF REFERENCES

- [1] David Caliga and David Peter Barker, “Delivering Acceleration: The Potential for Increased HPC Application Performance Using Reconfigurable Logic,” ACM 1–58113–2.093–X/01/0011, November 2001. <http://delivery.acm.org/10.1145/590000/582066/p32-caliga.pdf?key1=582066&key2=9009747011&coll=ACM&dl=ACM&CFID=37929187&CFTOKEN=45120840>, accessed January 7, 2005.
- [2] Andre DeHon and John Wawrynek, “Reconfigurable Computing: What, Why, and Implications for Design Automation,” ACM 1–58113–109–7/99/06, 1999. <http://ieeexplore.ieee.org/iel5/9516/30164/01385107.pdf?tp=&arnumber=1385107&isnumber=30164&arSt=610&ared=615&arAuthor=DeHon%2C+A.%3B++Wawrynek%2C+J.%3B>, accessed January 7, 2005.
- [3] Zhi Guo, Walid Najjar, Frank Vahid, and Kees Vissers, “A Quantitative Analysis of the Speedup Factors of FPGAs over Processors,” ACM 1–58113–829–6/04/0002, February 2004. <http://delivery.acm.org/10.1145/970000/968304/p162-guo.pdf?key1=968304&key2=3343287011&coll=ACM&dl=ACM-&CFID=38218966&CFTOKEN=71179759>, accessed January 7, 2005.
- [4] *SRC–6E C Programming Environment v1.2 Guide*, SRC–007–04, SRC Computers, Inc., Colorado Springs, February 5, 2003.
- [5] SRC Computers, Inc., “SRC–6E Training Course,” Training course notes, SRC Computers, Inc., Colorado Springs, 2003 (unpublished).
- [6] *User Hardware Interfacing to the Chain Port of the SRC MAP® REV D Board*, SRC–013–00, SRC Computers, Inc., Colorado Springs, May 19, 2004.
- [7] “Virtex-II Platform FPGAs: Complete Data Sheet,” DS031, Xilinx, Inc., San Jose, CA , October 14, 2003. From website: <http://direct.xilinx.com/bvdocs/publications/ds031.pdf>, accessed January 2, 2004.
- [8] Paul D. Buczynski, “AN/SPS–65(V)1 Radar System,” Class material, Naval Postgraduate School, Monterey, July 2002 (unpublished).
- [9] “MAXIM MAX108 $\pm 5\text{V}$, 1.5Gsp, 8-Bit ADC with On-Chip 2.2GHz Track/Hold Amplifier,” 19–1492 (Rev 1), Maxim Integrated Products, Sunnyvale, CA, October 2001. From website: <http://pdfserv.maxim-ic.com/en/ds/MAX108.pdf>, accessed April 1, 2004.
- [10] “MAXIM MAX104/MAX106/MAX108 Evaluation Kits,” 19–1503 (Rev 0), Maxim Integrated Products, Sunnyvale, CA, June 1999. From website: <http://pdfserv.maxim-ic.com/en/ds/MAX104EVKIT-MAX108EVKIT.pdf>, accessed April 1, 2004.

- [11] William D. Stanely, *Operational Amplifiers with Linear Circuits*, pp. 501–522, 167–172, Prentice Hall, Upper Saddle River, New Jersey, 2002.
- [12] “LMH6559 High-Speed, Closed Loop Buffer,” DS200641, National Semiconductor, Santa Clara, California, April 2003. From Website: <http://cache.national.com/ds/LM/LMH6559.pdf>, accessed August 2, 2004.
- [13] “LMH6642/6643/6644 Low Power, 130 MHz, 75 mA Rail-to-Rail Output Amplifiers,” National Semiconductor, Santa Clara, California, April 2004. From Website: <http://cache.national.com/ds/LM/LMH6642.pdf>, accessed August 2, 2004.
- [14] “4-Layer Production Service,” ExpressPCB, Santa Barbara, CA, July 2004. From Website: <http://www.expresspcb.com/ExpressPCBhtm/Specs4Layer-Production.htm>, accessed August 23, 2004.
- [15] Jon Varteresian, *Fabricating Printed Circuit Boards*, pp. 47–56, Elsevier Science, Woburn, Massachusetts, 2002.
- [16] “MC100EPT23 3.3 V Dual Differential LVPECL to LVTTL Translator,” MC100EPT/D (Rev 9), On Semiconductor, Denver, CO, October 2003. From Website: <http://www.onsemi.com/pub/Collateral/MC100EPT23-D.PDF>, accessed February 9, 2004
- [17] “MAXIM MAX9360/MAX9361 LVTTL/TTL/CMOS-to-Differential LVECL/ECL Translators,” 19–2327 (Rev 1). Maxim Integrated Products, Sunnyvale, CA, July 2002. From website: <http://pdfserv.maxim-ic.com/en/ds/MAX93-60-MAX9361.pdf>, accessed February 6, 2004.
- [18] “MAXIM MAX9316A 1:5 Differential (LV)PECL/(LV)ECL/HSTL Clock and Data Driver,” 19–2648 (Rev 0), Maxim Integrated Products, Sunnyvale, CA, October, 2002. From website: <http://pdfserv.maxim-ic.com/en/ds/MAX9316.pdf>, accessed February 6, 2004.
- [19] “MICTOR Vertical Connectors for Surface Mount Technology (SMT) Printed Circuit (PC) Board Applications,” (Rev B), Tyco Electronics Corporation, Harrisburg, PA, April 2003. From website: http://ecommas.tycoelectronics.com/commerce/DocumentDelivery/DDEController?Action=showdoc&DocId=Specification+Or+Standard%7F114-11004%7FB%7Fpdf%7FEnglish%7FS_114-11004_B.pdf, accessed February 3, 2004.
- [20] “.100” x .100” Low Profile Header,” TS–0770–10, 3M Interconnect Solutions Division, Austin, TX, April 2001. From website: <http://rocky.digikey.com/WebLib/3M/Web%20Data/2500%20Series.pdf>, accessed July 19, 2004.
- [21] “The ECL Translator Guide,” AN1672/D (Rev 7), On Semiconductor, Denver, CO, November 2002. From website: <http://www.onsemi.com/pub/Collateral/AN1672-D.PDF>, accessed February 17, 2005.

- [22] "Trace Carrying Capacity Per Mil Std 275," K & F Electronics, Inc., Fraser, MI. From website: <http://www.circuitboards.com/capacity.php3>, accessed February 18, 2005.
- [23] Thomas. G. Guthrie, *Design, Implementation, and Testing of a Software Interface Between the AN/SPS-65(V)1 Radar and the SRC-6E Reconfigurable Computer*, Master's Thesis, Naval Postgraduate School, Monterey, California, March 2004.
- [24] John F. Wakerly, *Digital Design Principles & Practices*, Third Edition, pp. 175-183, Prentice Hall, Upper Saddle River, New Jersey, 2001.

THIS PAGE INTENTIONALLY LEFT BLANK

INITIAL DISTRIBUTION LIST

1. Defense Technical Information Center
Ft. Belvoir, Virginia
2. Dudley Knox Library
Naval Postgraduate School
Monterey, California
3. Chairman, Code EC
Department of Electrical and Computer Engineering
Naval Postgraduate School
Monterey, California
4. Alan Hunsberger
National Security Agency
Ft. Meade, Maryland
5. Dr. Russell Duren
Baylor University
Engineering Department
Rogers, Texas
6. Douglas J. Fouts
Department of Electrical and Computer Engineering
Naval Postgraduate School
Monterey, California
7. Phillip E. Pace
Department of Electrical and Computer Engineering
Naval Postgraduate School
Monterey, California
8. Jon Huppenthal
SRC Computers, Inc.
Colorado Springs, Colorado
9. David Caliga
SRC Computers, Inc.
Colorado Springs, Colorado